Theses and Dissertations

12-15-2014

Thermal Ecology and Physiology of an Intertidal Predator-Prey System: *Pisaster Ochraceus* and *Mytilus Californianus*

Cristian J. Monaco
University of South Carolina - Columbia

Follow this and additional works at: http://scholarcommons.sc.edu/etd

THERMAL ECOLOGY AND PHYSIOLOGY OF AN INTERTIDAL PREDATOR-PREY
SYSTEM: *PISASTER OCHRACEUS* AND *MYTILUS CALIFORNIANUS*

by

Cristián J. Monaco

Bachelor of Marine Sciences
Universidad Católica del Norte - Chile, 2006

Professional title in Marine Biology
Universidad Católica del Norte - Chile, 2007

_____

Submitted in Partial Fulfillment of the Requirements

For the Degree of Doctor of Philosophy in

Biological Sciences

College of Arts and Sciences

University of South Carolina

2014

Accepted by:

Brian Helmuth, Major Professor

David S. Wethey, Major Professor

Sean P. Place, Committee Member

James L. Pinckney, Committee Member

Eric Sanford, Committee Member

Lacy Ford, Vice Provost and Dean of Graduate Studies

DEDICATION

Dedicated to my parents. Their unique blend has granted me with exactly the right

amounts of reality and magic!

ACKNOWLEDGEMENTS

This document could not have been produced without the support provided by a number of generous individuals and organizations. To me, this section is the most important in the entire dissertation because it implicitly holds the substance of my development over the last 5.5 years; that is, my understanding of the natural world has been shaped by and is contained within my personal interactions. As has been gracefully stated, "gratitude is the memory of the heart", so their contributions to my personal endeavors will forever remain.

First and foremost, my appreciation goes to my mentors Brian Helmuth and David Wethey. In their own personal styles, they provided with the right guidance and enthusiasm for my scientific inquiries to advance. From day one, Brian struck me for his infinite generosity, both material and intellectual. His kind spirit trespasses Helmuth's lab walls, as revealed by numerous conversations with random people from the scientific and non-scientific communities. Initially as a committee member, and later as a major advisor, David stood as the genius with all the correct answers. Perhaps more important is that, despite his vast experience and brilliancy, he always kept and open mind to my own viewpoints. These two giants gave me the keys not only to their labs, but also to a scientific community, which until then was only accessible to me through the literature.

The quality of my work was significantly increased thanks to the fine members of committee: Sean Place, Jay Pinckney, and Eric Sanford. Their service is very much

iv

appreciated. Not only did they invest the time to hear about my ideas during meetings, but also provided interesting thoughts to explore, and excellent feedback for my writing.

In Brian and David's labs I also benefited from close interactions with lab techs, postdocs, and fellow grad students. In a day-to-day basis and during lab meetings, I enjoyed learning about their study systems, as well as better ways for me to frame my own research. Lauren Yamane, Alli Matzelle, and Francis Choi were amazing lab techs that, in addition to keeping up with field, lab, and administrative labor, never hesitated to lend me a hand on even my most absurd requests. As our postdoc, Mackenzie Zippay brought an ideal blend of professional expertise, creative thinking, and contagious energy that permeated through the lab. Thanks to the grad students Shilpi Chhotray, Nick Colvard, Shadow Gulledge, Josie Iacarella, Nicole Kish, Alli Matzelle, Allison Smith, Alyson Tockstein, and Jessica Torossian. Aside from the labels given to these individuals, I respect them all as friends.

I am grateful to the grad students in the Biology Department who helped make the ride enjoyable. Their lessons were as valuable as those received from formal professors. In particular, thanks to Katie Allen, Wassim Basheer, Fernando Blanco, Chris Brandon, David Castillo, Laura Enzor, Richard Fandino, Matt Greenwold, Liz Fly, Kate Levasseur, Megan Riley, Rhiannon Rognstad, Jackson Sparks, Rachel Steward, Ben Toscano, and Amy Wahba.

Last but not least, my deepest acknowledgements go to my family. It is only because of their limitless love, patience, and high expectations that I got the work done.

ABSTRACT

Untangling natural systems' complexity requires understanding the mechanisms

responsible for organisms' responses to environmental change. Recently, significant

advances have been made by recognizing the relevance of direct and indirect effects,

which take place when multiple biotic and abiotic factors influence each other. I

examined potential direct effects of environmental variables on a predator-prey

interaction, as well as potential indirect effects of these variables on the interaction itself.

I placed emphasis on behavioral and physiological adaptations, which would potentially

contribute/modify these effects.

My study system was comprised of a rocky intertidal keystone predator, the sea

star *Pisaster ochraceus*, and its main prey the mussel *Mytilus californianus*. While

previous work had explored the influence of both seawater and aerial temperature on

their interaction, few studies had explicitly considered the physiological basis of such

responses. Given the direct links between *Pisaster* body temperature and physiological

performance, in Chapter 1 I asked, where exactly is *Pisaster* located? And, what

physiological consequences it might bring? Pisaster exhibited a size-dependent

distribution, with small animals found higher on the shore. Also, most individuals were

found in refugia at low tide, reflecting *Pisaster* risk-avoiding strategy, despite generally

mild conditions. We suggest that the strategy may help prevent exposures to extreme

(although rare) events.

Chapter 2 provided an opportunity to compare thermal performance between the predator *Pisaster* and prey *Mytilus*. Within an environmental stress model framework, I asked: which species would be more negatively impacted by thermal stress? To avoid influencing individuals' response, I tested this idea indirectly via thermal performance curves (TPC). I described TPCs for both species, which first allowed comparing them based on their intrinsic thermal sensitivities. Second, these curves were used to calculate thermal performance using field body temperature data. I collected data on body mass indices and heat-shock protein 70kDa to evaluate both species general physiological condition and levels of extreme thermal stress. Thermal sensitivity varied between species and site of origin. Contrary to previous findings, I observed that *Mytilus* performance resulted more negatively affected by temperatures than *Pisaster*, and no effects of movement behavior were detected.

Chapter 4 describes a Dynamic Energy Budget (DEB) model for *Pisaster*. I discussed the models' ability to simulate growth throughout ontogeny, shrinkage when food is scarce, and the combined effects of changes in body temperature and food availability. This model should prove useful in predicting *Pisaster* physiological responses to environmental change.

TABLE OF CONTENTS

LIST OF TABLES

LIST OF FIGURES

CHAPTER 1

INTRODUCTION

Dynamics in ecological systems result from multiple biotic and abiotic processes occurring simultaneously, at uneven rates, and in different directions. The complex nature of these processes translate into inherently nonlinear ecological dynamics (Peters et al. 2007). Understanding, and ultimately predicting such dynamics requires comprehensive examinations of the underlying mechanisms driving them (Denny & Helmuth 2009). The research described here revolves around the premise that, by focusing on the organism and its close interaction with the environment, one can identify and characterize the most relevant processes influencing organisms' condition, and then scale-up to higher levels of biological complexity.

Species' ecological roles are mediated by physical environmental variables that constrain individual fitness (Chase & Leibold 2003). A comprehensive understanding of the links between the physical environment and organismal performance has become particularly relevant in a period of rapid climate change (Harley et al. 2006a). Marine ecologists have long relied on the rocky intertidal system to characterize the drivers determining patterns of species' abundance and distribution. Given its steep gradients, both physical (e.g. temperature) and biological (e.g. ecological interactions), and the ease of performing observational and manipulative studies, the rocky intertidal is considered an ideal natural laboratory, and much of our current understanding of the interplay between the physical and biological factors that control species' presence originated from

research conducted in this system (Benson 2002). For example, the classical intertidal zonation studies by Connell (1961, 1972) revealed that while physical drivers set upper shore limits, biological factors are more important at setting lower limits. In a follow-on study, by manipulating the amount of sunlight experienced by competing intertidal barnacle species on the field, Wethey (1984) demonstrated that the intensity of species interactions could be regulated by prevalent physical conditions. As such, the influence of weather on predator-prey dynamics has gathered much attention, especially those involving keystone species capable of controlling community structure and functioning (Pincebourde et al. 2008, Zarnetske et al. 2012). Together, these studies provided solid evidence that ecological processes are highly context-dependent, a factor which needs to be considered when trying to forecast dynamics in managed and pristine natural systems.

More recently, as studies drawing the connections between environmental and ecological processes accumulate, the relevance of considering context-dependency in our predictions has been increasingly emphasized (Berlow & Navarrete 1997, Fields et al. 1993, Helmuth & Hofmann 2001, Russell et al. 2006, Williams & Morritt 1995). Specifically, while climate change's threat is often assumed to be associated with climate alone, a closer look at the individual may uncover non-climatic features of the system that either alter local environmental conditions (e.g. geography/topography, timing of low tide) or else affect vulnerability to changes in the environment (e.g., inter-individual variability in stress-response [behavior and physiology], ecological interactions), which could potentially modify the biotic and abiotic conditions organisms encounter (Mislan et al. 2009, Russell et al. 2011).

Environmental heterogeneity in the intertidal zone, both on a spatial and temporal scale, can determine complex patterns of abundance and distribution (Wethey 1983, Wethey 1984). Recent studies have demonstrated that individuals' body-temperature can greatly depart from air-temperatures measured by both weather-stations nearby or researchers on-site (Helmuth 1998), and significantly vary depending on the microhabitat being used (Denny et al. 2011, Helmuth 2002, Seabra et al. 2011). Depending on the species being scrutinized, mismatches can attributed to a variety of "filters" that transform the environmental signals into conditions truly experienced by the individual, thus defining its niche (sensu Kearney 2006). For intertidal species, these filters may include physiology, behavior, morphology, as well as interactions between organisms.

One of the most thoroughly studied intertidal communities is the one found on western coast of the United States. Notably, there is a series of ecological and physiological studies done with two conspicuous components: the sea star *Pisaster ochraceus* and the mussel *Mytilus californianus*. These species have been good study models to observe not only the direct effects that temperature might have over different populations, but also the indirect effects over vital rates such as the feeding rates of the star on the mussel (Pincebourde et al. 2008). As keystone species, *Pisaster* has the ability to modify its community's structure by preventing *Mytilus* from monopolizing the substrate (Paine 1966, Paine 1974); thus, it is of primary importance to address the effects that temperature shifts would exert on *Pissater* physiology and fitness. Specifically, it is now crucial to quantify the way how environmental temperatures vary, the way that organisms perceive those temperature variations, and the consequences of those

variations on the organism's vital rates (e.g. growth, reproduction, feeding) (Helmuth et al. 2006a).

A major strategy that intertidal organisms utilize to filter environmental signals is behavior. While often seemingly random, movement throughout the intertidal may very well follow predictable trajectories when enough details of the system are known. For example, *Pisaster* foraging bouts have been linked to seawater warming due to relaxations of upwelling periods (Sanford 1999). Once the tide recedes, many sea stars can be observed exposed to aerial conditions, which may be physiologically challenging. Previous work has clearly demonstrated that *Pisaster* avoids the risks associated with being aerially exposed (Burnaford & Vasquez 2008, Garza & Robles 2010). Interestingly, earlier studies have also identified a particular pattern of distribution characterized by larger sized individuals occupying lower shore levels (Feder 1956, Fly et al. 2012). Although informative, these studies did not explore whether the distribution patterns in *Pisaster* are consistent over time and space, the influence of body size on the relationships, and the role of alternative environmental drivers in controlling the patterns. Chapter 2 examines these aspects using both observational and experimental approaches. I present data of repeated surveys conducted on two populations of *Pisaster* located ~760km apart, Bodega (California) and Strawberry Hill (Oregon), which document individuals' microhabitat use (e.g. crevices, tide pools, exposed) in relation to body size. This information is coupled with environmental variable data collected by closely located weather stations and biomimetic temperature loggers deployed *in situ*. Lab experiments designed to test the effect of body size on *Pisaster* sensitivity to temperature and wind speed provide material to test alternative hypotheses about the mechanisms leading to

shore-level size gradients in intertidal organisms. Our results confirm the idea that *Pisaster* favors a risk-avoiding strategy, despite generally mild thermal conditions recorded during the period of our surveys. As an imperfect thermoregulator, and given the risk of reaching potentially lethal temperatures at some low tides, this seems a plausible strategy for *Pisaster*.

In Chapter 3, we turn our attention to both the predator and the prey, and examine which might be more affected by its thermal environment. I couch this question within an environmental stress model (ESM) framework. ESMs have provided means for conceptualizing the impacts of environmental stressors on ecological interactions such as predation and competition (Menge & Olson 1990, Menge et al. 2002). Given that ongoing climate change is challenging species via multiple stressors (e.g. direct effects of temperature and indirect effects on species interactions), frameworks that allow discriminating between them and incorporating their variability into our predictions are especially useful.

Depending on which species results more negatively affected by environmental stress, ESMs may serve to explicitly forecast the dynamics of a particular system. Although great progress has been made on this field, studies often ignore important elements of the system, which may alter the outcomes. In the rocky intertidal, for instance, species cope with an extremely heterogeneous environment, where even closely located individuals can experience radically different conditions (Denny et al. 2011, Seabra et al. 2011). Given the ability of *Pisaster* to move among different microhabitats throughout the intertidal, it is conceivable that individuals may buffer against potential heat stress by moving to sheltered locations during low tides. An earlier study

investigated this predator-prey interaction following an ESM framework, but ignored this potential role of behavior because their methods involved caging animals at different heights (Petes et al. 2008b).

I followed an alternative approach that may be useful to circumvent the problems encountered by that earlier study. Instead of directly assessing performance, I first described thermal performance curves (TPC) for both species and then calculated mean thermal performance based on body temperatures recorded in the field using biomimetic temperature loggers. In parallel, I made observation of *Pisaster* microhabitat use that allowed incorporating the role of movement behavior into the calculations of mean thermal performance. Using these data I quantified the thermal performance of both *Pisaster* and *Mytilus*. The performance of *Pisaster* was calculated under static and mobile scenarios to further evaluate the role of behavior. Additionally, to evaluate how this approach compares to more traditional measurements of performance, I provide data on indicators of overall physiological condition (body mass index) and thermal stress (heat-shock protein 70kDa).

Chapter 4 represents an effort to model *Pisaster* energy budget using the relatively novel Dynamic Energy Budget model (Kooijman 1986, Sousa et al. 2010). DEB models describe flows of energy and mass throughout the organism to meet requirements of maintenance, development, growth, and reproduction. One of the powerful aspects of DEB is the use of the same parameters to describe the biology of all organisms, whereby differences between species and individuals can be captured by differences in parameter values (Sousa et al. 2010, van der Meer 2006). Also, DEB

models explicitly recognize that organisms inhabit a dynamic environment, so variability in temperature, for example, can be readily incorporated in our predictions.

I modeled *Pisaster* DEB using data collected from the literature as well as from experiments explicitly designed to estimate parameters. In put special attention on: (1) characterizing growth of the different life-stages of *Pisaster*, larvae, juvenile, and adults, (2) the ability of the model to simulate shrinkage when energy intake is not enough to cover maintenance requirements, and (3) the ability of the model to account for the combined effects of changes in body temperature and food availability. Having estimated the DEB parameter values for *Pisaster*, this model will provide means for understanding underlying physiological processes that ultimately influence its interaction strength with *Mytilus*. Consequently, this mechanistic model could help predict dynamics at higher levels (Nisbet et al. 2000).

CHAPTER 2

SIZE-DEPENDENT INTERTIDAL HEIGHT AND REFUGE USE IN THE KEYSTONE PREDATOR *PISASTER OCHRACEUS* NTRODUCTION[1]

ABSTRACT

Intertidal organisms live in a highly heterogeneous habitat. To better understand the influence of environmental variability on population dynamics it is essential to describe conditions at the individual level. We surveyed populations of the rocky intertidal sea star *Pisaster ochraceus* and characterized size-dependent distribution, defined by individuals' shore level and refuge use. By conducting surveys repeatedly at two field sites in California and Oregon, we examined temporal and geographical variability in habitat selection. We evaluated whether environmental drivers measured by sensor station (air temperature, solar radiation, seawater temperature, wave height, and wind speed), and body temperatures measured using biomimetic sensors, explained the observed distribution patterns. We experimentally tested the effect of size on animals' thermo- and desiccation-tolerance. Using biomimetic data, combined with a thermal performance curve framework and information of critical temperatures of different size classes, we investigated potential physiological and survival consequences of microhabitat use. Results showed that *Pisaster* is mostly found in refugia during low tide, thus favoring a risk-avoiding strategy, despite minimal consequences of temperature

---

[1] Monaco, CJ, Wethey, DS, Gulledge, S, and Helmuth, B. To be submitted to *Marine Ecology Progress Series.*

on physiological condition and survival estimated for the period of the surveys. When found protected, *Pisaster* exhibited size-dependent intertidal height (SDIH, larger animals lower on the shore), which varied spatially and temporally; but when found exposed, the SDIH pattern disappeared. The proportion of individuals found protected increased with air temperature, solar radiation, and body temperature. SDIH was not influenced by environmental variability. Size-dependent sensitivity to stressful temperatures and wind speed did not explain the observed distribution patterns. Altogether, our data suggest that, despite generally mild conditions, *Pisaster* risk-avoidance strategy buffers against rare but potentially highly stressful events. Because ectothermic organisms' microhabitat use drives body temperature, foraging, and energetics, knowing exactly where this keystone predator occurs could shed further light on its ecological role, and how this may change in coming years.

INTRODUCTION

The rocky intertidal zone is considered among the most environmentally variable habitats because of its complex topography and alternating exposure to air and water. Animals and algae in this habitat can experience dramatically different environmental conditions from even close neighbors due to micro-scale variation in abiotic stressors (Denny et al. 2011, Potter et al. 2013, Seabra et al. 2011). Coupled with differential physiological sensitivities, patterns of stress among intertidal organisms are thus extremely variable, leading to "winners" and "losers" (Somero 2002). Variability is also likely to occur among members of the same species, both in terms of physiological sensitivity as well as ability to respond to environmental variability in space and time. As an organism grows and progresses through its ontogeny, many factors can change including rates of

9

movement and availability of microhabitats; larger organisms for example may be able to travel farther but also may no longer fit in smaller microhabitats such as crevices (Raffaelli & Hughes 1978). Larger organisms can also be less physiologically vulnerable to sudden changes in the environment due to high thermal inertia and energy reserves (Allen et al. 2012, Stevenson 1985).

Consequently, intertidal organisms can exhibit what are apparently idiosyncratic physiological and behavioral responses to local environmental conditions (Judge et al. 2011, Kearney et al. 2009, Marshall et al. 2013, Moore et al. 2007, Williams & Morritt 1995). While often interpreted as random (and thus unpredictable) variation, these responses likely result from underlying mechanistic relationships that are revealed only when relevant details are included (Hallett et al. 2004). Given the direct relationship between how an organism senses and interacts with its immediate habitat, its physiological condition, and subsequent fitness, a lack of understanding of how species filter environmental signals and utilize their microhabitats may limit our ability to accurately anticipate population or community level dynamics (Monaco & Helmuth 2011). Therefore, deepening our understanding of the relationship between environmental stressors and organisms' behavioral and physiological toolkits for coping with these stressors is crucial.

By integrating temperature time-series data and observations of individuals' microhabitat use and behavior, studies are increasingly including aspects of the intra-site body temperature variability that would be expected for a complex rocky intertidal zone. For example, in response to varying levels of thermal and desiccation stress, gastropods (particularly limpets and snails) and crabs have been reported to vary in intertidal height

(Klaassen & Ens 1993, Williams & Morritt 1995), refuge use both of biogenic and non-biogenic origin (Cartwright & Williams 2012, Garrity 1984, Jones & Boulding 1999), or even social behavior such as "huddling" (Muñoz et al. 2008, Rojas et al. 2013), in response to varying levels of thermal and desiccation stress. A few studies have further explored how patterns of microhabitat use and movement among shore levels can be driven by organisms' body size (e.g. Hobday 1995, Klaassen & Ens 1993, Soto & Bozinovic 1998). Several hypotheses have been put forward to explain shore level size-gradients, primarily based on earlier studies conducted using intertidal gastropods. In a review of these patterns, Vermeij (1972) found that species common to the low intertidal zone typically show smaller size classes higher on the shore, presumably because predation and competition pressures over those vulnerable individuals decrease at those heights. Then, a study conducted using *Nucella* spp. snails suggested that individuals chose specific heights based on their preference for consuming specific prey sizes (Bertness 1977), thus highlighting the role of energy maximizing criteria, as opposed to just a risk of mortality. Subsequently, McQuaid (1982) noted that higher desiccation experienced by smaller individuals due to increased surface-area/volume prevents these individuals from occupying higher shore levels, as larger ones do. Raffaelli and Hughes (1978) also contributed to this discussion by showing that the availability and size of refuges can drive size-gradients across the intertidal zone.

Here we examine microhabitat use by a keystone predator, the rocky intertidal sea star *Pisaster ochraceus* (Brandt, 1835) (hereafter, *Pisaster*). Because of its role as keystone predator *Pisaster* has been the subject of extensive ecological and physiological research (Paine 1974, Sanford 1999). *Pisaster* inhabits exposed rocky shores on the

Pacific coast of North America, where cyclic tides, recurrent upwelling, and topographic complexity set the scene for an extremely heterogeneous thermal environment (Broitman et al. 2009, Helmuth & Hofmann 2001, Jackson 2010). Evidence shows that the impact of *Pisaster* on the intertidal community is indirectly mediated by body temperatures experienced during both periods of low and high tide (Pincebourde et al. 2008, Sanford 1999).

Pisaster forages during submersion at high tide, and then remains in place during low tide, often continuing to ingest its prey (Robles et al. 1995). As a result, depending on where a sea star finds itself when the tide recedes, it can either be exposed to potentially stressful thermal, wind, and solar radiation conditions, or protected in crevices, tide pools, or under algae (Burnaford & Vasquez 2008, Fly et al. 2012). Being exposed while foraging at high tide may also imply having to cope with the impact and drag of wave-generated forces (Denny et al. 1985). Unlike other smaller species, however, the size range of *Pisaster* (~0.1 to 20 cm arm length) is quite large and in some cases on par with the "grain size" of the physical habitat. Thus, a microhabitat that may serve as effective refuge for a small animal may be inaccessible for a larger individual (e.g. Raffaelli & Hughes 1978). Additionally, these highly mobile animals can travel several m per day during high tide (Robles et al. 1995) and individuals can thus be found at different elevations (from shallow subtidal to mid-high intertidal) (Garza & Robles 2010, Pincebourde et al. 2008), implying exposure to different degrees of physical stress (Marshall et al. 2013).

Although substantial progress has been made towards accurately characterizing the realized niche of *Pisaster*, most studies have ignored the potential relationship

between an individual's body size and its microhabitat choice (defined here by its refuge use and intertidal height). Consequently, our knowledge of this predator's body temperature and physiological condition throughout ontogeny is generally obscure. Importantly, previous studies have revealed that *Pisaster* vertical position in the intertidal zone appears correlated with body size, with larger individuals found lower on the shore (i.e. size-dependent intertidal height, hereafter SDIH) (Feder 1956, Fly et al. 2012). In *Pisaster*, because SDIH has not been systematically described over multiple tide cycles, or across different sites, its mechanism and overall ecological and physiological significance remain unknown. Although it is recognized that the majority of *Pisaster* individuals observed in the field during low tides are found protected in crevices, tide pools, or under kelp (e.g. Burnaford & Vasquez 2008, Fly et al. 2012), studies have yet to examine the influence of body size on microhabitat selection across geographic scales. Because our predictions of organisms' response to climate change are sensitive to our ability to accurately estimate body temperature (Helmuth 2002), improving our understanding of how the thermal niche of *Pisaster* shifts throughout ontogeny will provide a more complete picture of individual physiological condition and fitness, and ultimately the dynamics of populations. Here, we approach the issue through both field and laboratory-based observations.

First, using data from repeated field surveys (2010-2012) conducted at two sites located approximately 770 km apart, we aimed to characterize *Pisaster* refuge use and SDIH. Specifically we asked: how consistent are these patterns through space and time? Second, we tested whether the variability in these patterns could be explained by changes in environmental drivers; namely, air temperature, seawater temperature, solar radiation,

wind speed, and wave action. Third, we ran laboratory experiments to determine whether

differences in thermo- and desiccation-tolerance between size classes can help explain

the observed pattern. According to the oxygen limitation hypothesis (Pörtner 2002,

Pörtner 2006), and supporting evidence available in the literature (Peck et al. 2009, Peck

et al. 2013), we hypothesized that smaller individuals can withstand higher temperatures

than larger ones because they have a proportionately larger respiratory surface area

relative to volume of tissue. One might expect that the larger surface-area to volume

ratio exhibited by small animals would favor water loss during exposure to wind stress,

with a consequent reduction in performance, relative to larger individuals (Allen et al.

2012, Stevenson 1985). However, previous accounts for *Pisaster* (Feder 1956,

Landenberger 1969) have suggested that this is not the case. By exposing individuals

ranging in body size to desiccation ("drierite" treatment), Feder (1956) demonstrated that

smaller *Pisaster* are not more vulnerable to losing water through evaporation, nor of

showing earlier signs of physical distress (i.e. body wall flattening, failure of tube feet to

attach) (Landenberger 1969). We therefore hypothesized that size does not have a strong

effect on desiccation tolerance, and complemented this body of knowledge by following

an approach that recreated natural conditions more realistically. We exposed individuals

to a constant wind speed that paralleled average *in situ* measurements made during a

representative low-tide period, and measured performance during simulated high tides.

Finally, in an effort to place this study into a more realistic ecological context, we

collected information of the body temperature that individuals would have been

experiencing in the different microhabitats available in a typical rocky intertidal zone,

recorded using biomimetic data loggers. In light of these potential conditions and our

direct observations of microhabitat use, we aimed to further our understanding of the

mechanisms driving patterns of distribution in *Pisaster*, and their role in defining

zonation patterns. While previous studies have suggested that their upper limits of

distribution are likely not set by temperature (Robles et al. 2009), we also know that

physiological performance is strongly dependent on sub lethal temperatures (Pincebourde

et al. 2008). Because vertical movement may imply increased energy expenditure to

cope with physiological thermal stress (either acute or chronic, sensu Pincebourde et al.

2008), we expected *Pisaster* to behaviorally compensate for these costs by preferentially

seeking protected microhabitats (i.e. refuges).

MATERIAL AND METHODS

Study sites

We conducted field surveys at two study sites: Strawberry Hill (44°14'59.4" N,

124°06'54.7" W, Oregon, USA), and Bodega Marine Reserve (38°19'07.7" N,

123°04'27" W, California, USA), spanning ~770 km of coastline. We chose these sites

based on habitat suitability for *Pisaster*. Since the population size structure of *Pisaster*

may vary widely across habitat types (Rogers & Elliott 2013), we limited our analysis to

wave-exposed rocky shores, where this keystone predator plays a more critical ecological

role (Menge et al. 1994, Paine 1966, Paine 1974, Power et al. 1996). Both sites presented

dense mid-intertidal mussel beds, which promotes *Pisaster* presence and elicits its

keystone role (Menge et al. 1994, Paine 1974), and were topographically complex,

providing alternative microhabitats for sea stars to occupy, including crevices, tide pools,

kelps, and open spaces. At the time of the surveys, wasting disease (Bates et al. 2009,

Stokstad 2014) had not yet affected populations and abundances at all sites were high.

15

Intertidal distribution surveys

To describe *Pisaster* microhabitat use (SDIH and refuge use) at each study site and survey date, we sampled every individual encountered along 5, 2-m wide, belt-transects perpendicular to the coastline. Transects extended from the height of the highest *Pisaster* individual found to the low water level limit set by the spring-tide. We conducted all surveys during the time of negative tide heights, as predicted and verified by NOAA's CO-OPS (station IDs 9435380 and 9415020 for Strawberry Hill and Bodega, respectively). For each sea star, we recorded body size and described microhabitat use. We determined size from wet weight measurements taken with a portable balance (Ohaus SP202, 200g) or a spring scale (Pesola, 1000g), depending on the animal's size. We characterized the microhabitat in which each individual was found based on (1) intertidal height (cm above MLLW), measured using a surveying laser-level (Topcon), and (2) its refuge use, which was designated as either heat-protected (i.e. crevice, tide pool, under kelp) or exposed (i.e. flat, receiving solar radiation). We used regression analysis to determine SDIH from the data collected during each survey (see section *statistical analyses*).

To evaluate temporal dynamics in sea star distribution patterns we surveyed Strawberry Hill and Bodega on multiple spring tide periods during the summer of 2012 (Strawberry Hill: 24 May 2012, 22 June 2012, 20 July 2012, and 3 August 2012; Bodega: 22 May 2012, 8 June 2012, 20 June 2012, 19 July 2012, and 1 August 2012). Bodega was additionally surveyed repeatedly during the summers of 2010 (2 June 2010, 16 June 2010, and 28 June 2010) and 2011 (19 May 2011, 4 June 2011, 15 June 2011, 1 July

2011, and 14 July 2011); thus inter-annual comparisons could be performed. To examine spatial variability we compared data between sites collected in the same year (2012).

Foraging activity and distance to prey

We collected data to compare *Pisaster* foraging activity and potential access to its preferred prey, the mussels *Mytilus californianus* and *M. trossulus*. During the intertidal distribution surveys of 2011 and 2012 at Bodega, and 2012 at Strawberry Hill (see section *intertidal distribution surveys*), we recorded (1) whether sea stars were found consuming mussels (i.e. digesting with stomach everted), and (2) distance to closest mussel bed edge, when found not eating.

Influence of environmental drivers

We examined the effect of changes in relevant environmental variables on the intertidal distribution patterns (SDIH and refuge use) exhibited by *Pisaster*. We tested the effects of seawater temperature (Sanford 1999), air temperature (Pincebourde et al. 2008), wind speed (Landenberger 1969), wave action (Sanford 2002b), and solar radiation (Burnaford & Vasquez 2008) since all have been shown to affect sea star physiology, body temperature and/or behavior (Szathmary et al. 2009). We used data collected hourly by an on-site weather station (200m from survey area) maintained by the Bodega Ocean Observing Node (available at http://www.bml.ucdavis.edu/boon/). Because on-site weather data were not available for Strawberry Hill, we conducted this analysis only for Bodega. We manipulated the data series as follows. First, we extracted the data corresponding to one day prior to each population survey, making the assumption that any environmental cues (except sea water temperature) would have had their impact during the previous day's aerial exposure (Szathmary et al. 2009). Second, we filtered

17

environmental data according to the shore level at which they would influence the condition of *Pisaster*. Namely, we only used data recorded during high tide periods (> 1m above MLLW) for seawater temperature and wave action, and data recorded during low tide periods (≤ 1m) for air temperature, wind speed, and solar radiation. For each driver, we determined both the daily maximum value and the 75th percentile, which were then regressed against our field observations of *Pisaster* distribution. We report only the output obtained with the former, as results did not qualitatively differ when using the maxima or the 75th percentile.

The analysis addressed two main elements of *Pisaster* distribution that could potentially vary depending on environmental variability. First, we looked for relationships between SDIH and the five drivers. And second, we tested whether these drivers explained changes in the proportion of individuals found exposed during low-tide surveys (i.e. refuge use).

Size-dependent aerial thermotolerance: Lab experiment

To evaluate the effect of *Pisaster* body size on its aerial thermotolerance we conducted experiments to estimate and compare the lethal temperature (LT_{50}, temperature at which 50% of the individuals die) between two size classes, small (25 to 75g, N=34) and large (250-400g, N=33). We ran these experiments during July 2011, at the Bodega Marine Laboratory (BML, University of California – Davis).

We collected the specimens used for these experiments at Bodega Marine Reserve, CA (38°19'4.9" N, 123°4'24.8" W), and held them in tanks with running seawater and food (mussel *Mytilus californianus*) provided *ad libitum*. We withdrew their food supply 24h before the experiments to prevent contributions of food to wet

weight, and to standardize physiological condition. Before beginning the experimental treatments, we recorded each individuals' wet weight. We placed specimens (up to 2, avoiding contact between them) on gray acrylic-platforms positioned 25-cm above the bottom of 75-L tanks. Below the platform, we provided a constant stream of seawater to maintain high levels of ambient humidity. Above the platforms we mounted a heat-lamp (150-W) directed downwards, which could be moved vertically to adjust animal's temperature during each trial. Using a non-invasive infrared thermocouple thermometer (Omega Corporation), we measured the surface temperature of each individual's central disc every 15-min. We ran each trial for 6h. During the first 3h, we gradually increased body temperature from ambient seawater temperature (~12°C) to the treatment temperatures, which ranged between 24 and 40°C, with 2°C intervals. During the last 3h, we maintained the treatment temperature at constant levels. Then, we placed the individuals in recovery tanks with running seawater for 24h, after which we assessed survival by probing their tube feet and evaluating their response.

Size-dependent desiccation-tolerance: Lab experiment

To evaluate the effect of *Pisaster* body size on its tolerance to desiccation, we conducted experiments to quantify and compare the performance of individuals ranging in size (7.1 to 780.1g, N=26) after realistic, consecutive, 6-h daily exposures to a moderately high wind speed treatment of 3.5-4.0 m s^{-1}. We ran these experiments during July 2011, at the BML.

We collected and prepared the animals for this experiment following the same steps described for the *Thermotolerance Experiment*. To evaluate sea stars' response to desiccation, we determined each individual's performance on four consecutive days: (1)

One day prior to beginning the experiment, which defined a baseline, individual-specific value (reference), (2) day 1, after a first exposure to the wind speed treatment, (3) day 2, after a second wind exposure, and (4) day 3, after a final wind exposure. We assessed performance based on righting response time (*RT*) measurements (seconds) collected at each time point in the three consecutive trials, and the reference. We calculated an activity coefficient (*AC*) (Lawrence & Cowell 1996, Percy 1973) for each time point, based on the equation: $AC = 1000/RT$. We then calculated an average between the *AC*s from days 1, 2, and 3, corresponding to the period when the individual was subjected to the desiccation treatment. We finally calculated the difference between this after treatment *AC* and the reference *AC* of each individual, thus obtaining a relative measure of the effect of desiccation. These data were modified by adding a positive offset value in order to have only positive number, which were then analyzed in relation to body size.

Robo-sea star temperature records

To assess the temperatures individuals would have been experiencing in different microhabitats frequently occupied by sea stars (i.e. potential body temperature), we used biomimetic temperature loggers (iButton DS1922, 0.0625˚C resolution) modified to resemble the thermal properties of an average size *Pisaster*, ~ 200g (Szathmary et al. 2009). We deployed these biomimetic sensors, a.k.a. robo-sea stars, at Strawberry Hill and Bodega, during the summer of 2012, and continuously recorded (15-min sampling rate) *Pisaster* body temperature in exposed (high, mid, and low intertidal heights) and protected (crevices, and tide pools) microhabitats.

Physiological performance and survival consequences of body temperature

We used the robo-sea star temperature data to evaluate the physiological implications, as well as potential mortality effects, of selecting each microhabitat type. Physiological consequences were quantified based on a thermal sensitivity curve previously derived for *Pisaster* (Monaco et al. 2014). Mortality effects were examined via cumulative survival curves described for each microhabitat type, size class, and site.

Statistical analyses

All statistical analyses were conducted using R 3.0.1 (R Core Team 2013). To determine the effect of body size on individuals' intertidal height (i.e. SDIH) we ran regression analyses using data collected during each survey (e.g. Bertness 1977, Hobday 1995). To test whether microhabitat use would change the nature of these relationships, it was included in the models as a categorical variable. Due to lack of normality in the data (even after $\log_{10}$-transformations) we used generalized linear models (GLM) and generalized linear mixed effects models (GLMM) when appropriate, assuming gamma (with "identity" link function) error distributions, which yielded the lowest dispersion (determined using the "gamma.dispersion" function from the MASS package in R). Because the sample sizes were unbalanced between surveys, we computed the significance of model parameters via Likelihood Ratio Tests (LRT) using Type II sums of squares. We checked for homogeneity of variances by visual inspections of diagnostic plots of residuals vs. fitted data (R package *car*).

To determine whether SDIH and microhabitat use patterns varied among survey dates (i.e. temporal variability) at each site and year, we ran multiple regressions with date as an additional main factor. We did not combine data from different years to avoid

21

introducing variability due to unaccounted events (e.g. Bodega's population density was dramatically reduced in 2012). Similarly, to examine whether SDIH and microhabitat use patterns varied between sites (i.e. spatial variability), we ran multiple regressions with site as an additional main factor. We ran this comparison using data collected in 2012 because surveys at Strawberry Hill were only conducted that year.

To examine the relationships between SDIH and the five environmental drivers considered (both daily maxima and 75th percentile), we ran multiple regression analyses, where the slope of the regression lines between *Pisaster* intertidal height and wet weight (Table 2.1) was defined as the response variable, and all five drivers treated as independent variables. Similarly, we tested whether these drivers explained changes in the proportion of individuals found exposed during low-tide surveys using multiple logistic regression analyses, treating exposure (protected/exposed) as response and the five environmental drivers as independent variables. We observed collinearity between the explanatory variables air temperature and solar radiation (variance inflation factor > 10) (Quinn & Keough 2002) which is not surprising since the latter can often strongly drive the former. To avoid this issue, we ran the regressions twice, once including air temperature and excluding solar radiation, and vice versa.

Pisaster thermotolerance survival data for each size-class were fitted using logistic regression models estimated by generalized linear models with binomial error distributions. We determined LT_{50}s from these models, and contrasted them using a one-tailed z-score test (Quinn & Keough 2002).

The relationship between *Pisaster* relative performance after the desiccation treatment and body size was described by a 2-parameter asymptotic exponential model.

We used the asymptote in the fitted curve as reference marking the size at which individuals' *AC* was least affected by the desiccation treatment. Individuals performing < 1SE of the asymptote were regarded as significantly affected by desiccation.

To compare the temperature time series obtained from the robo-sea stars at different tidal elevations and microhabitat types, we calculated Mean Absolute Errors (MAE), and ran paired t-tests using daily maximum values. For each site, we defined the high intertidal exposed robo-sea star (expected to display the hottest temperatures) as the reference time series against which all other robo-sea stars were compared. Physiological implications of selecting each microhabitat were quantified based on a thermal sensitivity curve previously derived for *Pisaster* (Monaco et al. 2014). Specifically, using the thermal performance breadth parameter (i.e. temperature range where performance is ≥69% of maximum; Sharpe & DeMichele 1977), estimated to be 17.2-23.8°C, we calculated the percentage of time *Pisaster* would have spent below, above, and within that range at each microhabitat. Potential mortality effects of body temperature were evaluated based on cumulative survival curves described for each microhabitat, size class, and site. We calculated this using the logistic functions modeled from our size-dependent Thermotolerance Experiments, and the robo-sea stars' temperature records.

RESULTS

Pisaster intertidal distribution

Year-to-year changes in *Pisaster* demographics (density and size-frequency distribution) at Bodega Marine Reserve were marked. Because this is likely due to unaccounted population and community level phenomena such as massive invertebrate die-offs, presumably driven by harmful algal blooms, that took place in August 2011 (Rogers-

Bennett et al. 2012), we grouped the data by year and site, and examined temporal

dynamics occurring between survey dates. Overall, the patterns of size-dependent

intertidal distribution (i.e. the relationship between individuals' intertidal height and

refuge use, and body size) shown by *Pisaster* were highly variable (Figs. 1 and 2),

although some generalizations could be made. We provide specific findings below.

Table 2.1 shows the generalized linear model (GLM) regression coefficients for

the data collected during the different surveys. We surveyed the Bodega population three

times in 2010. Not surprisingly, most individuals were consistently found protected from

the elements either in crevices, tide pools, or under algae (Table 2.1). A logistic

regression analysis revealed that *Pisaster* refuge use (i.e. proportion of protected

individuals) was not affected by size (LRT, χ^2 = 0.2, df = 1, P > 0.05), although it did

vary among the three surveys (LRT, χ^2 = 34.8, df = 1, P < 0.01). While the first 2010

Bodega survey (2 June 2010) revealed no effect of size or refuge use on *Pisaster* shore

level, the second (16 June 2010) and third (28 June 2010) showed a negative relationship

between shore level and size, at least for those animals found in protected microhabitats.

In contrast, exposed individuals showed no significant relationship (Table 2.1; Fig. 2.1A-

C) in any of the three surveys. Additionally, a regression analysis to test the influence of

size, refuge use, and survey date on *Pisaster* shore level revealed the following: first, a

non-significant interaction between the effect of size and refuge use (i.e. parallel slopes)

(LRT, χ^2 = 1.7, df = 1, P > 0.05); and second, a significant effect of body size (LRT, χ^2 =

24.5, df = 1, P < 0.01) and refuge use on *Pisaster* shore level (LRT, χ^2 = 49.3, df = 1, P <

0.01), which did not change with survey date (LRT, χ^2 = 3.8, df = 1, P = 0.05) (Fig. 2.1A-

C). Thus, *Pisaster* shore level in the intertidal depended both on size and refuge use, and the pattern did not vary much among surveys conducted during the summer of 2010.

The Bodega population was surveyed 5 times in 2011. Again, most individuals were found protected from solar radiation (Table 2.1), and size had no significant effect on refuge use (LRT, $\chi^2 = 2.8$, df = 1, P > 0.05), although the proportion of exposed individuals varied among surveys (LRT, $\chi^2 = 7.9$, df = 1, P < 0.01). As for the 2010 survey, in 2011 we found that the relationship between shore level and size was conditioned by *Pisaster* refuge use. In four survey dates (19 May 2011, 15 June 2011, 1 July 2011, 14 July 2011), the slope of this regression was negative and significant for the protected individuals, and not different from zero for the exposed ones (Fig. 2.1D, F, G, H). In the remaining survey (4 June 2011), while protected animals exhibited no relationship between shore level and size, exposed individuals' size increased with intertidal elevation (Fig. 2.1E; Table 2.1). The regression analysis further confirmed that the slopes of the lines differed between protected vs. exposed groups (LRT, $\chi^2 = 7.1$, df = 1, P < 0.01), so we could not statistically compare their intercepts. However, a simple visual inspection of Figure 2.1D-H reveals exposed individuals occupying higher shore levels than protected ones with non-overlapping distributions. Additionally, a GLMM (with refuge use as random variable to remove its effect) showed that the relationship between shore level and size was weakly influenced by survey date (LRT, $\chi^2 = 4.0$, DF = 1, P = 0.045), indicating a slight effect of time on SDIH.

In the summer of 2012, the *Pisaster* population at Bodega had shrunk dramatically from 0.52 ± 0.03 ind. m^{-2} in 2011 to 0.08 ± 0.01 ind. m^{-2} (mean $\pm$ 1 SE). Possibly as a consequence, the total number of exposed sea stars was also reduced (Table

2.1). Because there were so few exposed individuals, we ran statistics for this year using

only data for protected individuals encountered. From the four surveys conducted, two

(22 May 2012, 20 June 2012) showed significant negative relationships between *Pisaster*

intertidal height and body size (Fig. 2.1I, K), and two (8 June 2012, 19 July 2012)

showed no relationship (Fig. 2.1J, L; Table 2.1). We ran a regression analysis to test for

statistical differences between the regressions described during each survey date. First,

despite having found significant slopes only for two of the regressions (Table 2.1), we

detected a non-significant interaction between the effect of size and refuge use (i.e.

parallel slopes) (LRT, $\chi^2 = 0.005$, df = 1, P > 0.05); and second, a significant effect of

survey date on sea stars' intertidal height (LRT, $\chi^2 = 16.4$, df = 1, P < 0.01) (Fig. 2.1I-L),

reflecting temporal variability.

In general, *Pisaster* intertidal distribution appeared less constrained at Strawberry

Hill than Bodega, as suggested by the broader and overlapping error bands (Figs. 2.1 and

2.2). Again, the majority of sea stars sampled were found protected (Table 2.1);

however, the proportion of protected individuals was lower than at Bodega, as revealed

by a GLM with site and survey date as main effects (LRT, $\chi^2 = 7.1$, df = 1, P < 0.01).

Also contrary to Bodega, at Strawberry Hill we found significant effects of size on

Pisaster refuge use (LRT, $\chi^2 = 8.3$, df = 1, P < 0.01). As for Bodega, the proportion of

protected individuals varied between surveys (LRT, $\chi^2 = 14.2$, df = 1, P < 0.01). From

the four Strawberry Hill surveys, the only significant regressions between individuals'

shore level and size were a negative and a positive relationship for the protected animals

from survey dates 05/24/2012 and 07/20/2012, respectively (Fig. 2.2A, 2.2C; Table 2.1).

A regression analysis to examine the variability of these regressions revealed significant

effects of both survey date (LRT, $\chi^2 = 4.5$, df = 1, P < 0.05) and individuals' refuge use

(LRT, $\chi^2 = 8.3$, df = 1, P < 0.01). Interestingly, the overall relationship between shore

level and size was positive (LRT, $\chi^2 = 4.0$, df = 1, P < 0.05), in contrast to the trend

observed at Bodega (Figs. 2.1 and 2.2; Table 2.1).

Overall, we found extensive evidence for the SDIH pattern, but only for animals

found protected. From the 16 surveys conducted, 13 showed negative relationships

between shore level and body size, nine of which were significant.

Foraging activity and distance to prey

We recorded foraging activity and distance to prey (i.e. closest mussel bed edge) for

Pisaster individuals sampled during the surveys conducted at Bodega in 2011 and 2012,

and Strawberry Hill in 2012. Although distance to prey was farther for individuals at

Strawberry Hill (mean ± SE; 256.66 ± 24.49 cm) than Bodega (mean ± SE; 75.27 ± 2.79

cm), the proportion of animals foraging was greater at the former (mean ± SE; 0.30 ±

0.02) than the latter (mean ± SE; 0.10 ± 0.02). These observations may account for the

higher proportion of exposed individuals observed at Strawberry Hill vs. Bodega (see

results in section *Pisaster intertidal distribution*).

Role of environmental drivers and how they translate to the organism

Contrary to our expectations, we found no overall relationship between any of the five

environmental variables evaluated (air temperature, solar radiation, seawater temperature,

wave height, wind speed) and the SDIH of *Pisaster* surveyed from Bodega. This was

true for both analyses, considering only protected or only exposed individuals (Appendix

A). With regard to refuge use, although the proportion of individuals found exposed was

consistently low (Table 2.1), a slight but significant decrease in the proportion of animals

exposed could be attributed to increases in both air temperature (Fig. 2.4A; LRT, χ^2 = 22.5, df = 1, P < 0.01) and solar radiation (Fig. 2.4B; LRT, χ^2 = 12.8, df = 1, P < 0.01) during the day prior to our field population surveys. While the model that included solar radiation as an independent variable did not detect an effect of seawater temperature on *Pisaster* exposure (Fig. 2.4C; LRT, χ^2 = 1.9, df = 1, P > 0.05), the model that considered air temperature revealed a positive influence (Fig. 2.4C; LRT, χ^2 = 4.3, df = 1, P < 0.05). We detected no relationship between proportion of *Pisaster* in refuge and the environmental drivers wave height (Fig. 2.4D; LRT, χ^2 = 0.48, df = 1, P > 0.05), or wind speed (Fig. 2.4E; LRT, χ^2 = 0.07, df = 1, P > 0.05).

Because ectothermic organisms' body temperatures are driven by multiple environmental variables of which ambient air temperature is but one (Broitman et al. 2009, Helmuth 2002), we further examined the influence of maximum temperatures recorded by robo-sea stars (which provide a closer estimate of the animal's body temperature) one day prior to the surveys. When looking for the effect of these potential body temperatures measured by robo-sea stars deployed at low, mid, and high intertidal heights on SDIH, as measured by the regression slopes in Table 2.1, we again found no significant relationships (LRT; P > 0.05 in all cases). However, as with air temperature measured by the weather station, we observed a positive association between temperatures recorded by robo-sea stars deployed at low intertidal heights and *Pisaster* refuge use on the next day (Fig. 2.4A; LRT, χ^2 = 10.2, df = 1, P < 0.01) and mid (Fig. 2.4B; LRT, χ^2 = 17.2, df = 1, P < 0.01). Although the high intertidal robo-sea star was weakly negatively associated with the proportion of protected individuals (Fig. 2.4C), the effect was non-significant (LRT, χ^2 = 0.2, df = 1, P > 0.05). Additionally, note that the

maximum potential body temperatures reached higher values than maximum air

temperatures (Fig. 2.3A vs. 2.4).

Size-dependent tolerance to thermal and desiccation stress

Large *Pisaster* individuals showed a significantly higher median lethal temperature

(LT_{50}) than small animals (mean ± SE; large = 33.3 ± 0.9 ˚C; small = 31.6 ± 0.5 ˚C; z = -

1.76; P = 0.04) (Fig. 2.5).

The effect of wind (and hence desiccation) on the activity coefficient of *Pisaster*

depended on individual size (Fig. 2.6). According to 2-parameter asymptotic exponential

model fitted, animals smaller than 105.8g significantly reduced performance below 1SE

of the estimated asymptote after exposure to continuous wind during simulated low tide

periods. From the 19 individuals larger than 105.8g treated, only four (21.1%) reduced

their activity coefficient below that threshold.

Robo-sea star temperature records

Pisaster body temperatures, as determined using robo-sea stars, showed variable patterns

among sites. Most of the observed variability can be attributed to periods when robo-sea

stars were aerially exposed during low tides. Figure 2.7 shows temperatures recorded at

Strawberry Hill and Bodega, in three exposed (high, mid, and low intertidal) and two

protected (crevice and tide pool) microhabitats. At both sites the high-intertidal robo-sea

star temperatures were consistently higher (paired t-tests, P < 0.01 in all cases) and more

variable (F-tests, P < 0.01 in all cases, except for the low-intertidal and tide pool robo-sea

stars at Strawberry Hill) than the other microhabitats considered. However, note that

MAE and variance ratios were greater at Bodega than Strawberry Hill (Fig. 2.7),

suggesting that the choice between contrasting microhabitats is more important for

Pisaster at the former site. Also, based on MAEs between microhabitats, we found that for Strawberry Hill the coolest microhabitats were crevices, and at Bodega either low intertidal, crevices, or tide pools (Figure 2.7). As a caveat, the relatively high temperatures recorded by low intertidal and tide pool robo-sea stars at Strawberry Hill is likely explained by their specific location: the former received more solar radiation than the rest, and the latter was in a rather shallow pool and may have not been always covered.

Between-site variations in temperature patterns were also observed. For exposed microhabitats, both mean and variance in daily maximum temperatures were greater at Bodega than Strawberry Hill. For example, high intertidal temperatures at Bodega were $22.5 \pm 0.6°C$, vs. $19.9 \pm 0.5°C$ (mean $\pm$ 1SE) at Strawberry Hill. For protected microhabitats, in turn, variance was higher at Strawberry Hill than Bodega, although the mean temperatures were still higher at Bodega. For example, this was observed for crevices, where temperatures were $13.4 \pm 0.2°C$ at Bodega, and $12.8 \pm 0.3°C$ (mean $\pm$ 1SE) at Strawberry Hill.

Physiological consequences

With regards to the potential physiological consequences of occupying different microhabitats, we found that the percentage of time spent at temperatures above the thermal performance breadth ($>23.8°C$) was minimal: $<5\%$ in every case (Table 2.2). However, note that at least for mid and high intertidal microhabitats, *Pisaster* at Bodega would have experienced slightly more time above this threshold than at Strawberry Hill. The proportion of time spent within the thermal performance breadth (17.2-23.8°C) was also low ($<5\%$) for every microhabitat, except the high intertidal at Strawberry Hill and

Bodega, reaching values of 7.51 and 6.45%, respectively. As a corollary, for all

microhabitats at both sites, *Pisaster* was estimated to have spent most of the time (>90%)

at body temperatures markedly lower than the optimal thermal performance breadth

(<17.2°C) (Table 2.2, Fig. 2.7).

Survival probability

Our survival analysis revealed that for the time window evaluated, the cumulative

probability of survival was markedly high at both sites, and for both size classes (Fig.

2.8). Only the high intertidal zone at Bodega showed potentially risky conditions for

large and small *Pisaster*, for which final cumulative survival was 0.87 and 0.59

respectively (Fig. 2.8B,D).

DISCUSSION

A growing body of literature has demonstrated that simplistic assumptions about

individuals' habitat can be misleading when trying to accurately establish relationships

between the physical environment and the organism (Helmuth 2002, Kearney 2006,

Wethey 1983). In many instances observed differences in conditions among

microhabitats can exceed those over large geographic scales (Denny et al. 2011).

Furthermore, as individuals' fitness results from the conditions experienced cumulatively

throughout ontogeny, earlier studies have encouraged considering all size classes in order

to better predict the impacts of combined climatic and non-climatic variables on natural

systems (Manzur et al. 2010). Here we explicitly tested these generalizations using a

mobile rocky intertidal predator, the sea star *Pisaster ochraceus*. Specifically, we

examined dynamics in *Pisaster* patterns of size-dependent microhabitat use, evaluated the

role of environmental variables and size-dependent sensitivity to desiccation and

temperature stress, and explored potential ecophysiological consequences of microhabitat use in *Pisaster*.

Pisaster intertidal distribution

As has been reported previously (Feder 1956, Fly et al. 2012), we observed evidence of size-dependent intertidal height in *Pisaster*, with larger individuals found lower on the shore. We found this in 2/3 of surveys of protected animals, but not for exposed animals. We additionally found that this pattern varied both temporally and geographically (Figs. 2.1 and 2.2; Table 2.1). Given that this species can travel several meters during high tide periods (Robles et al. 1995), it is not surprising that its distribution patterns changed over time. Interestingly, when considering the shifts in SDIH occurring between surveys (within years) (Table 2.1), the bulk of the variation seems driven by vertical displacements of larger size animals, whereas smaller individuals tend to remain at relatively fixed heights (Figs. 2.1 and 2.2). We speculate that two main elements determine such a phenomenon. First, our preliminary unpublished data suggests that, while submerged during high tide, larger *Pisaster* are more active and travel faster than small individuals. Second, *Pisaster* is known for avoiding physical stressors by seeking protection before low tide (Garza & Robles 2010, Robles et al. 1995); however, because larger animals cannot benefit from small crevices, as smaller individuals might, they are often forced to move towards the milder subtidal zone. As a result, the pattern of SDIH emerges only for animals found sheltered. In contrast, because exposed animals are presumably not seeking refuge, they do not exhibit SDIH. Since *Pisaster* generally requires leaving its refuge to reach a higher mussel bed and forage (Garza & Robles

2010, Paine 1974, Robles et al. 1995), which occurs regardless of body size, one can expect an absence in the SDIH pattern for exposed sea stars, as we observed here.

As expected based on previous research (Burnaford & Vasquez 2008, Fly et al. 2012, Pincebourde et al. 2008), most *Pisaster* individuals surveyed were found in microhabitats protected from the elements (Table 2.1), which reinforces the idea that this species favors avoiding physical stressors characteristic of low tide periods (Garza & Robles 2010, Robles et al. 1995). Microhabitat use varied substantially between survey dates and sites (relatively more exposed sea stars at Strawberry Hill than Bodega) (Table 2.1). Notably, however, while *Pisaster* size had no effect on microhabitat use at Bodega, at Strawberry Hill we observed a negative relationship between proportion of protected individuals and size (Results section *Pisaster intertidal distribution*). The observation that sea stars were generally more exposed at Strawberry Hill than Bodega could be due to mussel bed patches being more scattered at the former site; where Strawberry Hill is characterized by a number of large rock outcrops and high substratum heterogeneity, Bodega is a more or less gently sloping bench with comparatively less topographic complexity. This in turn is possibly a consequence of the higher predation pressure imposed by a dense population of *Pisaster* at Strawberry Hill (Results section *Foraging activity and distance to prey*). Also, we suggest that the negative relationship between size and refuge use at Strawberry Hill may be explained in part by the lower availability of mussels, and in part by the greater difficulties encountered by larger *Pisaster* in finding refuges.

Foraging activity and distance to prey

Although *Pisaster* at Strawberry Hill were on average farther from the closest mussel bed edge, they were eating more than *Pisaster* at Bodega. We also observed higher *Pisaster* density at Strawberry Hill than Bodega. These observations prompt the hypothesis that higher predation pressure at Strawberry Hill, driven by increased *Pisaster* density, has contributed (in concert with the presence of rock outcrops) to increased spacing between mussel beds to a point where sea stars are forced to cover greater distances to forage. These observed patterns, in turn, may explain why individuals are more exposed at Strawberry Hill, as well as why we observed a positive relationship between size and proportion of exposed animals at this site alone. As mentioned above, securing refuge may be harder for larger animals. For large *Pisaster*, foraging implies moving up the shore to capture prey and externally digest, and down to find a refuge again, so greater distances to mussel beds imply higher likelihood of being stranded at an exposed microhabitat once the tide is low. Of course this will have an impact on both body temperature and physiological condition, which we address below.

Role of environmental drivers and how they translate to the organism

Knowing that the patterns of *Pisaster* size-dependent distribution vary, the question then becomes: what, if anything, are the role of environmental drivers? We examined two aspects that define *Pisaster* distribution, the slopes of the regressions between intertidal height and size (i.e. SDIH), and refuge use (i.e. exposed/protected). We found no association between SDIH and any of the variables measured by the on-site sensor station (air temperature, solar radiation, seawater temperature, wind speed, and wave height), within the range of conditions during the study period (Appendix A). Our data, however,

showed that the proportion of individuals found in refugia was positively affected by air temperature and solar radiation (Fig. 2.3).

Both air temperature and solar radiation have long been recognized as important drivers of species' physiological and behavioral responses (Burnaford & Vasquez 2008, Jones & Boulding 1999). For ectotherms, both variables are important drivers of an organism's heat budget (Helmuth 1998), and hence body temperature; however, since their signal may be obscured by simultaneous changes in other variables affecting heat flows (some of which we addressed here) (Helmuth 2002), it seemed likely more informative to evaluate the effect of body temperatures measured *in situ* using biomimetic loggers (Szathmary et al. 2009). This approach, nevertheless, yielded results that paralleled our findings based on weather station measurements. Namely, although increases in body temperature recorded by robo-sea stars did not affect observed SDIH patterns, they were positively correlated with the number of individuals found protected (Fig. 2.4A,B). The lack of a relationship between proportion of protected individuals and biomimic temperatures measured in the upper (high) intertidal zone (Fig. 2.4C) reveals that individuals' response to changes in temperature is tightly dependent on the conditions truly experienced by the organism. Since few *Pisaster* were observed at high elevations, our high intertidal temperature measurements did not necessarily reflect the real conditions experienced by sea stars, and therefore might not be expected to drive their behavioral response. Lastly, the fact that temperature maxima recorded by robo-sea stars were higher than air temperatures measured by the weather station (Fig. 2.3A vs. 2.4), points to the relevance of solar radiation in raising *Pisaster* body temperature during low tide.

Body temperatures across microhabitats and potential consequences

On a hot day, the rocky intertidal can potentially offer a wide array of physical conditions that *Pisaster* may have to cope with. By discriminating between exposed and protected microhabitats, and recording potential body temperatures using robo-sea stars, we have captured some of the thermal variability (Fig. 2.7). Not surprisingly, exposed *Pisaster*, especially in the mid and high intertidal, are subjected to higher temperatures and greater variability than protected individuals. But how would this affect *Pisaster* physiological state? It is long known that body temperature regulates physiological rates and fitness (Hochachka & Somero 2002), but because of the asymmetric nature of organisms' thermal response, the effect is often difficult to assess (Martin & Huey 2008). One way of quantifying the cumulative impact of temperature on organisms' physiological condition is by means of a thermal performance curve (Monaco & Helmuth 2011). Plugging the temperature time series collected at the different microhabitats into a thermal performance curve derived by Monaco et al. (2014) revealed that, although the high intertidal may offer conditions that would allow relatively high physiological performance (Fig. 2.7), *Pisaster* is selecting for cool microhabitats (Table 2.1) conducive to low performance (Table 2.2). Such a response where organisms appear to behaviorally select for temperatures below their optimum has been widely documented for both marine and terrestrial ectotherms (e.g. Martin & Huey 2008, Tepler et al. 2011). Counterintuitively, one possible explanation for this suboptimal behavior is based on a fitness maximization criterion. The concept of "sub-optimal is optimal" (Martin & Huey 2008) maintains that ectotherms select temperatures lower than those that yield the highest fitness based on: (1) the negatively skewed shape of a thermal performance curve,

including that of *Pisaster* (Monaco et al. 2014), and (2) the fact that ectotherms are imperfect thermoregulators. A negatively (left) skewed curve means that, if field body temperatures are close to or at optimal, an increase in body temperature (to the right) generates a greater depression in performance than a decrease in temperature by the same amount. Accordingly, given the high thermal heterogeneity in the rocky intertidal, selecting for cool and thermally homogeneous microhabitats (e.g. crevices) may grant *Pisaster* a higher cumulative fitness than what can be expected from warmer (seemingly more profitable) microhabitats (e.g. exposed high intertidal) through the avoidance of rare but potentially very damaging extreme temperatures. A second, non-exclusive explanation considers the risk-probability of reaching lethal body temperatures. Thus, besides increasing performance, favoring protected microhabitats (Table 2.1) where conditions are cooler and homogeneous (Fig. 2.7), would protect *Pisaster* against reaching upper critical temperatures, typically slightly warmer than organisms' optimal temperature (Martin & Huey 2008). Indeed, our survival analysis revealed that during the period of the study, *Pisaster* cumulative probability of survival with respect to body temperatures was clearly high for all microhabitats where individuals are actually encountered (Fig. 2.8).

It is often assumed that intertidal organisms live very close to their thermal tolerance limits (Denny et al. 2011, Jones et al. 2009, Stillman 2002) but see Mislan et al. 2014). However, given *Pisaster*'s preference for cool microhabitats (Table 2.1), our analysis suggests that this is not true for this predatory sea star. As increasingly demonstrated by studies documenting thermoregulatory behavior in intertidal species (Iacarella & Helmuth 2012, Muñoz et al. 2005, Pincebourde et al. 2009), only

comprehensive approaches that consider the interaction of potential body temperature and ecophysiological performance will truly reveal how close to their limits organisms are.

Between-site comparisons showed that *Pisaster* at Strawberry Hill would have experienced temperatures above thermal performance breadth for less time than at Bodega (Table 2.2). Although the difference seems negligible, it does suggest that the potential risk associated with thermal stress at Strawberry Hill is lower. This reduced cost, along with the fact that distance to prey is greater at Strawberry Hill, may help explain the higher proportion of exposed individuals observed there, relative to Bodega (Table 2.1). Note that Strawberry Hill is usually regarded as a hotter site because the timing of low tide is closer to noon than lower latitude sites. Although our body temperature data did not conform to that expectation, longer records may detect such a trend.

Our measurements of potential body temperature coupled with regular observations of microhabitat use provide a unique perspective of this model system, which had not been explored before. Although we knew *Pisaster* preferentially seeks protected microhabitats, there are no previous accounts of what this means in terms of body temperature at a population level. We showed not only that *Pisaster* body temperature can be far from the air temperature recorded by a weather station (Broitman et al. 2009, Pincebourde et al. 2009, Szathmary et al. 2009), but also that refuge-seeking behavior can strongly buffer the conditions experienced by individuals (Kearney et al. 2009, Marshall et al. 2013). This is especially important when trying to predict population dynamics in response to environmental pressure driven, for example, by ENSO events or ongoing climate change (Helmuth et al. 2005).

Size-dependent tolerance to thermal and desiccation stress

Contrary to our expectation and previous literature (Peck et al. 2009, Pörtner 2002), we found that upper critical temperature (LT_{50}) is higher for the large size-class of *Pisaster* (Fig. 2.5). Similarly, although we expected no effect of size on *Pisaster* sensitivity to wind stress based on previous desiccation experiments (Landenberger 1969), results revealed that the performance of smaller individuals was strongly reduced, in comparison to larger animals, following realistic exposures to wind stress (Fig. 2.6). The latter finding matches biophysical predictions based on surface-area to volume ratio considerations (Allen et al. 2012, McQuaid 1982).

As such, neither of these results would explain the presence of larger animals lower on the shore. However, when considered in concert with our data of body temperature and microhabitat use, these results provide an alternative perspective that may better characterize the system. Although we observed an effect of body size on the intertidal height of *Pisaster*, it was only evident for individuals found in refugia. Furthermore, we found no relationship between body size and refuge use. These findings reveal that, regardless of body size, sea stars are securing protected microhabitats. However, because larger animals are often found lower on the shore, the strategy seems to differ between size classes. We suggest that larger *Pisaster* find refuge more easily lower on the shore, as opposed to small individuals who may benefit from a wider array of large and small features on the rock surface, including nooks and crevices, or even biogenic material provided for instance by mussel reefs or algae (Bertness et al. 1999, Cartwright & Williams 2012, Garrity 1984, Jones & Boulding 1999). This idea is further supported by observations of refuge use in relation to shore level. Indeed, we found

negative relationships between the probability of finding *Pisaster* individuals sheltered in refuges and their intertidal height at Strawberry Hill (Fig. 2.9A) and Bodega (Fig. 2.9B).

Altogether, our data are consistent with the observation discussed by Vermeij (1972) that, as a low intertidal organism, *Pisaster* exhibits a reduction in body size with shore level; however, negative biotic interactions do not appear to drive the pattern. As argued by Raffaelli and Hughes (1978), the shore-level size gradient shown by *Pisaster* might be better explained by the availability of proper refuges. Because most individuals are found in protected microhabitats (Table 2.1), among which potential body temperatures are quite similar (Fig. 2.7), conditions experienced between size classes are ultimately very similar. Thus, as long as suitable microhabitats are available, the refuge-seeking strategy exhibited by *Pisaster* (Garza & Robles 2010, Robles et al. 1995) is not dependent on size.

Conclusions

Pisaster size-dependent distribution, in terms of intertidal height and refuge use, varied with time and between sites. While the physical environment (notably air temperature and solar radiation) may have played an important role in driving sea stars' movement between protected and exposed microhabitats, we found no relationship between *Pisaster* SDIH and the environmental variables examined. As reported elsewhere, *Pisaster* follows a risk-avoiding strategy by favoring protected microhabitats, which we showed is not influenced by body size. Furthermore, given our observation that potential impacts of temperature on physiological condition and cumulative survival are minimal, such a strategy does not seem to obey immediate responses to prevailing conditions. Instead, our observation that individuals' responses to changes in body temperature were delayed

by one day supports the idea that *Pisaster* can behaviorally thermoregulate, but not perfectly (Martin & Huey 2008). Because vertical movements seemed primarily controlled by larger individuals, different sized *Pisaster* seem to vary in their ability to find refuge across the intertidal. While small animals may find protection easily in the mid-intertidal, large sea stars may need to seek protection lower on the shore. As such, the negative relationship between intertidal height and *Pisaster* size (i.e. SDIH) results from (1) a preference for cool, homogeneous microhabitats, and (2) the difficulties for large individuals to secure refuge within those microhabitats at higher vertical levels. Contrary to our expectations, the nominal difference in LT_{50} between size classes and the fact that wind stress has a greater effect on small individuals, suggest that size-dependent sensitivity to these stressors does not provide an explanation for their distribution patterns.

Additionally, their behavioral response appears subjected to local conditions of food availability. At Strawberry Hill, where *Pisaster* needs to travel farther for prey, the likelihood of being exposed during low tide is greater than at Bodega. Although this would presumably increase potential risks, our data show that sea stars actually forage more at Strawberry Hill. Indirect assessments of physiological condition reveal no major reductions in relative performance for animals from this site, in comparison to Bodega, where mussel prey is more readily available. Altogether, this supports the hypothesis that microhabitat selection by *Pisaster* is not triggered by a search for optimal, but for suboptimal physical conditions. Given the heterogeneous nature of the rocky intertidal, where extremes may be common, such a risk-avoiding strategy stands as a plausible adaptation.

41

Table 2.1 *Pisaster* size-dependent distribution surveys' information. Regression lines were fitted using GLM (gamma error distribution). Shaded rows represent protected groups. NaN (i.e. not a number) indicates that the parameter could not be calculated because no individual was found in that group. P-values < 0.05 or < 0.01 are followed by one or two * symbols, respectively.

Site/ Survey date	Microhabitat	N	% at Microhabitat	Slope Mean ± SE	P-value
Strawberry Hill					
05/24/2012	Protected	49	62.82	-0.147 ± 0.021	0.008**
	Exposed	29	37.18	0.089 ± 0.059	0.129
06/22/2012	Protected	37	71.15	0.091 ± 0.061	0.205
	Exposed	15	28.85	0.019 ± 0.070	0.789
07/20/2012	Protected	49	63.64	0.126 ± 0.052	0.042*
	Exposed	28	36.36	-0.022 ± 0.044	0.659
08/03/2012	Protected	66	92.96	0.027 ± 0.037	0.518
	Exposed	5	7.04	0.181 ± 0.179	0.246
Bodega					
06/02/2010	Protected	198	71.22	-0.021 ± 0.015	0.156
	Exposed	80	28.78	-0.003 ± 0.025	0.908
06/16/2010	Protected	234	84.78	-0.054 ± 0.012	0.000**
	Exposed	42	15.22	-0.015 ± 0.023	0.488
06/28/2010	Protected	267	88.41	-0.023 ± 0.009	0.010**
	Exposed	35	11.59	-0.004 ± 0.016	0.791
05/19/2011	Protected	107	74.31	-0.058 ± 0.022	0.007**
	Exposed	37	25.69	0.015 ± 0.039	0.713

06/04/2011	Protected	110	77.46	-0.004 ± 0.023	0.871
	Exposed	32	22.54	0.072 ± 0.024	0.004**
06/15/2011	Protected	153	82.26	-0.046 ± 0.015	0.003**
	Exposed	33	17.74	0.052 ± 0.050	0.314
07/01/2011	Protected	160	87.91	-0.062 ± 0.017	0.000**
	Exposed	22	12.09	-0.046 ± 0.123	0.713
07/14/2011	Protected	139	83.23	-0.055 ± 0.017	0.001**
	Exposed	28	16.77	0.015 ± 0.028	0.595
05/22/2012	Protected	37	100.00	-0.027 ± 0.010	0.010*
	Exposed	0	0	NaN	NaN
06/08/2012	Protected	19	100.00	-0.003 ± 0.012	0.804
	Exposed	0	0	NaN	NaN
06/20/2012	Protected	21	84.00	-0.023 ± 0.012	0.034*
	Exposed	4	16.00	0.040 ± 0.025	0.248
07/19/2012	Protected	20	90.91	-0.014 ± 0.013	0.304
	Exposed	2	9.09	NaN	NaN

Table 2.2 Potential physiological consequences for *Pisaster* of occupying different microhabitats. Data represents percentage of time experiencing potential body temperatures (as measured by robo-sea stars) that fall below (<17.2˚C), within (17.2-23.8˚C), and above (>23.8˚C) *Pisaster* thermal performance breath (69% of maximum performance). Thermal performance breath was determined from a performance curve empirically derived by Monaco et al. (2014).

Site	Microhabitat	% Below (<17.2˚C)	% Within (17.2-23.8˚C)	% Above (>23.8˚C)
Strawberry Hill	High intertidal	91.33	7.51	1.19
	Mid intertidal	98.88	1.12	0.00
	Low intertidal	97.77	2.20	0.03
	Crevice	100.00	0.00	0.00
	Tide pool	97.76	1.99	0.25
Bodega	High intertidal	90.99	6.45	2.56
	Mid intertidal	98.82	1.05	0.13
	Low intertidal	99.97	0.03	0.00
	Crevice	99.92	0.08	0.00
	Tide pool	100.00	0.00	0.00
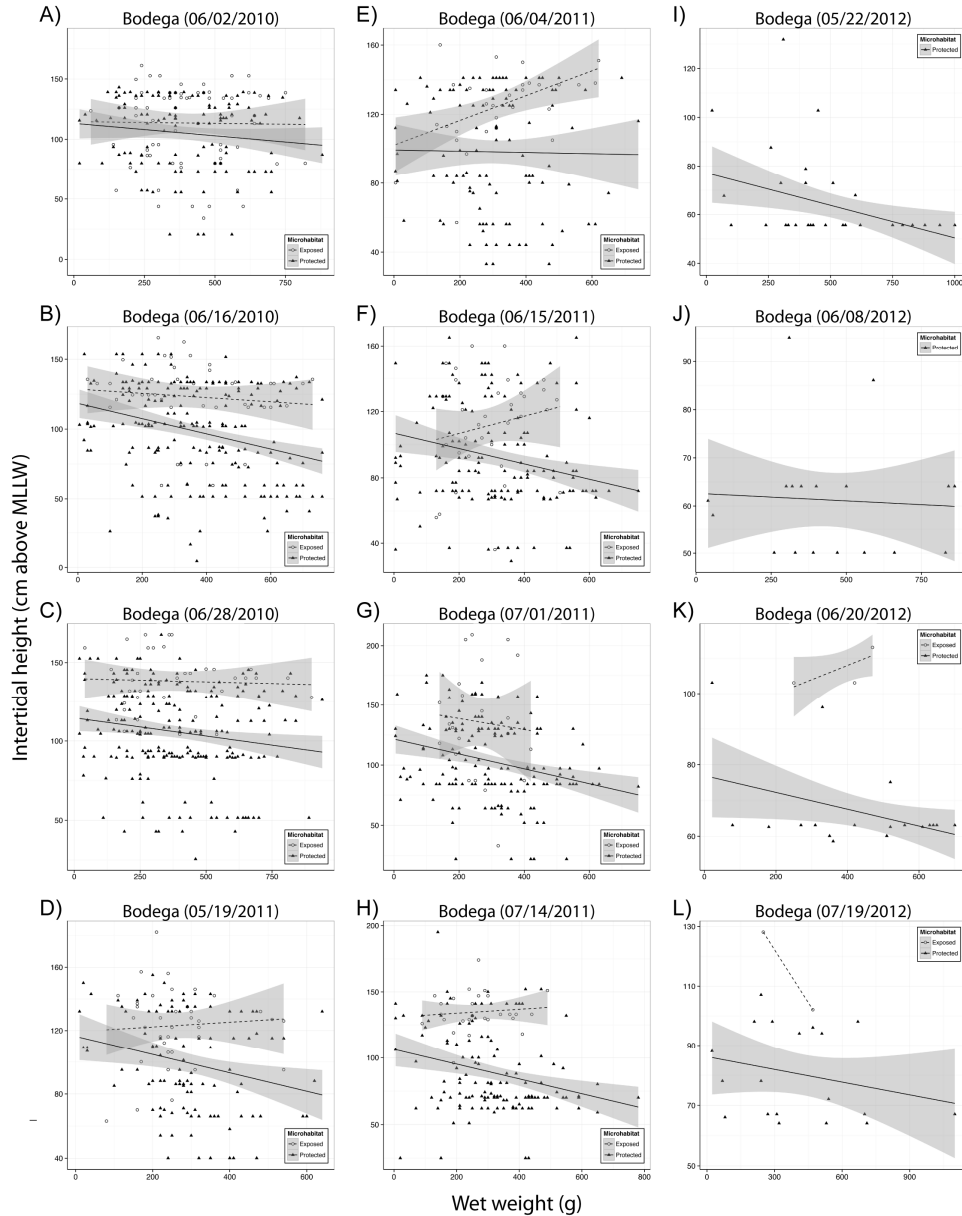
Figure 2.1 Relationships between *Pisaster* intertidal height (cm) and body size (wet weight) for the surveys conducted during different tide periods at Bodega. Data were grouped as protected or exposed, depending on whether individuals were protected from direct heat and solar radiation. Regression lines and standard errors (shaded areas), as estimated by GLM (with gamma error distribution), are provided. Panels A through C show data from surveys performed in 2010, D through H data from 2011, and I through L data from 2012.
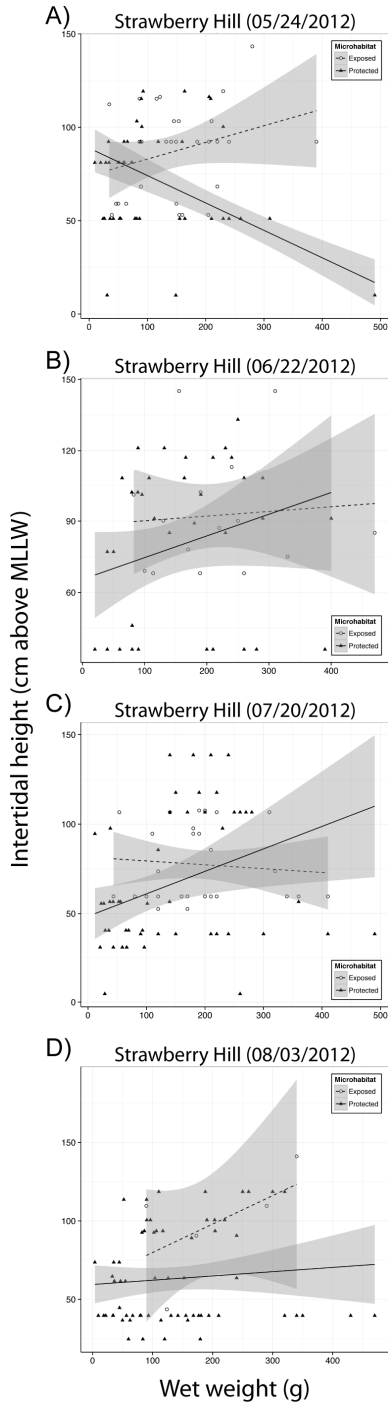
Figure 2.2 Relationships between *Pisaster* intertidal height (cm) and body size (wet weight) for the surveys conducted during different tide periods at Strawberry Hill. Data were grouped as protected or exposed, depending on whether individuals were protected from direct heat and solar radiation. Regression lines and standard errors (shaded areas), as estimated by GLM (with gamma error distribution), are provided. Panels A through D show data from surveys performed in 2012.
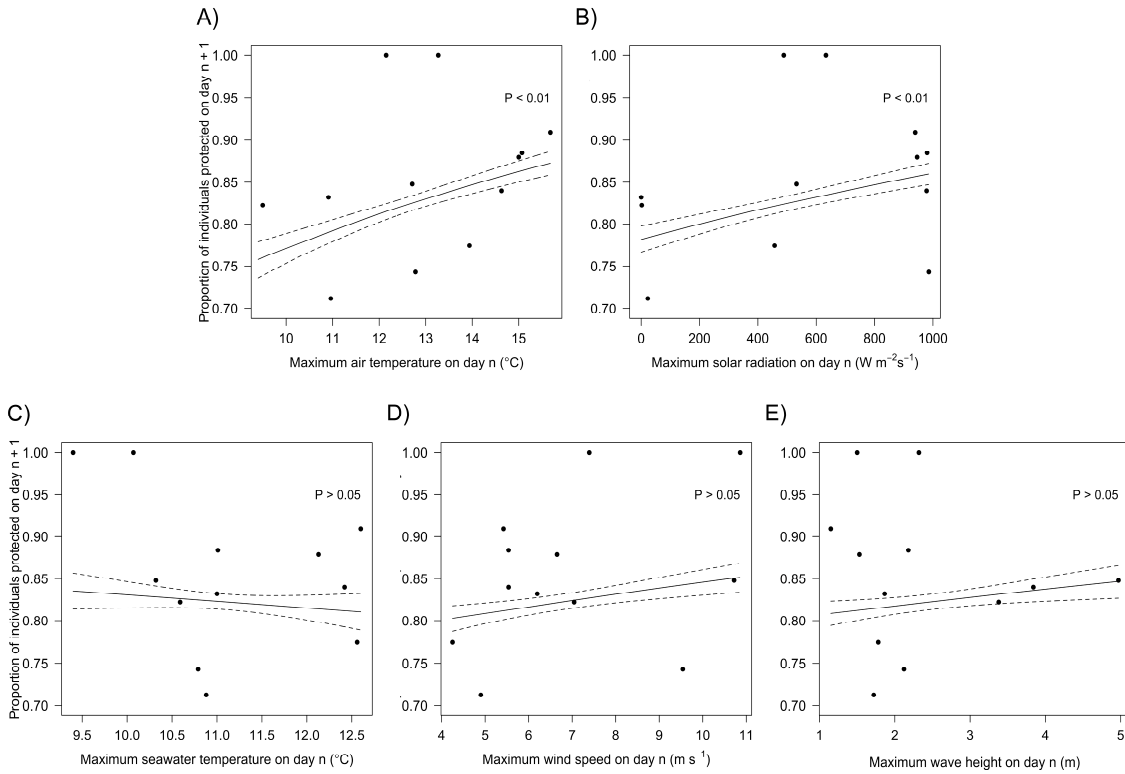
Figure 2.3 Proportion of *Pisaster* individuals protected in refuges on day n+1 vs. relevant environmental variables on day n: (A) air temperature, (B) solar radiation, (C) sea water temperature, (D) wave height, and (E) wind speed. Proportions were calculated for each survey conducted at Bodega. Raw data for environmental variables was retrieved from BOON weather station. For this figure we used the daily maximum values. The lines represent logistic regression fits ± 1SE.
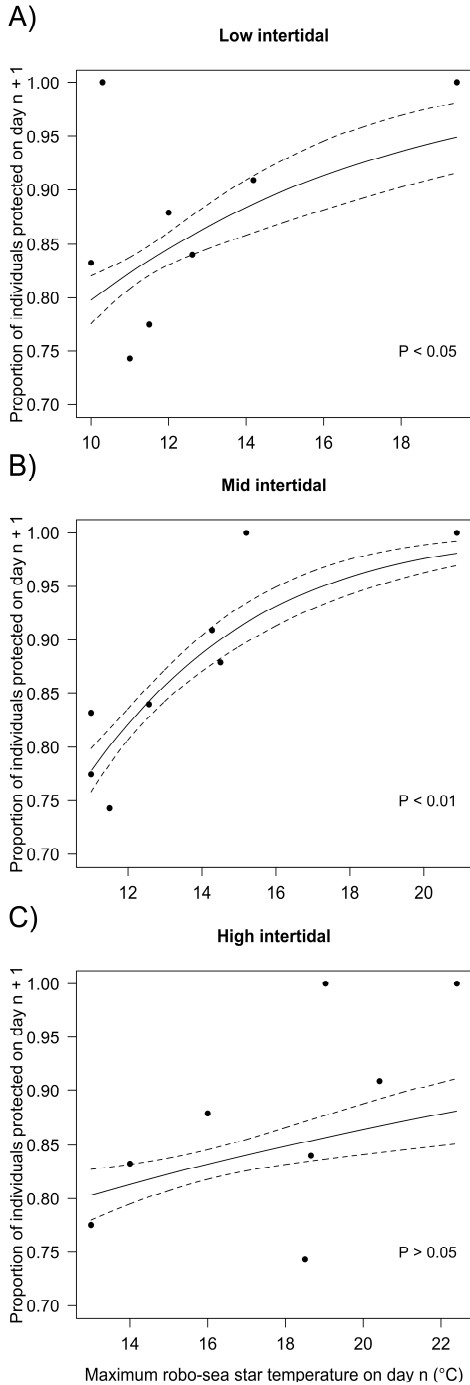
Figure 2.4 Proportion of *Pisaster* individuals protected in refuges on day n+1 vs. potential maximum body temperatures at day n experienced at three intertidal heights: (A) low, (B) mid, and (C) high (0, 1, and 1.5 m above MLLW, respectively). Data were collected at Bodega in 2011 and 2012. Temperatures were recorded using robo-sea stars. The lines represent logistic regression fits ± 1 SE.
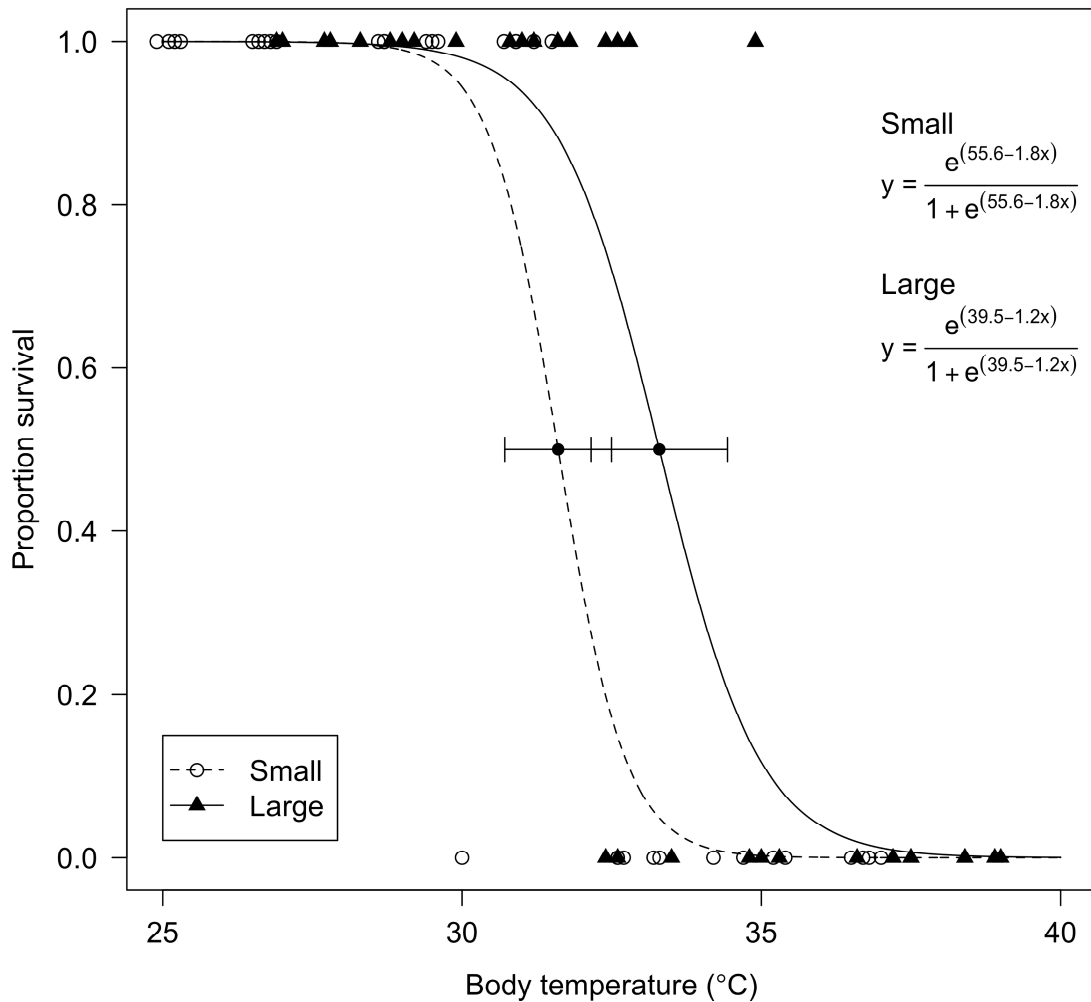
Figure 2.5 Proportion of *Pisaster* individuals surviving to a series of aerial body temperature treatments. Lethal temperatures were experimentally determined for two size classes, small (25 to 75g, N=34) and large (250-400g, N=33), by fitting independent logistic regression curves. The body temperatures ($\pm$ SE) at which 50% of individuals die (i.e. LT_{50}) are indicated by black dots on each logistic regression line. The logistic model equations for each size class, and their estimated parameter values, are also provided.
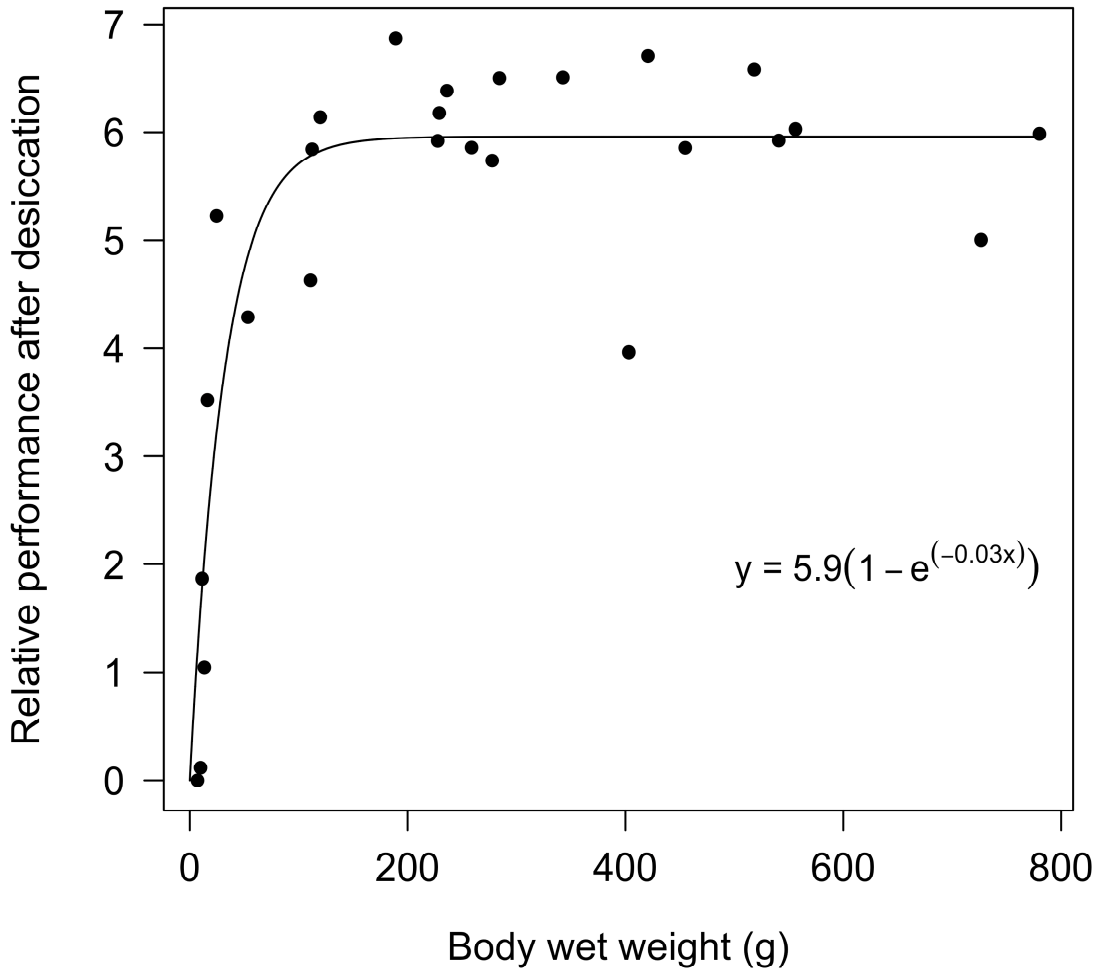
Figure 2.6 *Pisaster* relative performance after three days experiencing simulated 6-h low tide periods with 3-4 m s^{-1} wind speeds, in relation to body size (7.1 to 780.1g, N=26). A 2-parameter asymptotic exponential model was fitted to explore the trends. The equation and estimated parameters are also provided.
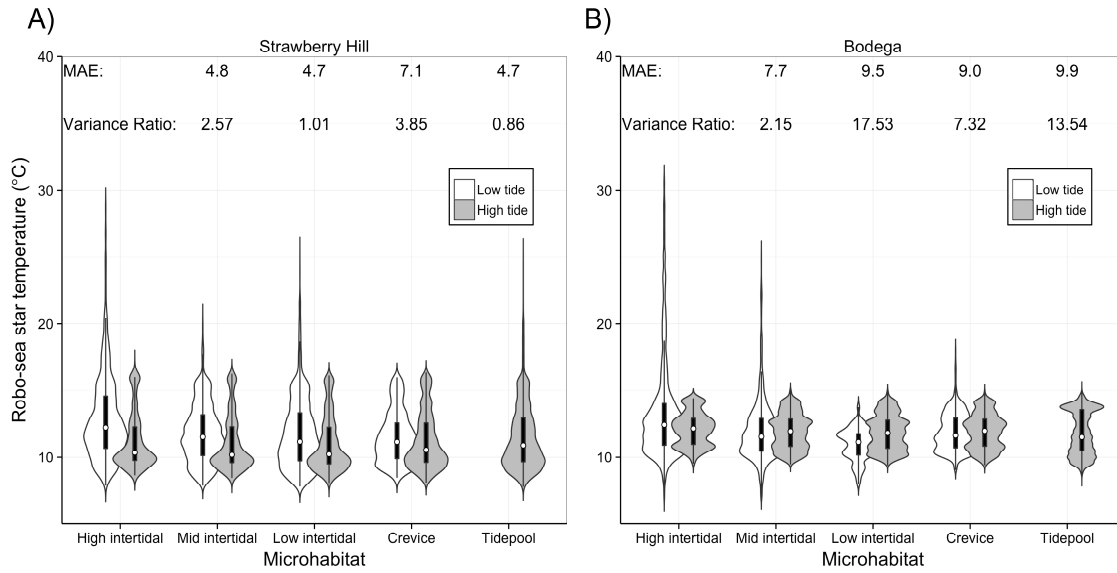
Figure 2.7 *Pisaster* body temperatures recorded by robo-sea stars (15-min sampling frequency) deployed on five different microhabitats at (A) Strawberry Hill and (B) Bodega between 06/22/12 and 08/10/12. High, mid, and low intertidal are exposed, while crevice, and tide pool are protected. Data are provided as violin plots with box-plots embedded. For each microhabitat, data were split between measurements taken while loggers were exposed to air (white) or submerged under water (gray). Comparisons between daily maxima temperatures of each microhabitat and the high intertidal (reference) were made based on Mean Absolute Errors (MAE) and variance ratios are given. These were calculated for each microhabitat without discriminating between tide periods.
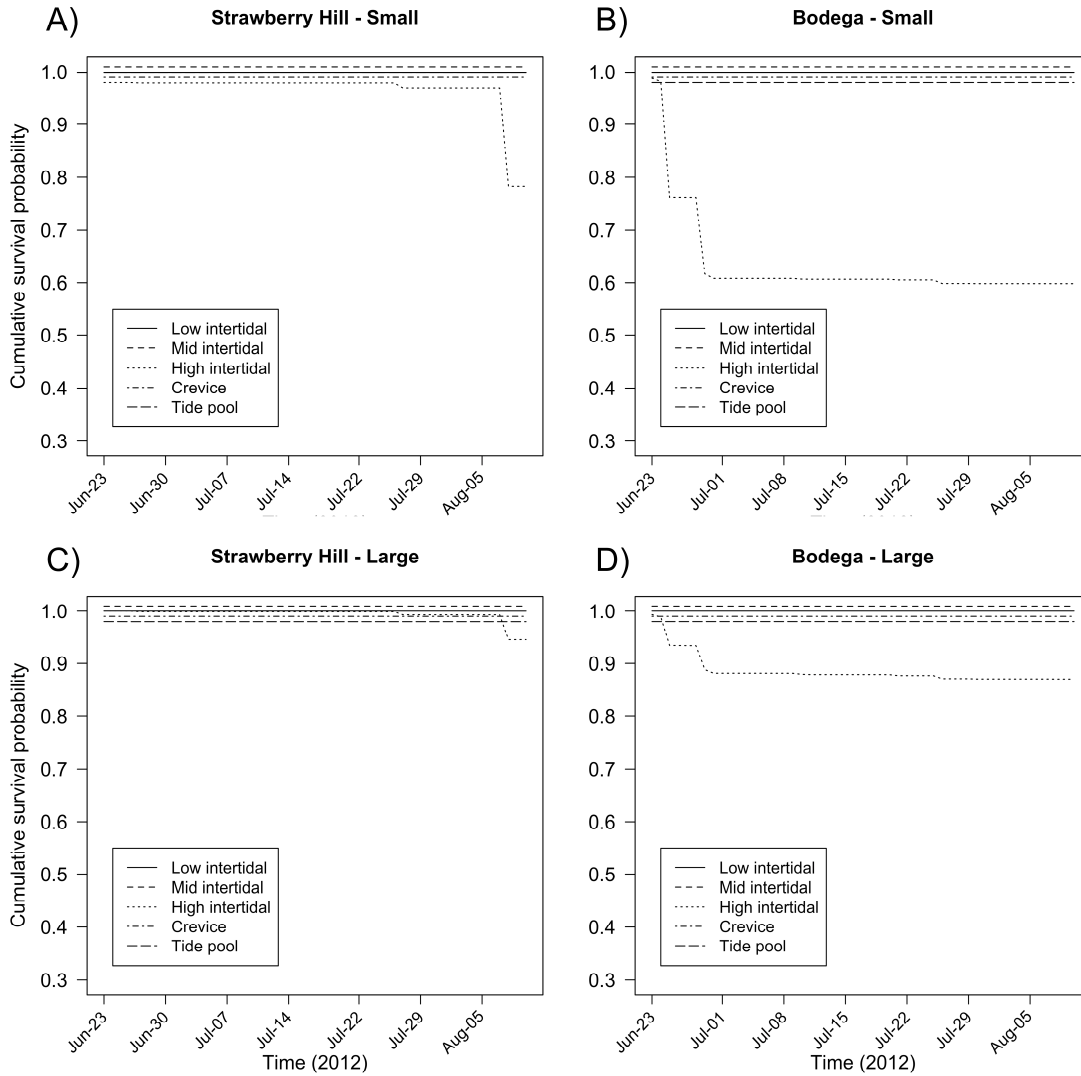
Figure 2.8 Cumulative survival curves for hypothetical small (25-75g) and large (250-500g) *Pisaster* individuals occupying various microhabitats (exposed high, mid and low intertidal, and protected in crevices or tide pools) available at Bodega and Strawberry Hill. Survival was calculated based on our empirical estimates of mortality in relation to body temperature (see sections about *Size-dependent tolerance to thermal stress*). We slightly displaced those curves that overlapped with each other.
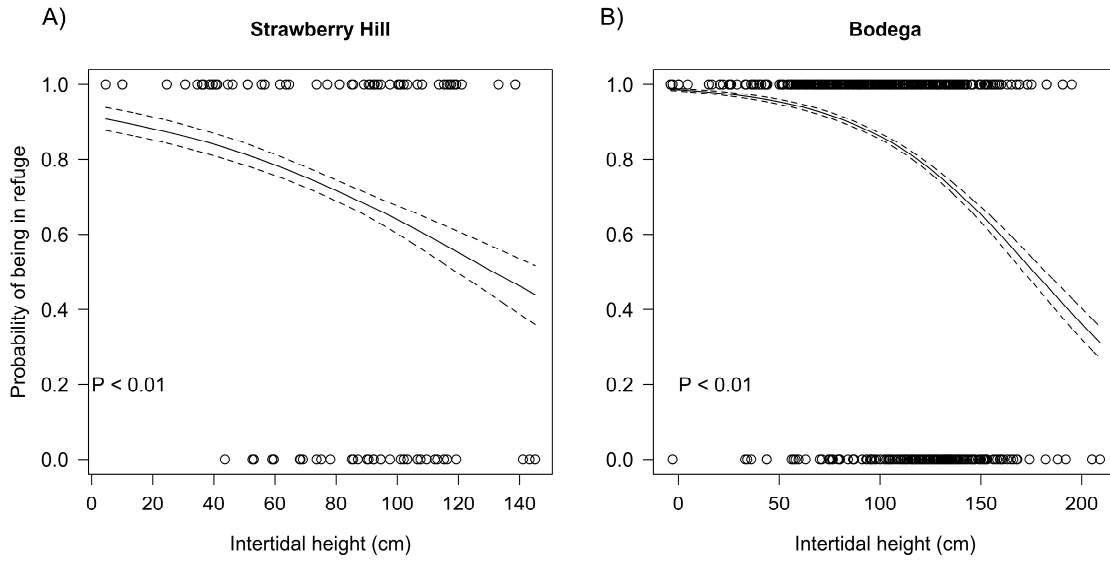
Figure 2.9 Probability of finding *Pisaster* individuals occupying refuge (i.e. crevices or tide pools) in relation to intertidal height at (A) Strawberry Hill and (B) Bodega. Data were collected at Strawberry Hill in 2012, and Bodega in 2010, 2011, and 2012. The lines represent logistic regression fits ± 1 SE. P-values for the models' significance are also provided.

CHAPTER 3

THERMAL SENSITIVITY AND BEHAVIOR'S ROLE IN DRIVING AN INTERTIDAL PREDATOR-PREY INTERACTION[2]

ABSTRACT

Untangling the effects of direct and indirect ecological drivers should improve our ability to mechanistically predict dynamics in natural systems. Environmental stress models (ESM) have been useful frameworks to identify these effects. Their practical application, however, may be limited when we fail to recognize the roles of behavioral and physiological responses. The rocky intertidal has long served to develop the theory behind ESM. We examined the role of thermal sensitivity and behavior on the mean performance of the keystone predator *Pisaster ochraceus* and its main prey *Mytilus californianus*. Unlike other studies that involved caging experiments, we propose a novel approach that merges the thermal performance curve (TPC) framework and observations of microhabitat use to provide a more ecologically realistic perspective of organisms' response to stress in the field. First, by deriving aquatic and aerial TPCs for both species and from two sites, we found differences in parameter values that correspond with the individuals' origins. For example the thermal sensitivity parameter Arrhenius temperature (T_A) resulted higher at the most thermally variable site. *Pisaster* and *Mytilus* seem to buffer against thermal heterogeneity. Second, we calculated mean thermal

_____

performance based on these curves and *in situ* body temperatures recorded with biomimetic sensors. This approach revealed that the thermal performance of *Pisaster* was higher than that of *Mytilus*, contrary to previous caging experiment results. Third, to test predictions from our indirect approach, we measured an indicator of overall physiological condition (body mass index) and a marker for extreme thermal stress (heat-shock proteins 70kDa). *Mytilus* body mass index was higher at the more thermally variable sire, Strawberry Hill. In contrast, *Pisaster* showed no differences in body mass index between sites, possibly because extreme body temperatures were not significantly different between sites. The same pattern was observed for heat-shock protein expression. Thus, these species seem to be responding more to high extremes than mean temperature values. We found no evidence that *Pisaster* movement influences thermal performance. Other environmental forces (e.g. solar radiation) must be driving *Pisaster* preference for sheltered microhabitats.

INTRODUCTION

Predicting natural systems' dynamics as a function of environmental drivers requires a mechanistic understanding of the biotic and abiotic factors controlling individual level processes (Denny & Helmuth 2009, Tomanek & Helmuth 2002). This task is particularly timely given the increasing threat posed by climate change on ecosystems globally (Burrows et al. 2011, Helmuth et al. 2006b, Parmesan & Yohe 2003). To this end, great efforts have been oriented towards modeling the independent effects of most relevant components. However, climate change is predicted to impact populations via multiple physical (e.g. temperature) and biological (e.g. ecological interactions) stressors with the potential for seemingly unpredictable synergistic, antagonistic, or additive outcomes

(Wernberg et al. 2011, Williams et al. 2011). It has been argued that such outcomes may result from interactions between the different drivers, which can be conceptualized as direct and indirect effects. For example, the direct effects of increasingly warmer temperatures may indirectly force phenological mismatches between key interacting species, thereby disrupting community dynamics (Ohlberger et al. 2014).

Environmental stress models (ESM), a useful framework to anticipate the output of ecological interactions along gradients of environmental drivers (Menge & Olson 1990, Menge et al. 2002, Menge & Sutherland 1987), can be used as heuristic tools for untangling direct from indirect effects. The theory behind ESMs has seen promising advances over the last 10 to 20 years. Importantly, in addition to considering negative interactions such as predation and competition, ecologists have acknowledged the importance of positive interactions (e.g. facilitation) in driving natural systems' dynamics, especially under climate change scenario (Bertness & Leonard 1997, Buckley 2013, Leonard 2000), and efforts to conceptually include them into the ESM framework have arisen (Bruno et al. 2003).

However, empirical studies applying the ESM framework, although informative, have often lacked the ecological realism that is necessary to accurately characterize context-dependency. In particular, studies have failed to incorporate aspects of behavior (e.g. microhabitat choice) and physiological responses, despite acknowledging their importance (Petes et al. 2008b). Because ecological interactions, microhabitat use, and physiological responses are tightly interdependent in many aquatic and terrestrial systems (Dahlhoff et al. 2001, Porter et al. 1975), studies would benefit by considering them in concert (Monaco & Helmuth 2011).

When applied to predator-prey systems, ESMs have been shown to take one of two forms; as consumer stress model (CSM) or prey stress model (PSM). The system behaves as CSM if predators appear more negatively affected by the environment than the prey (Menge & Sutherland 1976); alternatively, if prey suffer more from environmental stressors, the system is labeled as PSM (Menge et al. 2002, Trowbridge 1998). Depending on whether we use CSMs or PSMs, predictions about the dynamics of our species may follow fundamentally different trajectories (Menge et al. 2002). Thus, for ESMs to serve their purpose, it is essential to accurately identify the variant exhibited by our particular study system.

Because of its steep physical and biological gradients, the rocky intertidal has long served as a natural laboratory to develop and test ESMs. With the constant rise and fall of tides, intertidal organisms frequently cope with physical forces such as solar radiation, temperature, wind speed, and wave action, which have been shown to mediate species interactions in predictable manners (Sanford 1999, Wethey 2002). These gradients, however, are also inherently variable in time and space (Broitman et al. 2009, Denny et al. 2011, Porter et al. 1975). Furthermore, because the thermal niche may vary between interacting species, a temperature gradient may affect them differently (Helmuth 2002). In order to correctly identify the type of ESM, one may need to account for this variability, which is especially problematic for mobile species. Intertidal caging experiments provide a means for manipulating and testing the effect of environmental stress gradients (Menge et al. 2002, Petes et al. 2008b), but because of cage effects that impair the species natural behavior, these efforts may yield misleading results.

Here we describe an alternative approach to circumvent this problem, which relies on field observations of individuals' microhabitat use, biomimetic temperature logger records (Fitzhenry et al. 2004, Seabra et al. 2011, Szathmary et al. 2009), and the thermal performance curve (TPC) framework (Huey & Kingsolver 1989, Huey & Stevenson 1979, Woodin et al. 2013). Biomimetic temperature loggers are commercial sensors that have been modified to resemble the material properties of and organism, and therefore capture its body temperature with relatively high accuracy. Thermal performance curves describe the dependence of organisms' vital rates (e.g. metabolism, feeding, growth, reproduction) on temperature. By quantifying thermal performance indirectly using TPCs and *in situ* continuous measurements of body temperature, one can avoid influencing the organism's condition due to experimental manipulations.

As organisms' temperature dependence is an attribute of the species or population (Angilletta 2009), one can employ TPCs to compare thermal performance between them (Dell et al. 2011). TPCs can be used to evaluate temperature effects on each interacting species, and subsequently compare between them, thus estimating which might be winners or losers (Somero 2010).

The predictive power of this framework can be further improved if working with keystone species in the system, whose dynamics may disproportionately influence their communities. To examine potential direct and indirect effects of temperature, we focused on a major predator-prey interaction in rocky shores from the Pacific coast of North America, the predatory sea star *Pisaster ochraceus* (hereafter, *Pisaster*) and its main prey, the mussel *Mytilus californianus* (hereafter, *Mytilus*). By foraging on *Mytilus*, a dominant competitor for space, *Pisaster* facilitates the presence of other invertebrates and

alga, thus fulfilling a keystone ecological role (Paine 1966, Paine 1974). Recent work

has demonstrated that temperatures during high and low tides (and their interaction) may

drive the strength of interaction between these species (Pincebourde et al. 2012,

Pincebourde et al. 2008, Sanford 1999). To understand the underlying mechanisms

orchestrating these dynamics, the authors have advised looking at the physiological basis

of the effect of temperature. By combining data on metabolic rates during

submergence/exposure periods, Fly et al. (2012) quantified energetic costs of occupying

different shore levels for *Pisaster*, and found no marked differences between being lower

or higher, where its interaction with *Mytilus* mostly occurs. Following the ESM

framework Petes et al. (2008b) experimentally tested which species were more greatly

affected by the environment in the low zone, concluding that the system behaved as

CSM. However, their method of caging individuals might have influenced their results,

particularly because they constrained the ability of *Pisaster* to move among microhabitats

and potentially ameliorate stress (Huey 1991).

Here we examined the physiological performance of both species *Pisaster* and

Mytilus, revisiting the question of which is more negatively impacted by their

environment. First, to explore the role of physiology, we combined information of

empirically derived TPCs with observations of realized body temperatures. Second, to

evaluate the role of movement behavior in *Pisaster* on its mean thermal performance, we

included observations of microhabitat use. And third, we complement this with empirical

indicators of overall physiological condition (body mass index, BMI) and heat stress

(heat-shock protein 70kDa production, Hsp70). To test whether results were

generalizable across sites, these analyses were conducted at two field sites Bodega Bay,

California and Strawberry Hill, Oregon (~760km apart) with contrasting thermal environments, as the times of the lowest low tides are closer to noon during summer months at the latter site (Helmuth et al. 2002, Place et al. 2008).

MATERIALS AND METHODS

Study sites

We conducted field surveys, collected tissue samples, and collected animals for lab experiments at two sites: Strawberry Hill (44°14'59.4" N, 124°06'54.7" W, Oregon, USA), and Bodega Bay (38°19'07.7" N, 123°04'27" W, California, USA) (Fig. 3.1). We chose these sites because (1) *Pisaster* and *Mytilus* were highly abundant and interacting widely, (2) environmental conditions were expected to be dissimilar, given the time of the lowest low tides being closer to midday at Strawberry Hill, and (3) the habitat is topographically complex at both sites, offering alternative microhabitats for *Pisaster* to refuge (crevices, tide pools, kelps, open spaces). At the time of the study, wasting disease had not yet impacted sea stars' populations (Bates et al. 2009, Stokstad 2014).

Field body temperature measurements

We used biomimetic temperature loggers customized to resemble the thermal properties of average size *Pisaster* (~200g) and *Mytilus* (~8cm shell length) (Broitman et al. 2009, Szathmary et al. 2009). While *Pisaster* preferentially forages on mussels < 8cm shell length (Paine 1976), our current biomimetic design for *Mytilus* cannot be shrunk due to size constraints set by the commercial temperature logger used (TidBit, Onset Computers) (Fitzhenry et al. 2004). Sea stars and mussels' biomimetics, aka robo-sea

stars and robo-mussels respectively, recorded potential body temperatures between June 22nd and August 10th 2012, once every 30 minutes.

Because *Pisaster* can occupy different discrete locations throughout the intertidal, we deployed robo-sea stars in microhabitats where sea stars are commonly present; namely, exposed to the elements (solar radiation, wind) in the mid-intertidal, in crevices, and tide pools. Robo-mussels, in turn, were deployed only on the mid-intertidal, where *Mytilus* is stationary and their interaction with *Pisaster* is strongest.

Surveys of *Pisaster* microhabitat use

To determine *Pisaster* microhabitat use during the period of the study, we conducted surveys on five different low spring-tide periods over the summer of 2012 at Bodega (May 27, June 7, June 25, July 23, and August 2) and Strawberry Hill (May 26, June 7, June 23, July 22, and August 5). Surveys involved describing the microhabitat of every individual sea star encountered within five, 2-m wide, belt-transects oriented perpendicularly to the coastline. We categorized each individual based on microhabitat use as exposed (i.e. unprotected from direct solar radiation and wind), in crevices, or submerged in tide pools.

Empirical indicators of physiological performance

Body mass indices (BMI):

We calculated body mass indices for both *Pisaster* (n = 10 animals site^{-1}) and *Mytilus* (n = 40 animals site^{-1}). Individuals were collected at Bodega on July 19th 2012 (mean *Pisaster* arm length $\pm$ SE = 11.21 $\pm$ 1.98cm; mean *Mytilus* shell length $\pm$ SE = 48.07 $\pm$

0.55cm), and Strawberry Hill on July 22nd 2012 (mean *Pisaster* arm length $\pm$ SE = 10.12

$\pm$ 1.19cm; mean *Mytilus* shell length $\pm$ SE = 51.28 $\pm$ 0.66cm), and transported fresh to

Bodega Marine Lab (BML, UC-Davis) for later analyses. We dissected sea stars

separating gonads and pyloric caecum from the body walls. We determined the dry

weight of gonads (*GDW*), pyloric caecum (*PDW*), and body walls (*BwDW*) by drying at

80˚C for 48h, and weighing them to the nearest 0.001g. *Pisaster* BMI was calculated as:

$(GDW + PDW) \cdot (GDW + PDW + BwDW)^{-1}$. Similarly, we dissected mussels by

separating all soft tissue (without discriminating between gonadic and somatic tissue)

from the shell. To determine the dry weight of tissue (*TDW*) and shell (*ShDW*), we dried

them at 80˚C for 24h, and weighed to the nearest 0.001g. We calculated *Mytilus* BMI as:

$(TDW) \cdot (TDW + ShDW)^{-1}$.

Heat shock protein expression:

We measured heat shock protein 70kDa (Hsp70) expression from sea stars (n = 5 animals

site^{-1} sampling^{-1}) and mussels' (n = 6 or 7 animals site^{-1} sampling^{-1}) tissue samples

collected on the same five spring-tide periods when microhabitat use surveys were

conducted at Bodega and Strawberry Hill (*section 2.3.*). We collected all samples during

negative low tide periods. We chose individuals found on the lower edge of the mussel

bed (mid-intertidal zone), where these species interact the most. Tissue samples were

removed *in situ* (tube-feet for *Pisaster*, and gills for *Mytilus*), and quickly frozen using

dry ice. Within 24h of sampling, tissues were stored at BML in -80˚C freezers. We

shipped the samples on dry ice over night to the University of South Carolina, where they

were stored again at -80˚C for subsequent immunochemical detection of Hsp70.

We quantified Hsp70 expression using dot blot analysis. Previously, we had optimized the concentrations of protocol constituents using western blot analysis, as modified from (Hofmann & Somero 1995) and (Helmuth & Hofmann 2001). Although we were unable to discriminate between the bands of constitutive and inducible Hsp70 isoforms on our gels, preliminary assessments of *Pisaster* heat shock response after short-term (i.e. days) high temperature treatments revealed increases in Hsp70 expression, which can be considered as changes in the inducible isoform given the temporal resolution of the experiments (Kinsey and Place, unpublished data). Therefore, we regarded our measurements as total Hsp70 (i.e. constitutive + inducible) expression. Because we were interested on dynamics occurring over weeks and months, not distinguishing between the two isoforms does not impair our ability to examine *Pisaster* and *Mytilus* heat shock response.

We homogenized samples (~ 0.05g) in 0.5mL of homogenizing buffer [50mM Tris-HCl pH 6.8, 4% (w/v) SDS, cOmplete protease inhibitor cocktail]. Homogenates were incubated at 100˚C for 5min, centrifuged at $12000 \times g$ for 15min, and the supernatant stored at -20˚C. To determine total protein concentration of aliquots reserved from the sample extracts, we used a Bradford protein assay (Pierce Coomassie Plus).

We then loaded 10µg of extracted proteins onto a hydrated 0.2-µm nitrocellulose membrane placed flat in a 96-well dot blot apparatus (Bio-Rad). Samples were allowed to migrate by gravity for 30min. Blotted membranes were then washed in phosphate-buffered saline [PBS; 8.1 mmol l^{-1} Na_2HPO_4, 2.7 mmol l^{-1} KCl, 137 mmol l^{-1} NaCl, 1.5 mmol l^{-1} KH_2PO_4, pH 7.4] for 10min, blocked [blocking solution; 5% non-fat dry milk in PBS-Tween20 0.1%] for 1h, and washed in PBS-Tween20 0.1% for 5min three times.

We incubated the blots in a 1:2000 dilution of primary antibody solution [ENZO anti-Hsp70 pAb-ADI-SPA-757, 80% blocking solution, 20% fetal bovine serum, 0.02% thimerosal, 1mmol l^{-1} PMSF] for 1.5h, washed in PBS-Tween20 0.1% for 5min three times, and then incubated in a1:6000 dilution of secondary antibody solution [Santa Cruz goat anti-rabbit lgG-HRP-SC2004, blocking solution] for 1h. Blots were washed once in PBS-Tween20 0.3% for 5min, twice in PBS-Tween20 0.1% for 5min, and once in PBS for 5min. Next, we incubated them in an enhanced chemiluminiscence reagent (ECL; Thermo Scientific SuperSignal) for 5min, exposed films for 40min, and digitized them using an imaging system (Fotodyne). Dot intensity was determined using the software ImageJ. We calculated relative values of Hsp70 for the samples based on readings obtained from positive controls (purified recombinant Hsp70, ENZO ADI-SPP-758), which were loaded along with the tissue samples in every dot blot.

Theoretical quantification of physiological performance

Estimating thermal sensitivity curves

First we parameterized aquatic thermal sensitivity curves for both *Pisaster* and *Mytilus*, from Bodega and Strawberry Hill, using empirical metabolic rate data. Second, to describe aerial thermal sensitivity curves, we used the information gathered for submerged conditions, coupled with data on physiological responses to temperature under exposed conditions obtained from the literature. We fitted all four curves based on formulations by Sharpe and DeMichele (1977):

$$\dot{k}(T) = \dot{k}(T_1) \cdot \exp\left\{\frac{T_A}{T_1} - \frac{T_A}{T}\right\} \cdot \left(1 + \exp\left\{\frac{T_{AL}}{T} - \frac{T_{AL}}{T_L}\right\} + \exp\left\{\frac{T_{AH}}{T_H} - \frac{T_{AH}}{T}\right\}\right)^{-1}$$

(Eq. 1)

Where $\dot{k}(T)$ is a physiological rate at body temperature T, $\dot{k}(T_1)$ is a reference value for a physiological rate at body temperature T_1 (typically 20˚C), T_A is Arrhenius temperature, which determines the thermal sensitivity at temperatures where enzymes are active (analogous to Q_{10}), T_L and T_H are the lower and upper temperatures marking the organism's thermal performance breath (i.e. where enzymes are considered active), and T_{AL} and T_{AH} are the Arrhenius temperatures for the rates of decrease at the low and high margins of the curves (Freitas et al. 2007, Monaco et al. 2014).

Aquatic thermal sensitivity: Sea stars and mussels were collected at Strawberry Hill (June 24th, 2012), stored in coolers packed with kelps and icepacks on the bottom to maintain them cool and humid, and transported by ground to the Bodega Marine Lab (~ 11h trip). At the lab, we acclimated *Pisaster* and *Mytilus* in separate tanks with running seawater at ambient temperature (~12˚C) for 5d. Food supply was *ad libitum* for both sea stars (mussels provided in excess) and mussels (IAP Algae Paste, Spat Formula, diluted in the tanks and stopping the water flow for 2h, twice a day). The same protocol was followed for individuals collected at Bodega (July 7th, 2012), though instead of transporting the animals, we kept them in coolers for the same time as those collected at Strawberry Hill.

The sensitivity of both *Pisaster* and *Mytilus* to changes in seawater temperature was determined from metabolic rate measurements taken at six temperatures: 10, 13, 18, 21, 24, and 27˚C. Following the acclimation period, we placed two individual *Pisaster* and two *Mytilus* in 60-L aquaria (3 per treatment) filled with 1-µm filtered seawater at ambient temperature (~ 12˚C). Treatment seawater temperatures were adjusted by

keeping the aquaria in climate-controlled rooms available at BML. The two highest temperatures were reached using 100-W aquarium heaters (Marineland Visi-Therm, USA). Water temperatures were changed at ~ $1°C\ h^{-1}$. We kept the individuals at their treatment temperatures for 4d, after which we measured oxygen consumption rates. To ensure water quality, tanks were fitted with air stones and submersible pumps. Water chemistry (salinity, pH, ammonia, nitrite, and nitrate) was monitored every other day using a saltwater test kit (API, USA), and partial water changes were performed when necessary (every 1-2d).

To measure oxygen consumption we placed individual sea stars and mussels in watertight chambers (2.88 and 0.7-L, respectively) filled with aerated, 1-µm filtered seawater, at its corresponding treatment temperature. A magnetic stir-bar kept the water circulating during measurements. Over the top of each chamber, we fitted Clark-type electrodes (HANNA-9146, USA), and measured dissolved oxygen concentration (ppm) at 10 and 40 min after sealing the chamber. Trials were discontinued if oxygen levels dropped below 70% of initial readings. To control for background variability in oxygen content, we conducted measurements in two animal-free chambers at each of the treatment temperatures. We standardized the change in oxygen concentration by the animal's dry weight, and expressed as standard metabolic rate (SMR, $µmol\ O_2\ h^{-1}\ gDW^{-1}$). The experimental design yielded six replicates per temperature, per site, for *Pisaster* and *Mytilus*. All animals maintained at the warmest treatment temperature, 27°C, died within two days of beginning the thermal conditioning period, so a value of zero was assigned to them when fitting thermal sensitivity curves.

To estimate aquatic thermal sensitivity parameters we normalized the oxygen consumption data for each treatment by the highest value. We estimated the parameter T_A from the slope of a linear model between ln(SMR) and the inverse of treatment temperature in K, for the range of temperatures where SMR increased exponentially (Freitas et al. 2007). To estimate the parameters T_L, T_H, T_{AL}, and T_{AH}, we used the Levenberg-Marquardt non-linear least squares optimization method (R package minpack.lm) (Moré 1978).

Aerial thermal sensitivity: Data to fit aerial thermal sensitivity curves for each species and site were obtained from the literature. Although information was not available for the whole thermal range, key parameters that constrain the curves (e.g. lethal temperatures) were found, which combined with the aquatic thermal sensitivity parameters from each site, allowed fitting site-specific aerial thermal sensitivity curves for each species. For *Pisaster* we obtained data of aerial physiological rates, relative to measurements taken in water at the same temperatures, from Fly et al. (2012), and critical temperatures from Monaco et al. (unpublished) and Pincebourde et al. (2008). For *Mytilus* we obtained data on aerial physiological rates, relative to measurements taken in water at the same temperatures, from Bayne et al. (1976). Critical temperatures were taken from Denny et al. (2011) and Mislan et al. (2014). Note that Mislan et al. (2014) also found that upper critical temperature of *Mytilus* collected at Bodega did not differ from that of individuals collected at Boiler Bay, a site located in close proximity to Strawberry Hill, suggesting no difference in upper thermal limits between the latter and Bodega.

The manual fitting protocol involved a grid search method. First the parameter T_H was varied until the deviance between the model prediction and the critical temperatures were minimized. Then T_A was varied until the model best matched the observations of relative aerial physiological rates. The other thermal sensitivity parameters (T_L, T_{AL}, and T_{AH}) were assumed to remain operationally constant between periods of immersion and emersion.

Calculating mean thermal performance

We calculated *Pisaster* and *Mytilus* relative thermal performance at Bodega and Strawberry Hill for the time period when our biomimetic sensors were deployed. The thermal sensitivity models estimated for each species were run using the temperature records from each biomimetic sensor and tide height data (to inform when loggers were submerged/emersed) as inputs, thus generating relative performance time-series for the prey and each of the microhabitats where the predator is found. We downloaded the tide height data from NOAA's CO-OPS (station IDs 9435380 and 9415020 for Strawberry Hill and Bodega, respectively).

Accounting for Pisaster behavior

We evaluated the role of movement on *Pisaster* thermal performance by recreating three scenarios: mobile, static, and optimal predator. The static scenario was computed using the thermal performance curves and the mid-intertidal robo-sea stars. On the mobile scenario, to account for *Pisaster* movements throughout the intertidal during the period when temperature measurements were taken, we ran 500 simulations by which hypothetical individuals were allowed to choose between microhabitats (exposed mid-

intertidal, crevice, tide pool) every 12h. Their selection was limited by the probability of occupying a specific microhabitat, as informed by our surveys conducted during the same period (*section 2.3.*). For the optimal scenario we hypothetically allowed *Pisaster* to instantaneously move to the microhabitat reporting the highest performance for each time point.

Statistical analyses

We ran all calculations and statistical analyses using the software R 3.0.1 (R Core Team 2013). From the field body temperatures recorded via biomimetic loggers we determined the daily maximum values and compared between site and species using a 2-way ANOVA.

The thermal sensitivity parameter T_A was compared between site, species, and aquatic/aerial condition using one-tailed z-score tests. To compare relative thermal performance data between species/scenarios at each site we calculated Root Mean Square Errors (RMSEs), and to test for correlation between them we computed Kendall's W coefficient of concordances. To compare variances between species/scenarios and sites we conducted Levene's tests (Quinn & Keough 2002).

We compared BMI between sites (categorical) for each species using Welch's two sample t-tests because data were heterocedastic (Levene test, $P < 0.01$). We analyzed Hsp70 data separately for each species using 2-way ANOVAs. For the lab experiment data, temperature (continuous) and site were considered as fixed factors, whereas for the field collected data, date (categorical) and site were the fixed factors.

When assumptions of normality and homocedasticity were not satisfied for Hsp70 data (even after log-transformations), we ran two ANOVAs, one using raw data and another using rank-transformed data. If results were qualitatively the same between the tests, we reported results from the former; otherwise we provided results from the latter.

RESULTS

Biomimetic temperature records

When comparing daily maxima body temperatures recorded using biomimetic loggers, we found significant effects of both species (2-way ANOVA; $F_{(1,196)} = 50.78$, $P < 0.001$) and sites (2-factor ANOVA; $F_{(1,196)} = 8.42$, $P = 0.004$). Mussels experienced higher extreme temperatures than sea stars at both sites, and Strawberry Hill appeared warmer than Bodega for both species (daily maximum mean ± SE: *Pisaster*/Bodega, 12.62 ± 0.19; *Pisaster*/Strawberry Hill, 13.39 ± 0.30; *Mytilus*/Bodega, 19.86 ± 0.35; *Mytilus*/Strawberry Hill, 21.85 ± 0.69) (Fig. 3.2). Despite these differences in extremes, the variability in temperature records did not significantly change with species (Levene's test; $F = 0.023$, $P = 0.88$) and site (Levene's test; $F = 0.027$, $P = 0.87$) (Fig. 3.2).

Theoretical indicator of physiological performance

Thermal sensitivity curves

Pisaster and *Mytilus* mean metabolic rate increased with water temperature up to a maximum point between 20 and 25°C, varying with species and site (Fig. 3.3). Using this portion of the data, following Freitas et al. (2007), we fitted linear regression models between ln(metabolic rate) and temperature in Kevin, and determined the slopes, which represent the parameter Arrhenius temperature (T_A) for each site and species (*Pisaster*/Bodega, slope = -6221±778, t = -3.49, P = 0.01, R^2 = 0.64; *Pisaster*/Strawberry Hill, slope = -3182±435, t = -3.08, P = 0.008, R^2 = 0.42; *Mytilus*/Bodega, slope = -4187±353, t = -4.91, P < 0.001, R^2 = 0.65; *Mytilus*/Strawberry Hill, slope = -5140±394, t = -6.47, P < 0.001, R^2 = 0.74). Knowing T_A values, we were able to estimate the remaining parameters by fitting Eq. 1 to each species/site dataset using Levenberg-Marquadt non-linear optimization models (*Pisaster*/Bodega, T_L = 274.3, T_H = 297.9, T_{AL} = 186458, T_{AH} = 218569, number of iterations = 6, RSS = 0.342; *Pisaster*/Strawberry Hill, T_L = 292.7, T_H = 299.5, T_{AL} = 4040.3, T_{AH} = 925180, number of iterations = 5, RSS = 0.339; *Mytilus*/Bodega, T_L = 280.3, T_H = 298.2, T_{AL} = 6654.1, T_{AH} = 247263, number of iterations = 6, RSS = 0.338; *Mytilus*/Strawberry, Hill T_L = 278.5, T_H = 298.2, T_{AL} = 5434.9, T_{AH} = 281782, number of iterations = 7, RSS = 0.20), yielding the respective aquatic thermal sensitivity curves (Fig. 3.4). Next, it was possible to fit aerial thermal sensitivity curves using the aquatic thermal sensitivity parameters as baselines and data on aerial metabolic rates obtained from the literature (Fig. 3.4). The RMSEs for fitted versus observed relative thermal sensitivity data were 0.024, 0.031, 0.012, and 0.006, for *Pisaster*/Bodega, *Pisaster*/Strawberry Hill, *Mytilus*/Bodega, and *Mytilus*/Strawberry Hill, respectively.

The rounded parameter values that define these curves are shown in Table 3.1. The thermal sensitivity parameter T_A was higher at Bodega than Strawberry Hill for both *Pisaster* (z = 3.41, P < 0.001) and *Mytilus* (z = -1.80, P = 0.03). While *Mytilus* T_A was higher for aquatic than aerial conditions, it appeared similar for *Pisaster*. The parameter T_L was lower at Bodega than Strawberry Hill for *Pisaster*, but did not differ between sites for *Mytilus*. Aquatic T_L was estimated for each site and species, but kept constant during the aerial thermal sensitivity curve fitting, so it did not differ between submergence/emergence. For both species the parameter T_H was higher when considering aerial conditions. The latter parameter did not change between species for aquatic conditions, but was higher for *Mytilus* than *Pisaster* when exposed to air. Parameters T_{AL} and T_{AH} were kept constant for aquatic and aerial conditions. Their values were generally high, reflecting the steepness of the slopes at the borders of the thermal performance curves (Fig. 3.4; Table 3.1).

Relative thermal performance

At Bodega (Fig. 3.5A; Table 3.2), we observed that relative performance (mean±SE) was lower for *Mytilus* (0.398±0.002) than any of the *Pisaster* scenarios evaluated: static (0.453±0.002), mobile (0. 481±2×10^{-4}), and optimal (0.505±0.001), with RMSEs = 0.13, 0.15±9.6×10^{-5} and 0.15, respectively. Despite our expectation, no clear differences were detected between the three *Pisaster* scenarios, although the optimal was slightly higher than the static and mobile scenarios (RMSE = 0.10 and 0.10±2.3×10^{-4}, respectively). Concordances between species/scenarios were significant in all cases, revealing strong association between them (P-value < 0.01 in all cases; Table 3.2).

At Strawberry Hill (Fig. 3.5B; Table 3.2) the patterns were comparable to Bodega. Relative performance was lower for *Mytilus* (0.357±0.002) than any of the *Pisaster* scenarios: static (0.371±0.002), mobile (0.362±2×10^{-4}), and optimal (0.411±0.002), with RMSE = 0.12, 0.13±1.4×10^{-4} and 0.12, respectively. Again, the *Pisaster* scenarios showed no marked differences, except that the optimal was higher than static and mobile (RMSE = 0.17 and 0.17±2.5×10^{-4}, respectively). Also at Strawberry Hill we observed significant concordance between species/scenarios (P-value < 0.01 in all cases; Table 3.2).

When comparing between sites, we found that *Pisaster* and *Mytilus* mean thermal performance was higher at Bodega for every scenario. In terms of variability, however, variances were greater at Strawberry Hill for both species and for every scenario: *Mytilus* (Levene's test; F = 36.801, P < 0.001), *Pisaster* static (Levene's test; F = 99.49, P < 0.001), *Pisaster* mobile (Levene's test; F = 90839, P < 0.001), and *Pisaster* optimal (Levene's test; F = 360, P < 0.001) (Fig. 3.5).

Empirical indicators of physiological performance

Body mass indices (BMI)

Pisaster BMI showed no differences between sites (Fig. 3.6A; Welch's t-test, t$_{(17.2)}$ = -0.8, P > 0.05). In contrast, *Mytilus* BMI was significantly higher at Strawberry Hill than Bodega (Fig. 3.6B; Welch's t-test, t$_{(52.3)}$ = -11.4, P < 0.01).

Heat shock protein (Hsp70) expression

Lab experiments showed that *Pisaster* expression of Hsp70 was not affected by temperature (2-way ANOVA; $F_{(4,50)} = 0.11$, $P > 0.05$), site ($F_{(1,50)} = 0.01$, $P > 0.05$), and their interaction ($F_{(4,50)} = 0.13$, $P > 0.05$). Likewise, for *Mytilus* we did not see a detectable change in expression of Hsp70 with temperature (2-way ANOVA, $F_{(4,48)} = 0.48$, $P > 0.05$), site ($F_{(1,48)} = 0.002$, $P > 0.05$), and their interaction ($F_{(4,48)} = 2.42$, $P > 0.05$) (Fig. 3.7A,B).

Our field tissue samples revealed that *Pisaster* Hsp70 production remained constant across survey dates (2-way ANOVA; $F_{(4,41)} = 1.18$, $P > 0.05$) and sites ($F_{(1,41)} = 1.76$, $P > 0.05$), and their interaction was non-significant ($F_{(4,41)} = 0.81$, $P > 0.05$) (Fig. 3.7C,D). In turn, *Mytilus* Hsp70 production in the field varied with survey date (2-way ANOVA; $F_{(4,54)} = 5.98$, $P < 0.01$), but did not change between sites ($F_{(1,54)} = 0.42$, $P > 0.05$), and no interaction between them was detected ($F_{(4,54)} = 2.45$, $P > 0.05$). When comparing level of variability between sites, *Mytilus* was significantly greater at Strawberry Hill (SD = 0.41) than Bodega (SD = 0.15) (Levene's test; $F = 5.48$, $P = 0.02$) (Fig. 3.7C,D).

DISCUSSION

By coupling information of organisms' thermal sensitivity, their potential body temperatures experienced on the field, and behavior, this study provides a unique perspective of the thermal physiology of two key species from the Pacific coast of North America, the predator *Pisaster ochraceus* and its main prey *Mytilus californianus*. Furthermore, embedded within an environmental stress model framework, this approach

stands as a powerful tool to uncover and predict mechanisms driving ecological dynamics associated with this and other predator-prey systems.

Body temperatures

By measuring temperatures using thermally-matched biomimetic sensors, we captured the real conditions that *Pisaster* and *Mytilus* would have experienced in the field (Fitzhenry et al. 2004, Szathmary et al. 2009). These records indicated that extreme high body temperatures differed between species and sites (Fig. 3.2). Higher temperature extremes at Strawberry Hill are likely due to the timing of low tide being closer to noon (Helmuth et al. 2002, Place et al. 2008). To explore the links between body temperatures and thermal performance, we first described thermal sensitivity curves (physiology) for both species from Bodega and Strawberry Hill, and then evaluated whether *Pisaster* movement behavior might influence its mean performance relative to that of *Mytilus*.

Role of physiology

The thermal sensitivity curves we described for *Pisaster* and *Mytilus* provide a means for quantifying mean levels of relative performance during continuous periods of high and low tides. While previous work had described aquatic thermal sensitivity curves for *Pisaster* (Monaco et al. 2014), we know of no previous studies that explicitly described it for *Mytilus*, although raw data for parameterizing the curve has long been available in the literature (Bayne et al. 1976). Aerial thermal sensitivity curves had not been described for either species. Given that both species spend significant amount of time exposed at low tides, during which body temperatures fluctuate even more than at high tides (Elvin & Gonor 1979, Hofmann & Somero 1995), getting a handle on the relationship between

76

aerial body temperature and physiological performance is especially relevant. Note, however, that we had limited data to fit the aerial curve, so further efforts using more data to describe it are warranted.

A wealth of empirical and theoretical evidence suggests that the thermal ecology and physiology of ectothermic organisms are aligned (Angilletta 2009). For instance, Freitas et al. (2007) showed that the thermal sensitivity (i.e. T_A) and higher critical temperatures (i.e. T_H) of various ectothermic species found in the Dutch Wadden Sea depend on the thermal environment where they are found. The same concepts apply for species distributions along larger (e.g. geographical) and smaller (e.g. vertical intertidal gradients) spatial scales (Monaco et al. 2010, Stillman & Somero 2000, Zippay & Hofmann 2010). Accordingly, we expected that the body temperatures experienced by *Mytilus* and *Pisaster* would correlate with their thermal sensitivity parameters. Displaying a low T_A may offer a physiological buffer against potentially stressful temperatures that might be reached at a more thermally heterogeneous environment (Hochachka & Somero 2002), such as Strawberry Hill (Fig. 3.2). It has also been suggested that a reduction of the temperature dependence of metabolism (i.e. lower T_A) is an energy conserving strategy for intertidal organisms (Marshall & McQuaid 2011) (but see Huang et al. 2014). Thus, based on homeostatic considerations, lower T_As were expected for the species and site showing the higher temperature variability. We observed this relationship on most cases (Table 3.1). As expected, both species showed lower T_A at Strawberry Hill than Bodega. Similarly, due to greater temperature variability for *Mytilus* during low tide, T_A was lower for aerial than aquatic conditions (Table 3.1). In a previous study using *Mytilus edulis*, van der Veer et al. (2006)

empirically estimated T_A to be 7022±551, which is higher than what we report here for *M. californianus*. This may be explained in part because *M. edulis* can be subtidal, and is presumably adapted to more homogeneous conditions, and in part due to differences in local thermal conditions experienced by the individuals subjected to the experiments.

Surprisingly, T_A did not vary much between aerial and aquatic conditions in *Pisaster* as much as it did for *Mytilus* (Table 3.1). We propose two complementary hypotheses for explaining this. First, related to the body temperatures experienced at low and high tides. At low tides, most *Pisaster* individuals are found protected in sheltered microhabitats such as crevices. Temperature differences between low and high tide are not dramatically different in sheltered or shaded microhabitats (see Chapter 2), so physiological adjustments (in the form of T_A reductions) may not be necessary. Mussels, in turn, experience radically different body temperatures between periods of low and high tide (Elvin & Gonor 1979, Hofmann & Somero 1995), and they have had to develop physiological mechanisms to cope with such insults. Our second hypothesis is related to such mechanisms. During aerial exposure *Mytilus* can readily sustain anaerobic metabolism (Connor & Gracey 2012), with a consequent reduction in oxygen consumption, and a lower T_A value. In contrast, evidence suggests that *Pisaster* may strongly rely on aerobic metabolic pathways regardless of the tide (Fly et al. 2012, Stickle 1988). It is likely that *Pisaster* has not evolved a dependence on anaerobiosis because of the generally mild thermal conditions it encounters. Additionally, when aerially exposed, higher than aquatic oxygen partial pressures and diffusion through body walls may allow sustaining aerobic metabolism. Because *Mytilus* has valves, and the fact that it does not

normally gape as other mussels do (Fitzhenry et al. 2004), presumably prevent it from maintaining aerobiosis.

Despite the lower T_A at Strawberry Hill, organisms still exhibited significantly higher variability in thermal performance than Bodega (Fig. 3.5). Thus, both predators and preys are reaching extreme high and low levels of performance, which can be associated with a higher risk of experiencing critical conditions. *Pisaster* generally selects for sheltered microhabitats to prevent such situation (see Chapter 2). However, Figure 3.5 also revealed that mean performance was lower at Strawberry Hill, so the risk of sporadic exposures to stressful temperatures may be offset by long-term mild conditions.

The upper temperature at which enzymes stop functioning properly, represented by the parameter T_H in the thermal performance curve framework, is also useful to assess and compare thermal sensitivities between species and populations (Freitas et al. 2007). Other studies have employed analogous metrics of upper thermal limits (e.g. LT_{50}, Arrhenius break-point temperature), finding evidence of phenotypic plasticity in some cases and local adaptation in others (Hollander 2008, Sanford & Kelly 2011, Stillman & Somero 2000). Overall, given the long larval dispersal potential shown by *Pisaster* and *Mytilus*, populations are likely not genetically isolated (Addison et al. 2008, Harley et al. 2006b), so differences could be attributed to plasticity. In terms of aerial T_A, while *Mytilus* showed no differences between sites, we observed a higher upper limit for *Pisaster* from Strawberry Hill than Bodega (Table 3.1). This trait would presumably be selected depending on the high temperatures experienced locally. Accordingly, given the higher extremes observed at Strawberry Hill (Fig. 3.2), the result found for *Pisaster* was expected. From our comparisons of mean thermal performance (Fig. 3.5), it appears that

increasing T_H is a response to the risk-probability of experiencing higher maximum temperatures, and not necessarily due to differences in means. Although *Mytilus* also experienced higher temperature extremes at Strawberry Hill, their T_H did not appear to change between sites. Similarly, Mislan et al. (2014) found no difference in *Mytilus* lethal high body temperature between Boiler Bay, a site close to Strawberry Hill, and Bodega. However, note that, although in close proximity, Strawberry and Boiler Bay may exhibit different climatic conditions for mussels (Dahlhoff & Menge 1996).

When applying these performance curves to conduct inter-species comparisons, our data showed that regardless of scenario tested (static, mobile, or optimal), the thermal performance of the predator, *Pisaster*, was higher than that of its main prey, *Mytilus* (Fig. 3.5; Table 3.2), thus fitting the prey stress model (PSM) variant within the environmental stress model framework. This finding contradicts the results by Petes et al. (2008b), presumably in part due to differences in methodology. They directly assessed performance of individuals caged along an intertidal vertical (stress) gradient. Although informative, caging experiments may unnaturally influence the physiological condition of the organisms, thus potentially leading to wrong conclusions. Notably, it is known that *Pisaster* preferentially avoids exposure to the elements during low tides (Burnaford & Vasquez 2008, Robles et al. 1995), which could not be considered in the study by Petes et al. (2008b) because the individuals were prevented from moving. Here we favored an alternative approach, by which thermal performance was indirectly quantified using biomimetic temperature loggers deployed on the field, and thermal performance curves described for each species.

The role of behavior

Our approach additionally allowed testing for the role of the predator's movement behavior. Because *Pisaster* preferentially avoids exposure to the elements during low tides (Burnaford & Vasquez 2008, Robles et al. 1995), we hypothesized that thermal performance would differ when microhabitat use was considered, as opposed to static individuals that stayed fixed in the mid intertidal. Interestingly, at both sites evaluated, static predators performed almost as well as mobile predators (Fig. 3.5; Table 3.2). *Pisaster* has the ability to incorporate seawater into its coelomic cavity at high tide, and use it to increase thermal inertia at low tide (Pincebourde et al. 2009). Since our robo-sea stars are made of sponges that soak up water too, we were able to account for this phenomenon. This high thermal inertia in *Pisaster* may explain the lack of differences we found between static and mobile predators. While unexpected, our observations conform to the results from previous studies evaluating the effects of prey addition/removal on the intertidal distribution of *Pisaster* (Robles et al. 1995). Their experiments showed that *Pisaster* could move vertically on the shore depending on availability of profitable prey items. Because sea stars would remain in the low intertidal when food was available, the authors argued that reaching higher shore levels would imply additional energy costs to cope with thermal stress. Note, however, that this expectation was not supported by calculations from Fly et al. (2012), who found very modest differences in thermal energy costs for individuals located at different shore levels.

Although we found marginal differences in performance between mobile and static predators (Fig. 3.5; Table 3.2), this does not mean that they did not exist. Our method only accounted for the thermal response, ignoring other relevant variables that

have been demonstrated to influence behavior and potentially fitness in *Pisaster*, most noticeably, solar radiation (Burnaford & Vasquez 2008) and desiccation (Feder 1956, Landenberger 1969). Since *Mytilus* inhabits higher shore levels than *Pisaster*, it is better adapted to cope with these factors. The differential effect of these factors on this predator-prey interaction, and not temperature, may help explain the results by Petes et al. (2008b), which lead them to define this system as consumer stress model.

The optimal predator scenario data provided an interesting viewpoint of the system. Although its thermal performance was higher than both the static and mobile predator scenarios, the differences were nominal (Fig. 3.5; Table 3.2). This means that among those options available for *Pisaster*, none represented a strikingly advantageous one. Including higher shore levels in the analyses may alter results; however, we deliberately ignored *Pisaster* thermal performance at higher shore levels and focused on the zone where their interaction with *Mytilus* is strongest.

Empirical indicators of physiological condition

We accompanied our indirect metric of thermal performance with direct, empirically determined indicators of physiological condition, BMI and Hsp70. Because these were measured from field-collected individuals, they potentially represent the net effect of biotic and abiotic factors on the surveyed populations, as well as the influence of behavior on thermal performance. Although these are not directly comparable to our estimates based on thermal performance curves, they should be correlated.

Both indicators BMI and Hsp70 have been used to examine physiological condition in sea stars and mussels. BMI, a ratio between soft tissues produced and total

somatic mass (including calcareous components such as shells or skeletons), provides broad insights about the individual's general capacity to grow and reproduce. BMI variability has been primarily associated with changes in temperature and food availability, as well as their interaction (Fitzgerald-Dehoog et al. 2012, Sanford & Menge 2007, Schneider et al. 2010). Organisms grow more if food is available. Their response to temperature, however, depends on where on a thermal performance curve they lie. Since both sites have dense mussel beds, we assume that food was not limiting and speculate on the effects of temperature. Although not significantly, *Pisaster* BMI was marginally higher at Bodega (Fig. 3.6A), which might be explained by the lower mean thermal performance observed there (Fig. 3.5; Table 3.2). Additionally, *Pisaster* variability in thermal performance was greater at Strawberry Hill, which might have lead to the slightly lower (although non-significant) BMI.

Mytilus BMI resulted higher at Strawberry Hill (Fig. 3.6B). The link with thermal performance, however, is not particularly clear given that mean performance at Strawberry Hill was lower (Fig. 3.5; Table 3.2). One explanation might be that the high extremes observed at Strawberry Hill, and not necessarily the mean values, are stimulating growth. An alternative explanation is related to food availability, which for bivalves may be given by differences in food supply or proportion of time spent submerged (feeding) (Honkoop & Beukema 1997). Because we collected mussels from approximately the same intertidal elevation at both sites, we assume that time foraging did not differ between populations. To test whether food availability varied, we compared levels of chlorophyll-a ($\mu g\ L^{-1}$) determined via satellite imaging (data retrieved from data.cencoos.org) 1km offshore from each site. Monthly measurements taken

during the five months preceding the animal collections revealed no differences between the two sites. Thus, we have no evidence to suggest that food availability explained the pattern in BMI.

As revealed by total Hsp70 expression data, we did not observe signs of sub-lethal thermal stress on the species and populations examined. First, our lab experiment showed no change in Hsp70 along an ecologically realistic range of body temperatures (Fig. 3.7A,B). This was expected given that the inducible isoform of Hsp70 is known to up-regulate in situations of more critical cellular damage (Feder & Hofmann 1999). The levels detected are most likely explained by the constitutive isoform, which is always present (Petes et al. 2008b, Place et al. 2008). We also found no differences between sites, indicating that these populations do not differ in their baseline. However, our lab experiment does not tell whether populations would respond differently under more stressful scenarios, which are possible as shown in Figure 3.2. Based on the high extremes in thermal performance data, one might expect the Strawberry Hill populations to exhibit an increased heat shock response, but this may vary between species. The heat shock response of *Mytilus* has been shown robust; individuals can acclimate to warmer conditions and up-regulate Hsp70 (Halpin et al. 2004, Petes et al. 2008b). As expected for mobile ectotherms (Huey 1991), *Pisaster* appears not physiologically adapted to cope with such insult (Petes et al. 2008b), which it avoids by relying on behavior and its high thermal inertia (Pincebourde et al. 2009).

Second, our field-collected individuals showed no signs of thermal stress both over time and between sites (Fig. 3.7C,D). Interestingly, *Mytilus* response was more variable than *Pisaster*, which again speaks to the robustness of the prey's heat shock

response (Halpin et al. 2004, Petes et al. 2008b). Also, the variability in Hsp70 production was greater at Strawberry Hill than Bodega, which also may be a consequence of the higher variability in body temperatures (Fig. 3.2) and thermal performance (Fig. 3.5) observed there.

Overall, as empirical indicators of physiological performance, BMI and Hsp70 corroborated the insights gathered through our observational-modeling approach. However, because BMI and Hsp70 depend on other intrinsic (e.g. phenotypic plasticity) and extrinsic (e.g. physical forces, food availability) processes besides temperature, which interact in complex ways, caution must be taken when drawing direct connections between them.

In summary, this study provides a novel approach for applying the ESM framework when species' nuances (behavior, physiology) do not allow for traditional experimental techniques. Using a combination of field observations and modeling, we were able to quantify thermal performance of the predator *Pisaster* and its main prey *Mytilus*. This approach deliberately sought for ecological realism. Under the thermal conditions experienced by these species over the time window evaluated at two sites, we found that the system behaved as a PSM.

Our results may have implications for future climate change scenarios. Since *Pisaster* has a generally higher T_A than *Mytilus*, warmer conditions may increase performance of the prey more than that of the predator, potentially releasing some predation pressure. On a similar analysis Freitas et al. (2007) found the opposite, as the system's preys showed lower thermal sensitivity. Given the keystone role of *Pisaster*

(Paine 1966, Paine 1974), ecological implications of this prediction may reach the community level.

An important caveat to the way we applied our approach here is that we ignored potential effects of relevant environmental parameters on individual's performance. Follow-ons to this study may incorporate these elements. The impact of multiple environmental stressors, for example, has recently regained popularity in the marine ecology literature, especially given the urgency imposed by ongoing climate change (Harley et al. 2006a). In particular, food availability may condition organisms' thermal performance response (Fitzgerald-Dehoog et al. 2012, Freitas et al. 2007), which could be considered by monitoring predators' predation and prey's availability of phytoplankton.

Conclusions

Our approach to the ESM framework provides a means for quantifying mean thermal performance in the field. Applying this approach revealed that the thermal performance of *Pisaster* is higher than that of *Mytilus*, which defines the system as PSM. *Pisaster* and *Mytilus* appear to buffer against thermal heterogeneity, characteristic of their intertidal environment, by reducing thermal sensitivity. Thus, the role of physiology appears important in driving responses in this predator-prey system. Our data lend support to the idea that variability in environmental drivers may be more important than mean values. As such, we found that thermal performance (estimated using thermal performance curves), BMI, and Hsp70 production may be responding to high temperature extremes, as opposed to mean temperatures. Movement behavior did not appear related to thermal performance. At least for the period considered, the physiological cost of thermal stress

86

did not drive *Pisaster* microhabitat use. *Pisaster* movement behavior may be driven more by alternative environmental forces such as solar radiation and desiccation, and less by temperature.

Table 3.1 Thermal sensitivity parameter values estimated for *Pisaster* and *Mytilus* individuals collected at Bodega and Strawberry. Parameter values for aquatic and aerial conditions are provided. See Materials and Methods for a description of estimation procedures.

| | *Pisaster ochraceus* | | | |
| | Bodega | | Strawberry Hill | |
	Aquatic	Aerial	Aquatic	Aerial
T_A	6200	6500	3200	3300
T_L	274	274	293	293
T_H	298	304	300	307
T_{AL}	186458	186458	4040	4040
T_{AH}	218569	218569	925180	925180

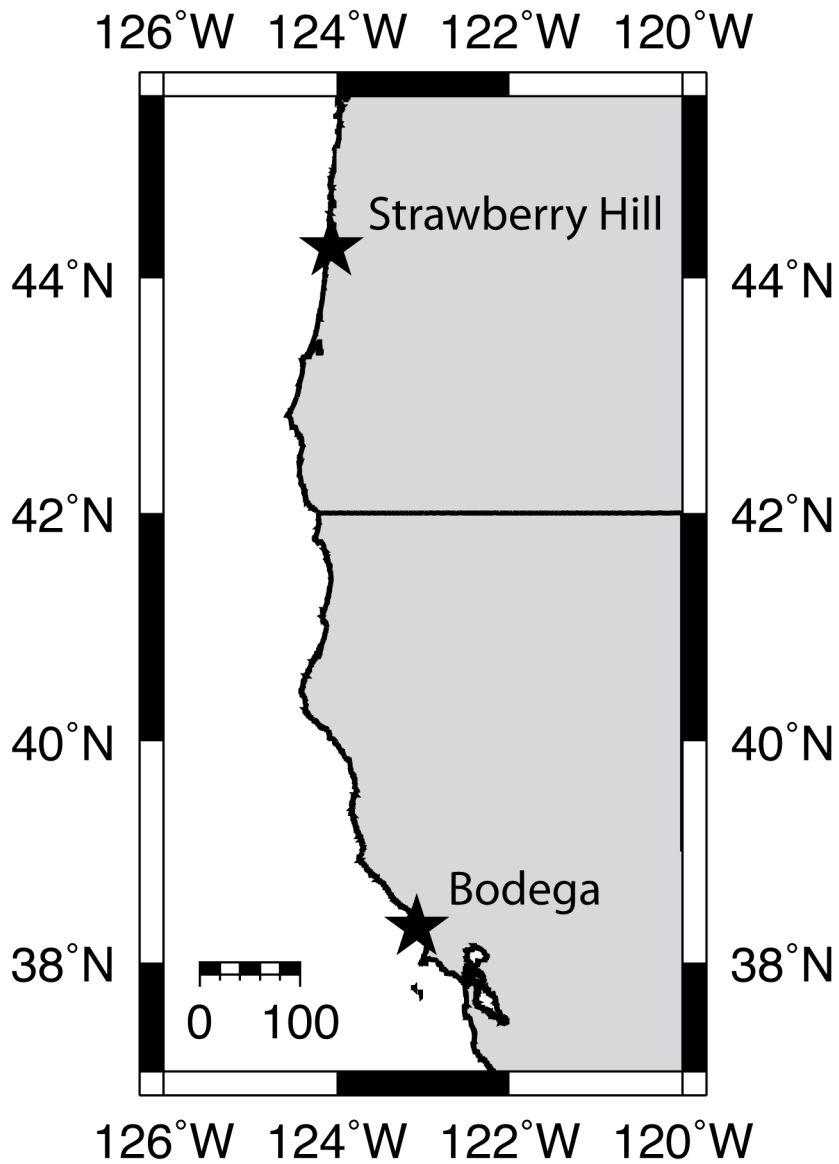| | *Mytilus californianus* | | | |
| | Bodega | | Strawberry Hill | |
	Aquatic	Aerial	Aquatic	Aerial
T_A	4200	3000	5100	3500
T_L	280	280	279	279
T_H	298	308	298	308
T_{AL}	6654	6654	5435	5435
T_{AH}	247263	247263	281782	281782

Table 3.2 Statistical results from multiple comparisons between relative thermal performances exhibited by groups of species/scenario, as illustrated in Figure 3.4. Comparisons were made using Root Mean Square Error (RMSE) and the non-parametric test Kendall's W. Comparisons that included the mobile predator involved 500 independent contrasts (one for each simulated mobile individual), in which cases statistics mean ± SEs are shown. Results are provided for both sites Bodega and Strawberry Hill.

	RMSE	Kendall's W		
		W	χ^2	P-value
Bodega				
Prey vs.				
Static predator	0.13	0.77	3604.4	$2*10^{-186}$
Prey vs.				
Mobile predator	0.15 ± 9.610^{-5}	0.62 ± 5.210^{-4}	$2884.6*2.4$	$610^{-20}\pm5*10^{-20}$
Prey vs.				
Optimal predator	0.15	0.75	3487.1	$5*10^{-146}$
Static vs.				
Mobile predator	$0.12\pm1.4*10^{-4}$	$0.76\pm5.7*10^{-4}$	3538.1 ± 2.7	$8*10^{-118}\pm8*10^{-118}$
Static vs.				
Optimal predator	0.11	0.90	4183.1	0
Mobile vs.				
Optimal predator	0.06 ± 2.310^{-4}	0.80 ± 6.710^{-4}	3723.3 ± 3.14	$110^{-161}\pm110^{-161}$
Strawberry Hill				
Prey vs.				
Static predator	0.12	0.72	3324.8	310^{-110}
Prey vs.				
Mobile predator	0.13 ± 1.410^{-4}	0.65 ± 7.110^{-4}	2979.9 ± 3.3	$810^{-28}\pm0$
Prey vs.				
Optimal predator	0.12	0.70	3232.9	710^{-90}

Static vs. Mobile predator	$0.09 \pm 1.3 \cdot 10^{-4}$	$0.74 \pm 6.7 \cdot 10^{-4}$	3420.4 ± 3.1	$2 \cdot 10^{-89} \pm 4 \cdot 10^{-88}$
Static vs. Optimal predator	0.10	0.77	3572.9	$5 \cdot 10^{-181}$
Mobile vs. Optimal predator	$0.11 \pm 2.5 \cdot 10^{-4}$	$0.75 \pm 8.4 \cdot 10^{-4}$	3447.1 ± 3.9	$3 \cdot 10^{-89} \pm 3 \cdot 10^{-88}$

Figure 3.1 Map illustrating the location of our study sites Bodega (California) and Strawberry Hill (Oregon). About ~760km of coastline separate them.
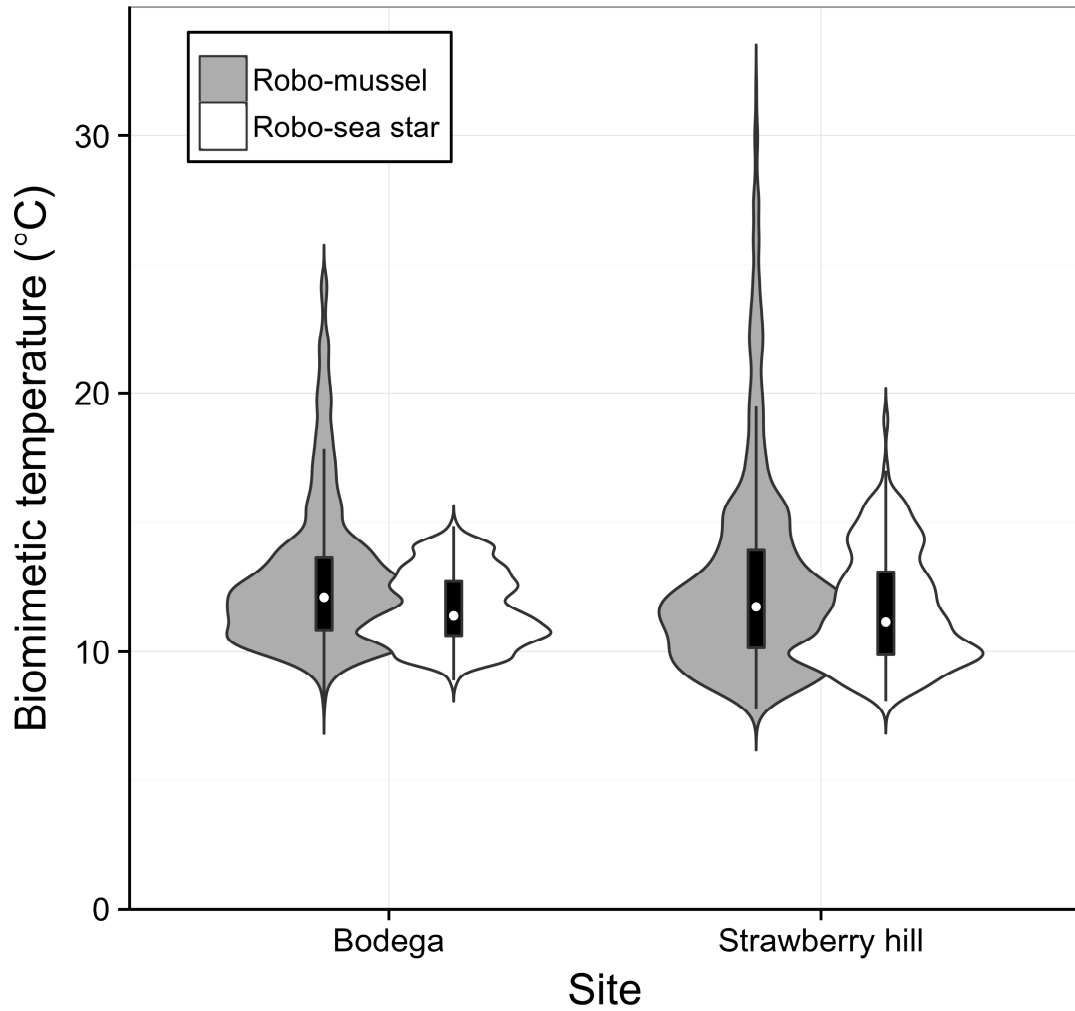
Figure 3.2 *Pisaster ochraceus* and *Mytilus californianus* biomimetic temperatures recorded in the mid intertidal zone at Bodega and Strawberry Hill during summer months of 2012 (June 22nd through August 10th). Data were collected every 30 min.
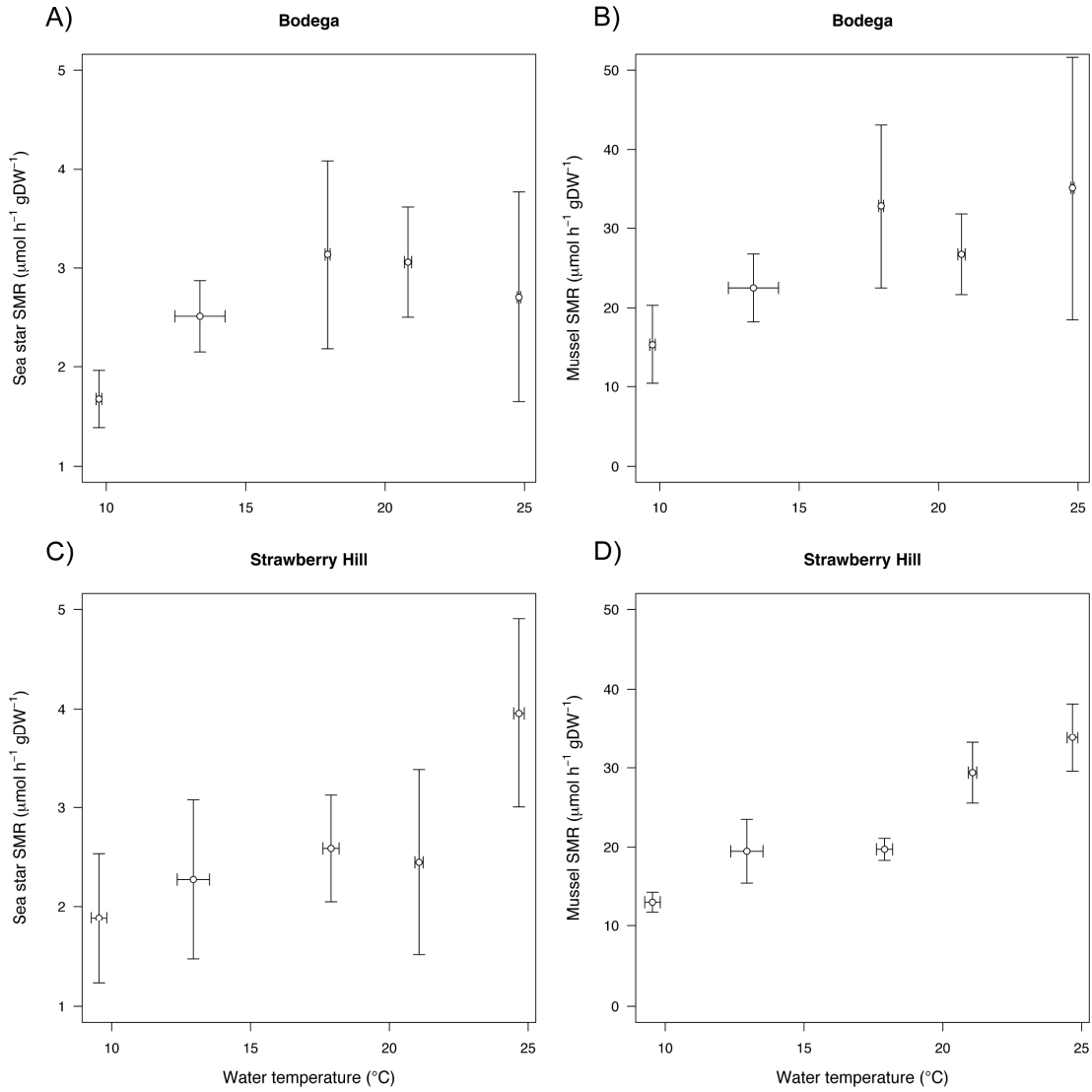
Figure 3.3 Standard metabolic rate (SMR) of the sea star *Pisaster ochraceus* and mussel *Mytilus californianus* collected from Bodega and Strawberry Hill. No data is provided for the 27°C treatment because all animals died during the first treatment day.
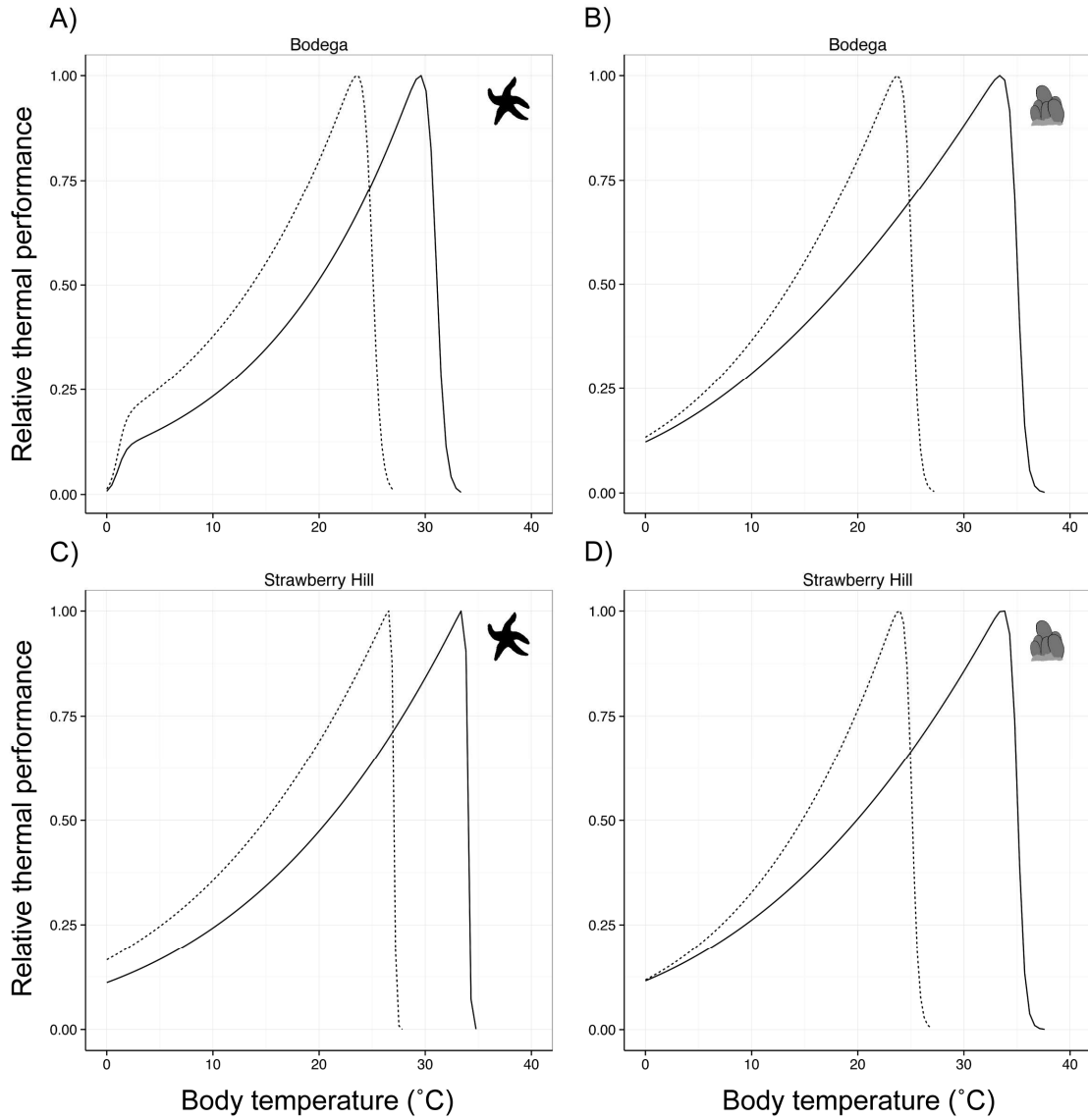
Figure 3.4 Aquatic and aerial thermal sensitivity curves described for *Pisaster ochraceus* and *Mytilus californianus* from Bodega (Panels A and B) and Strawberry Hill (Panels C and D). We estimated the aquatic curves' parameters using empirical SMR measurements (Fig. 3.3), and the aerial curves' parameters using information from the literature.
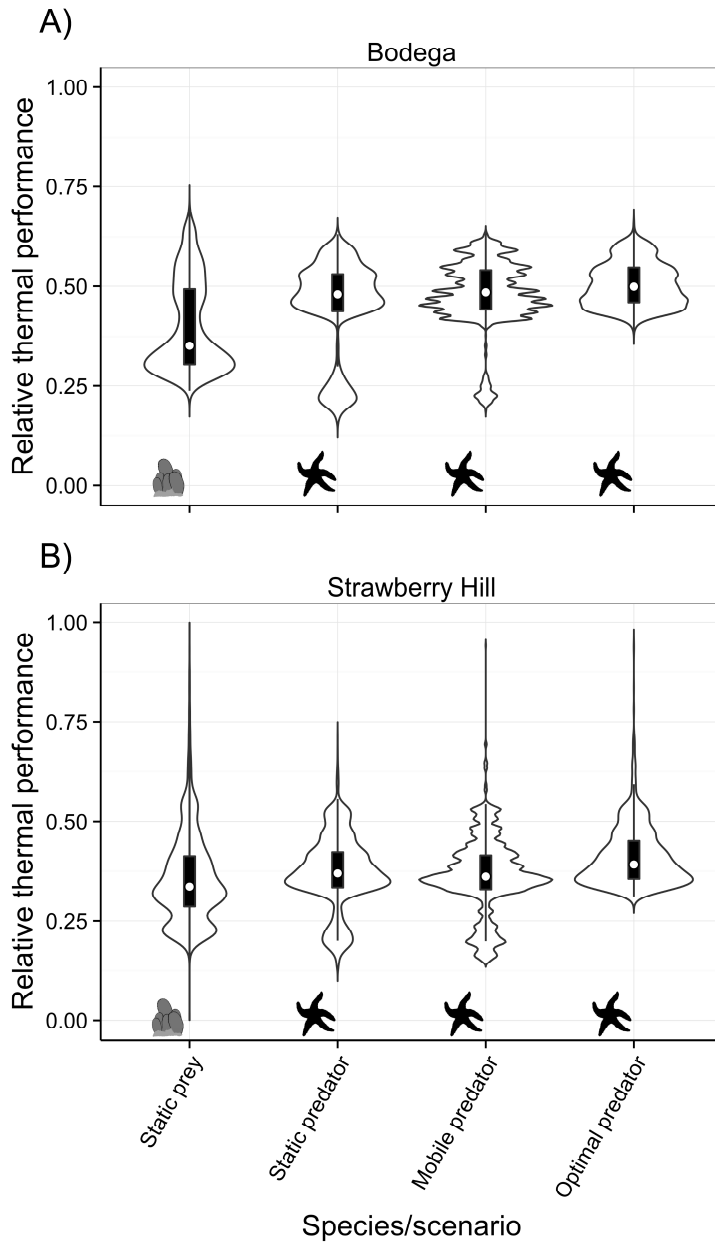
Figure 3.5 Cumulative thermal performance calculated for *Mytilus californianus* (prey) and *Pisaster ochraceus* (predator) using species- and site-specific thermal performance curves and body temperatures recorded *in situ* by biomimetic sensors. The static scenarios represent individuals that remain immobile. The mobile predator considers movements between microhabitats, as informed by regular surveys of microhabitat use. The optimal scenario represents the hypothetical situation where *Pisaster* occupies the microhabitat that reports the highest performance. Panels A and B show data from Bodega and Strawberry Hill, respectively.
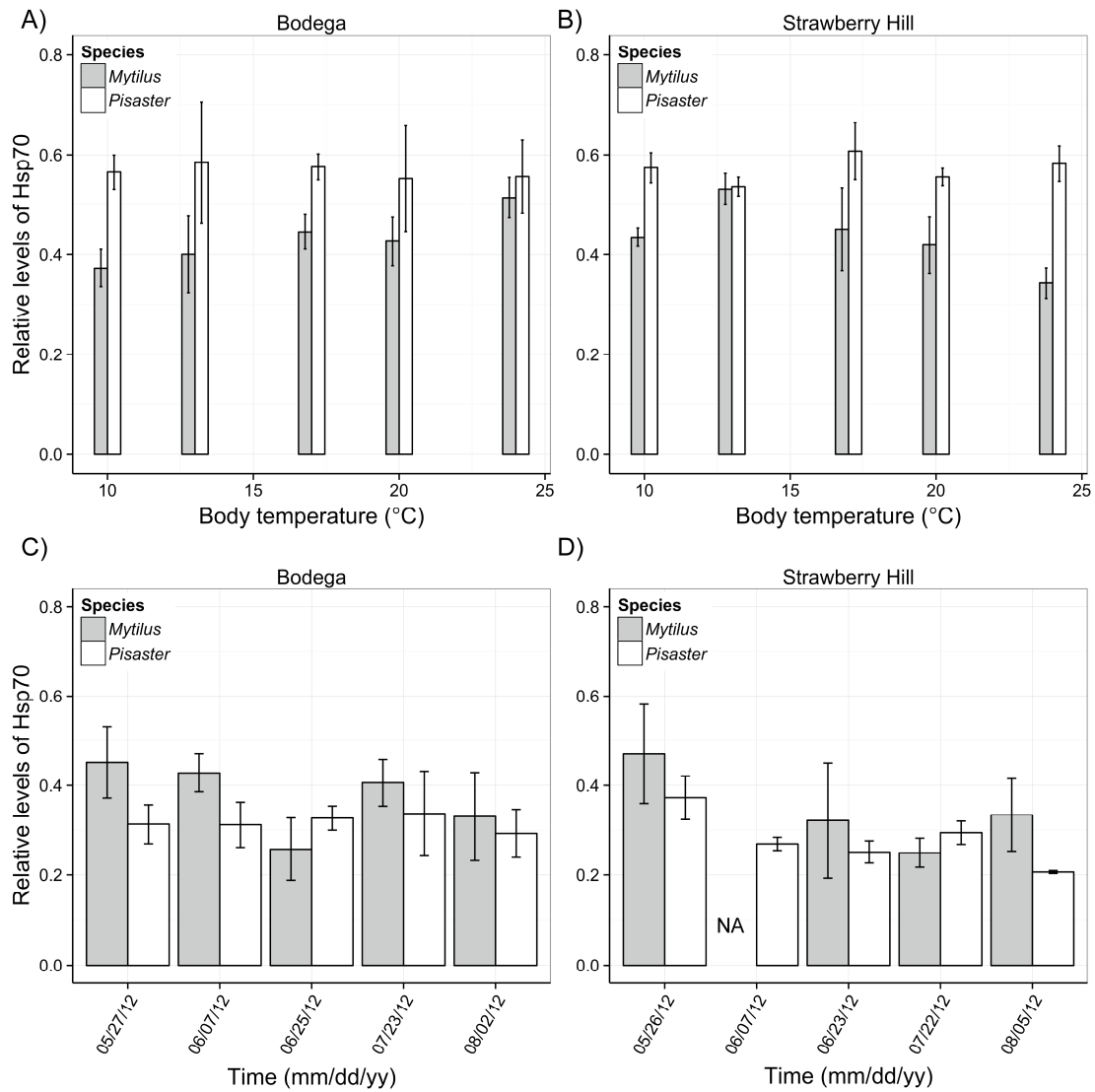
Figure 3.6 Total heat shock protein 70 (Hsp70) expression (i.e. constitutive and inducible isoforms are not differentiated) measured from *Pisaster ochraceus* tube feet and *Mytilus californianus* gill tissues. In Panels A and B, tissues were sampled after individuals had been kept at one of six seawater temperature treatments (10, 13, 18, 21, 24, and 27°C) for 4d. In panels Panels C and D, tissues were collected in the filed and immediately frozen in dry ice. Bars represent mean ± 1SE.
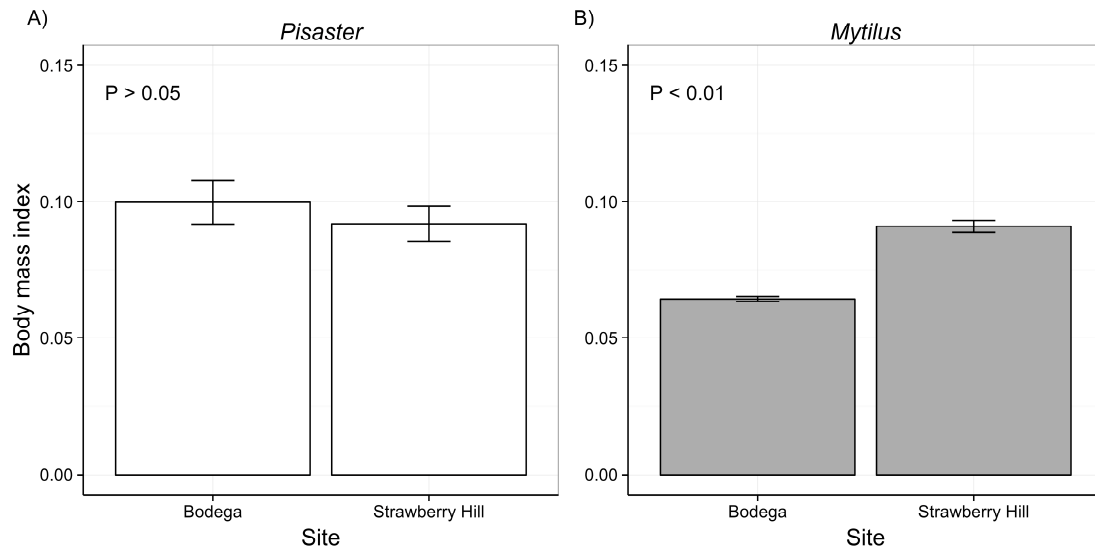
Figure 3.7 Body mass indices (BMI) of (A) *Pisaster ochraceus* and (B) *Mytilus californianus* individuals collected at Bodega and Strawberry Hill during the summer of 2012. P-values obtained from Welch's t-tests indicate whether differences between sites were significant.

CHAPTER 4

A DYNAMIC ENERGY BUDGET (DEB) MODEL FOR THE KEYSTONE PREDATOR

PISASTER OCHRACEUS[3]

ABSTRACT

We present a Dynamic Energy Budget (DEB) model for the quintessential keystone

predator, the rocky-intertidal sea star *Pisaster ochraceus*. Based on first principles, DEB

theory is used to illuminate underlying physiological processes (maintenance, growth,

development, and reproduction), thus providing a framework to predict individual-level

responses to environmental change. We parameterized the model for *P. ochraceus* using

both data from the literature and experiments conducted specifically for the DEB

framework. We devoted special attention to the model's capacity to (1) describe growth

trajectories at different life-stages, including pelagic larval and post-metamorphic phases,

(2) simulate shrinkage when prey availability is insufficient to meet maintenance

requirements, and (3) deal with the combined effects of changing body temperature and

food supply. We further validated the model using an independent growth data set.

Using standard statistics to compare model outputs with real data (e.g. Mean Absolute

Percent Error, MAPE) we demonstrated that the model is capable of tracking *P.

ochraceus*' growth in length at different life-stages (larvae: MAPE=12.27%; post-

---

metamorphic, MAPE=9.22%), as well as quantifying reproductive output index.However, the model's skill dropped when trying to predict changes in body mass (MAPE=24.59%), potentially because of the challenge of precisely anticipating spawning events. Interestingly, the model revealed that *P. ochraceus* reserves contribute little to total biomass, suggesting that animals draw energy from structure when food is limited. The latter appears to drive indeterminate growth dynamics in *P. ochraceus*. Individual-based mechanistic models, which can illuminate underlying physiological responses, offer a viable framework for forecasting population dynamics in the keystone predator *Pisaster ochraceus*. The DEB model herein represents a critical step in that direction, especially in a period of increased anthropogenic pressure on natural systems and an observed recent decline in populations of this keystone species.

INTRODUCTION

Improving our ability to anticipate responses of natural systems to environmental change is among the most pressing challenges facing modern ecological theory (Denny & Helmuth 2009). Efforts have been confounded by the inherently complex nonlinear dynamics of such systems (Monaco & Helmuth 2011, Mumby et al. 2011, Peters et al. 2007). However, the physiological responses of individuals may be considered as the underlying basis of all ecological dynamics, thus providing a solid foundation for advancing the field of ecological forecasting (Denny & Helmuth 2009). Studies at the organismal level have emphasized that some of the first responses to climate change may lie not in mortality but in changes in growth and reproduction (Newell 1970, Petes et al. 2007) and in the strength of species interactions (Kordas et al. 2011, Petes et al. 2008b, Wethey 2002). Particularly promising are bioenergetics studies that quantify flows of

energy and mass through an individual, which in turn dictate levels of physiological performance including feeding, growth and reproduction. This provides a mechanistic framework that can help characterize physiological responses to current and projected environmental drivers as a consequence, for example, of increasing temperatures (Kearney et al. 2010).

Predictive frameworks based on bioenergetics have been used for a wide range of species from a variety of taxa, and range in complexity from fairly simple to very elaborate (Kooijman 2010). However, given the complex nature of some of the threats currently faced by natural systems (e.g. climate change, ocean acidification, pollution), where intertwined direct and indirect effects can impact multiple species simultaneously, the most efficient approach may be to concentrate on ecologically important players, whose dynamics can exert cascading effects on populations and communities (Connell et al. 2011, Kordas et al. 2011). Following this reasoning, keystone species (Mills et al. 1993, Paine 1966) may serve as ideal candidates for investigating and modeling the physiological mechanisms that ultimately mediate ecological processes (Sanford 2002b). Particularly, keystone predators – consumers that can remove competitive dominants or otherwise have impacts on an ecosystem disproportionate to their abundance (Duggins 1980, Fauth & Resetarits 1991, Paine 1966) – have received much attention. Despite our generally good understanding of the links between the physiological condition of many species and their interactions with their environment (i.e. eco-physiology), few quantitative physiological models have been developed for keystone predators, and specifically there is a pressing need for models of feeding, growth and reproduction, and their response to changes in environmental drivers (André et al. 2010).

Here we describe a Dynamic Energy Budget (DEB), an individual-based mechanistic energetics model (Kooijman 1986, 2010), for the quintessential keystone predator, the rocky-intertidal sea star *Pisaster ochraceus* (Brandt 1835) (hereafter, *Pisaster*). By preferentially foraging on a dominant space-competitor, the mussel *Mytilus californianus*, *Pisaster* has profound impacts on intertidal community assemblages (Menge et al. 1994, Paine 1966). Exploiting the virtues of DEB theory, we describe a model that can (1) predict *Pisaster* growth at larval and post-metamorphic stages when prey are abundant and available *ad libitum*, (2) characterize shrinkage when food is removed, and (3) illuminate dynamics in physiological processes driven by cumulative effects of temperature and prey availability. This model represents a critical first step in exploring, and forecasting how variation in environmental drivers will likely affect the physiological performance and rates of foraging of this keystone predator (Sanford 2002a). Such an understanding is especially timely given the recent widespread mortality of *Pisaster* being observed on the Pacific coast of North America (Eric Sanford, pers. comm.).

While several bioenergetics models seeking to relate metabolic organization to aspects of physiological performance exist, DEB theory is gaining increased popularity because of its ability to model underlying physiological processes (maintenance, growth, development, and reproduction) based on first principles, that are common to all life forms including different taxa and life stages (Sousa et al. 2010). Unlike net-production models (e.g. scope for growth), which maintain that assimilated energy is partitioned between maintenance and growth/reproduction, DEB theory assumes that energy is first stored as reserves, and then distributed among physiological processes (Filgueira et al.

2011). This topology offers solutions for multiple biological problems (Kooijman 2010), three of which we emphasize here given their importance for *Pisaster*. Firstly, we rely on the capacity of the DEB to mechanistically describe the whole life cycle of a generalized organism without having to modify the structure of the model throughout ontogeny (Nisbet et al. 2012). This is accomplished by explicitly accounting for energetic requirements associated with the life-history processes of maturation and maturity maintenance. Incorporating these costs is non-trivial from both physiological and ecological standpoints, as highlighted by a growing body of literature revealing that challenges faced by individuals early in life can impair performance at later stages (Emlet & Sadro 2006, Gebauer et al. 1999, Hettinger et al. 2013, Pechenik 2006, Richmond et al. 2007). Since the keystone role of *Pisaster* is restricted to its benthic life stages, efforts to model the influence of environmental variables on its physiological condition have mainly focused on post-metamorphic stages (but see George 1999, Gooding et al. 2009, Pincebourde et al. 2012, Sanford 2002b). Notably, however, an important portion of its existence occurs as a planktotrophic larva (Strathmann 1971). The model presented here exploits the capacity of DEB theory to account for maturation and maturity maintenance and, building upon available data for both larval (George 1999) and post-metamorphic stages (Feder 1956), provides a means for simulating growth trajectories of *Pisaster* throughout ontogeny.

Secondly, a reserve compartment provides organisms with a physiological buffer against environmental fluctuations, by which vital rates and dynamics of structural mass are partially independent of changes in prey availability. DEB theory thus offers a framework for accounting for time history aspects of environmental signals. Weight-loss

102

and shrinkage (i.e. reduction in structure to pay for somatic maintenance (Kooijman 2010)) are common for some intertidal organisms such as annelids, echinoderms, and cnidarians (Feder 1956, Linton & Taghon 2000, Sebens 1987, Tenore & Chesney 1985) frequently having to cope with severe energy limitations due to abiotic (e.g. waves, heat and desiccation stress) and biotic conditions (e.g. competition, low prey availability). In an attempt to improve the accuracy of the model with respect to starvation, we include an additional parameter calibrated using data from controlled laboratory observations.

Thirdly, organisms rarely face single stressors in nature (Sokolova & Lannig 2008); instead, the environment tends to challenge individuals through cumulative effects of multiple factors. As has been well established, the relative importance of predatory species on their communities is largely determined by their sensitivity to varying conditions of body temperature and food (Bertness & Schneider 1976, Burrows & N. 1989, Dell et al. 2013, Freitas et al. 2007, O'Connor et al. 2009). Surprisingly, despite widespread recognition of the critical ecological role of keystone predators, few models have been developed that account for the interactive effects of these variables on their physiological condition. Developing such models is particularly necessary for species experiencing extreme variability in environmental conditions. Throughout its wide range of distribution along the west coast of North America (between Alaska and Baja California), *Pisaster* encounters large temporal and spatial variation in temperature and prey availability, so a model capable of accounting for the cumulative effects of simultaneous changes in these variables should prove especially useful. If we are to predict responses of individuals to natural and/or anthropogenic pressures it is therefore crucial to account for multiple sources of stress (Howard et al. 2013). Due to logistic and

103

conceptual challenges, designing experiments that provide comprehensive, yet easy-to-interpret data has troubled eco-physiologists hoping to bridge the gaps between empirical observations and estimates of fitness (Sokolova 2013). Based on individual bioenergetics, DEB theory provides a general (i.e. non taxon-specific) framework that can be utilized to uncover physiological mechanisms by which multiple stressors combine to impact performance in organisms (Flye-Sainte-Marie et al. 2009, Kooijman 2010, Sokolova 2013). To incorporate these effects, the model described here is based on empirically-derived estimates of temperature sensitivity, feeding functional response, and starvation dynamics of *Pisaster*.

The DEB model builds on both observational studies, which provide information of the basic biology of *Pisaster*, and manipulative studies addressing the effects of changes in body temperature on metabolic, feeding, and growth rates. These data were obtained both from the literature and from our own experiments, which were especially designed for DEB modeling purposes. Our aim is to provide an individual-based mechanistic model that can characterize the physiological condition of *Pisaster* throughout ontogeny, and in response to cumulative effects of changes in body temperature and prey availability across its geographic range.

MODEL DESCRIPTION

Dynamic Energy Budget (DEB) theory describes energy and mass flows in an individual organism (Fig. 4.1) throughout its life history. In its purest form DEB considers an archetypal individual that is representative of all individuals of the species, although several authors have extended the theory to examine intraspecific variability, such as occurs along latitudinal gradients (Freitas et al. 2007). The model herein was first

developed following the assumptions of a standard DEB model (i.e. one reserve compartment, one structure compartment, isomorphic growth). While excellent comprehensive descriptions of the standard DEB model and its fundamentals are provided elsewhere (Kooijman 2010, Sousa et al. 2010, van der Meer 2006), we offer a basic explanation of the formulations that orchestrate our generalized model in the Appendix B. As illustrated in Figure 4.1, the model tracks dynamics of four state variables (reserve, structure, maturation, and reproductive buffer), which depend on energy flows (units of J d^{-1}; represented by arrows). Energy assimilated from food at rate $\dot{p}_A$, first enters the reserve compartment. Energy can then be mobilized at rate $\dot{p}_C$, and allocated depending on the parameter kappa (k) (Kooijman 1986, 2010), which amounts to a fixed fraction of energy used for somatic maintenance at rate $\dot{p}_M$, plus growth at rate $\dot{p}_G$. The remainder, $\dot{p}_C(1-k)$, goes to maturity maintenance at rate $\dot{p}_J$, plus reproduction at rate $\dot{p}_R$.

The standard DEB model (Appendix B) was modified to incorporate relevant aspects of *Pisaster* life-history. Specifically, we accounted for growth during larval stage, the ability of individuals to shrink (i.e. compensate for somatic maintenance costs using structure) when starved, and species-specific rules for energy expenditure in spawning. The steps taken to incorporate these aspects into the standard model (Appendix B) are detailed below.

Pisaster ochraceus **DEB model structure**

Since relevant information for the different life-stages of *Pisaster* was available in the literature, it was possible to build a model that encompasses the whole life-span of a generalized individual, accounting for changes in morphology, energy allocation rules,

and growth patterns that follow when transitioning between stages (Jusup et al. 2011, Nisbet et al. 2000, Pecquerie et al. 2009).

Including a larval stage implies deviations from the standard DEB model due to violations of the isomorphy assumption arising from the stark morphological differences between *Pisaster* larval and post-metamorphic stages (planktonic ciliated swimming larva vs. benthic juvenile and adult). Standard DEB models use one shape coefficient, δ_M, to convert physical lengths, L_W (e.g. larval length), to structural lengths, L (a useful theoretical measure of size that directly relates to the state variable structure and is not influenced by the organism's shape), through the equation $L = \delta_M \cdot L_W$. Because morphology differs between the larval and post-metamorphic stages, the relationship between physical and structural length needs to be described independently for each stage, which we do here by estimating two shape coefficients, $\delta_{M.lrv}$ and δ_M, respectively. Violating the isomorphy assumption also implies that surface-area is proportional to volume[1] instead of volume$^{2/3}$ – as for isomorphs (Kooijman et al. 2011). As a consequence, growth during larval development is accelerated (George 1999), which is therefore better described by an exponential rather than the asymptotic von Bertalanffy growth model (Kooijman et al. 2011). Indeed, using data from George (1999) and Pia et al. (2012), we found that larval surface-area was proportional to volume$^{0.97}$, an exponent that is not statistically different from 1.0. It has been argued that, as a result, the processes of assimilation and mobilization rates (Appendix B, equations 1 and 3, respectively) increase during larval development (Jusup et al. 2011, Kooijman 2010). Since somatic maintenance is proportional to volume (Appendix B, Eq. 4), there

is no limit to the increase in structure (Kooijman et al. 2011), in agreement with observations (George 1999, Jusup et al. 2011, Pecquerie et al. 2009).

The increase in both processes $\dot{p}_A$ and $\dot{p}_C$ during the larval phase has been modeled by means of a shape correction function, M (following Jusup et al. 2011):

$$M\left(L, E_H\right) = \begin{cases} 1 & E_H < E_H^b & \text{(fertilization to feeding larva)} \\ L/L_b & E_H^b \leq E_H < E_H^j & \text{(feeding larva to metamorphosis)} \\ L_j/L_b & E_H^j \leq E_H & \text{(life after metamorphosis)} \end{cases}$$

(1)

where L is structural length (cm) and E_H is energy allocated to maturation (J). L_b and L_j correspond to structural lengths (cm) at birth and metamorphosis, respectively. Parameters E_H^b and E_H^j are defined as the energy invested in maturity (J) for reaching "birth" as a feeding larvae and metamorphosis, respectively (Table 4.1). Because M is applied to those processes containing the parameters $\{\dot{p}_{Am}\}$ and $\dot{v}$ (Appendix B, equations 1 and 3), it may strongly influence all processes that depend on them. Importantly, it will have an impact on the expected asymptotic body length, L_∞ (Kooijman et al. 2011).

As is the case for many marine invertebrates (e.g. anemones, urchins), sea stars have indeterminate growth, and size dynamics may vary dramatically according to habitat conditions. When starved during extended periods these organisms lose weight (Feder 1956, Sebens 1987). Initially, there is a reduction of stored reserves (Ren & Schiel 2008, Sarà et al. 2013), but once these are depleted, the overarching priority given to the process of somatic maintenance, $\dot{p}_M$, would presumably lead to a reversing of energy/mass flux from structure to cover the costs of living, and the organism shrinks (

107

$\dot{p}_G$ becomes negative, Fig. 4.1) (Kooijman 2010). The assumption that somatic

maintenance is prioritized has been empirically confirmed for *Pisaster ochraceus* (Nimitz

1971, 1976) and its congener, the subtidal *Pisaster giganteus* (Harrold & Pearse 1980).

Histological studies with *Pisaster* further revealed that during prolonged starvation

energy reserves contained in the pyloric caecum decrease to levels insufficient for gonad

production (Nimitz 1971, 1976), thus compromising reproduction in favor of somatic

maintenance.

Due to thermodynamic constraints, mobilizing energy from structure to somatic

maintenance is less efficient than mobilizing it from the reserve compartment (Kooijman

2010, Sousa et al. 2010). To account for the physiological adjustments during periods of

prolonged starvation (i.e. when mobilized energy cannot cover somatic maintenance,

$k \cdot \dot{p}_C - \dot{p}_{VM}$), we introduced a new parameter, $\left[\dot{p}_{VM} \right]$ (J d^{-1} cm^{-3}), which adjusts the rates

at which structure shrinks, $-\dot{p}_G$, and somatic maintenance is paid, $\dot{p}_{VM}$ (J d^{-1}):

$$\dot{p}_G = \kappa \cdot \dot{p}_C - \dot{p}_{VM}$$
$$\dot{p}_{VM} = \left[\dot{p}_{VM} \right] \cdot L^3$$

(2)

Also, to characterize the effect of starvation on maturity and maturity maintenance, we

followed the approach used by Augustine et al. 2011 (Augustine et al. 2011). During

periods when mobilized energy cannot cover maturity maintenance, i.e. $\dot{p}_C \cdot (1-\kappa) < \dot{p}_J$,

change in maturity ($\dot{p}_R$; Appendix B, Eq. 8) is calculated as:

$$\dot{p}_R = -\dot{k}_J \cdot \left(E_H - \frac{\dot{p}_C \cdot (1-\kappa)}{\dot{k}_J} \right)$$

(3)

The rules for emptying the reproductive buffer are defined based on species-specific considerations. Evidence shows that gametogenesis in *Pisaster* is driven by annual changes in photoperiod (Pearse et al. 1986). Gonadal volume increases towards the winter months, and gametes are released during late spring and early summer depending on latitude (Fraser et al. 1981, Mauzey 1966, Sanford & Menge 2007). Our model makes the simple assumption that all individuals empty their reproductive buffer as gonads every 365d.

Going from the DEB model to traditional metrics of growth and reproduction

DEB model quantities can be converted from more traditional metrics reported in the literature to estimate parameter values used in the model. Conversely, comparison of metrics generated from DEB to traditional metrics (not used in model parameterization) provides an opportunity to independently train and validate model outputs. Two commonly used metrics of the size of sea stars are arm length, L_w (cm), and wet weight, W_w (g). Arm length can be obtained from the quotient between structural length and shape coefficient (Appendix B). Wet weight is calculated from structure, reserve and reproductive buffer (Kooijman 2010):

$$W_W = d_V \cdot L^3 + \rho_E \cdot (E + E_R)$$

(4),

where d_V (g cm^{-3}) is density of structure, assumed to equal 1, and ρ_E (4.35·10^{-5} g J^{-1}) is weight-energy ratio for a generalized reserve molecule (Lika et al. 2011a), calculated from the per carbon atom molecular weight w_E (23.9 g mol^{-1}) and chemical potential of reserves $\bar{\mu}_E$ (550 kJ mol^{-1}): $\rho_E = w_E / \bar{\mu}_E$. Note that ρ_E transforms energy to weight of reproductive buffer as well.

Additionally, estimates of reproductive potential are often employed as proxies for fitness. Reproductive potential in asteroids, commonly known as Reproductive Output index (*RO*, dimensionless) or Gonadal Index, the ratio between the gonadal and somatic mass (Mauzey 1966, Petes et al. 2008a, Sanford & Menge 2007), can be described in DEB terms by the following equation:

$$RO = \frac{\rho_E \cdot E_R}{d_V \cdot L^3 + \rho_E \cdot E}$$

(5).

PARAMETER ESTIMATION AND MODEL TRAINING

The DEB parameter values for *Pisaster* were estimated by the covariation method (Lika et al. 2011a, Lika et al. 2011b) implemented in the MATLAB 2010 software package DEBtool (available at http://www.bio.vu.nl/thb/deb/deblab/debtool/), which employs a Nelder-Mead numerical optimization to minimize the difference between observed and predicted values based on a weighted least-squares criterion. The estimation procedure simultaneously uses both real data from observational and manipulative studies and pseudo-data from theory in the parameter fitting process (Jusup et al. 2011, Matzelle et al. 2014). This approach is possible because DEB theory is formulated under the premise that all living organisms regulate metabolic processes using more or less the same mechanisms. Given this assumption we can describe these processes with a set of DEB parameters, and it follows that differences between species are underpinned by variations in parameter values among common mechanisms (Lika et al. 2011a).

The covariation method can accommodate diverse data sets that provide information about the basic biology of the target species, including size/age at transitions between life stages, growth, feeding, or reproductive output measurements, as well as

110

data sets generated to estimate DEB theory quantities. We used the covariation method to (1) estimate DEB parameters for which we had no real data (e.g. $\delta_{M.lrv}$), and to (2) optimize the estimates obtained for parameters we determined empirically (e.g. δ_{M}) (Table 4.1). Our training phase used field and laboratory measurements of size at age, laboratory functional response data, field and laboratory measurements of reproductive output, and laboratory measurements of thermal sensitivity of metabolism. The data sets used for parameterizing and training the DEB model for *Pisaster* are detailed below. All information collected from figures found in the literature for which no data tables were provided was extracted using *DataThief III* (Tummers 2006). All animals used for experimental and observational purposes were collected with permission granted by the California Natural Resource Agency, Department of Fish and Game (Scientific Collection Permit, ID Number: SC-11078).

Data sets

Growth and shrinkage: Growth time-series are of great value for estimating DEB parameters, but only if accurate body temperature and food availability data are also available (Kearney et al. 2010, Kooijman et al. 2008). Because body temperature and food availability data are often limited, parameter estimations may be based on observations made over short time windows. This reduces confidence in the model's ability to simulate performance over prolonged periods of time, where digestion limitations are possibly defining maximum feeding and growth rates (Zwarts & Blomert 1992). We used growth data for the larval and adult stages available from George (1999) and Sanford (2002a), respectively. Data retrieved from both sources were collected from individuals fed *ad libitum* (i.e. *f*=1), and both studies reported water temperatures.

Changes in larva width, $L_{W.lrv}$(cm), were used as a metric of larval growth, while changes in arm length, L_W (cm), were used to assess growth during post-metamorphic stages.

We conducted a laboratory experiment to quantify long-term changes in size during starvation (i.e. f=0), and ultimately to determine the parameter $\left[\dot{p}_{VM} \right]$. Mature individuals (~100g) were kept in a 2600-L recirculating seawater tank (temperature controlled at 12˚C; provided with a protein-skimmer; water chemistry monitored every other week and partial water changes conducted accordingly) for 467d (N=5) and 152d (N=1), and wet body weight, W_W (g), was measured at irregular intervals ranging from 1 to 10wk. Data collected for each individual were compared to DEB predictions obtained from the parameterized model. Values of $\dot{p}_{VM}$ were adjusted until a minimum deviation between observations and predictions was found, based on a root-mean-square error (RMSE) criterion. Shrinkage volume-specific cost of maintenance during prolonged starvation, $\left[\dot{p}_{VM} \right]$, values from all individuals were averaged to determine the overall best estimate.

Life-stage transitions: Growth data were complemented with information about size and age at transitions between stages: "birth", defined as the onset of larval feeding, occurs around day 9-10 after fertilization (Fraser et al. 1981), when $L_{W.lrv} = $ ~0.03cm (12˚C) (George 1999); larvae reach competency to metamorphose and settle after ~50d post-fertilization (12-15˚C) (Vickery & McClintock 2000); and puberty has been estimated under field conditions around age 5y, when wet weight is ~70-90g (Menge 1975).

Reproductive potential: Reproductive potential can be estimated from studies conducted in the field or in the laboratory, as long as relative levels of resource availability are known (e.g. Jusup et al. 2011, Pecquerie et al. 2011). We used field data from Sanford and Menge (2007); specifically the highest value for Reproductive Output index reported, i.e. $RO = 0.23$. Similar values have been reported from laboratory experiments where *Pisaster* was given *ad libitum* food supply (Pearse et al. 1986).

Feeding functional response: We estimated the half-saturation coefficient X_κ through a mesocosm experiment conducted at Bodega Marine Laboratory (BML, UC-Davis) in July 2012. Feeding rates of individual sea stars (200g wet weight) were measured in five food density treatments (5, 11, 21, 32, and 48 mussels m^{-2}; *Mytilus californianus*; 2-cm shell length). Five 300-L tanks supplied with running seawater were each divided in fourths (0.57m^2) to allow for 20 simultaneous feeding rate observations. Sea stars were collected at Bodega Bay, CA (38°18'16" N, 123°03'15" W) and kept individually under running seawater for one week prior to the experiment. Individuals were starved for six days, and fed *ad libitum* on day seven to standardize hunger. On day eight each animal received a randomly chosen food density treatment, and was allowed to forage for seven hours. Eaten mussels were then quantified and their tissue dry weight determined from an empirical relationship based on mussel shell length:

$DW_{tissue} = 0.0088 \cdot L_{shell}^{2.7}$ (N=98, r^2=0.98). Feeding rates, expressed as consumed

DW_{tissue} h^{-1}, were then scaled by the maximum value to obtain *f*. The relationship between food density and *f* (Appendix B, Eq. 1) was fitted using a non-linear least-square regression, which yielded an estimate for X_κ.

Temperature sensitivity: The sensitivity of *Pisaster* to changes in temperature was determined from O_2 consumption measurements taken in five water temperature treatments: 10, 14, 18, 20, 24 and 26°C. Sea stars (mean ± SE = 105.4 ± 5.2g wet weight, N=48) were collected at Bodega Bay, CA (38°18'16"N 123°03'15"W) and kept in tanks with running seawater (10.8 ± 0.7°C, mean ± SD) and *ad libitum* food supply (*Mytilus californianus* mussels) at BML for 5d before experimental temperatures were adjusted. Pairs of individuals were then transferred to 60-L aquaria filled with 1-µm filtered seawater at ambient temperature (~12°C). Experimental water temperatures were achieved by keeping the aquaria in climate-controlled rooms. The two highest treatment temperatures were reached using 100-W aquarium heaters (Marineland Visi-Therm, USA). Water temperatures were changed at a rate of ~1°C h^{-1}. Individuals were kept at desired temperature treatments for 4d before measuring O_2 consumption rates. To maintain water quality, tanks were equipped with air-stones and submersible pumps. Water chemistry (salinity, pH, ammonia, nitrite, and nitrate) was monitored every other day using a saltwater test kit (API, USA), and partial water changes were performed when needed (every 1-2d). Individuals were then placed in cylindrical watertight chambers (2.88L) filled with aerated, 1-µm filtered seawater, at its corresponding treatment temperature. A magnetic stir-bar kept the water circulating during measurements. A Clark-type electrode (HANNA-9143, USA), fitted over the top of each chamber, was used to measure dissolved O_2 concentration (ppm) at 10 and 40 min after sealing the chamber. Trials were terminated early if oxygen concentration dropped below 70% of the initial reading. The change in O_2 content was standardized by the

animal's dry mass. For each temperature treatment, two sea star-free chambers were used as blanks to account for background changes in O_2 concentration.

The temperature sensitivity experiment was run twice (August 2011 and July 2012). This data set was complemented by measurements of growth rate taken at ~5°C by Gooding et al. (2009). These data were then used to optimize thermal sensitivity parameters (Table 4.1). Arrhenius temperature, T_A, was estimated from the slope of an Arrhenius relationship (Freitas et al. 2007) using measurements taken at 10, 14, 18 and 20°C. Once T_A was known, a grid-search was conducted to find the combination of parameter values for T_L, T_H, T_{AL}, and T_{AH} that minimized the RMSE between observed and simulated data. Maximum and minimum parameter values evaluated by the grid-search were determined by the range of values reported for a collection of species modeled through DEB, available on-line (http://www.bio.vu.nl/thb/deb/deblab/). The fitted curve was then scaled in relation to its maximum value to force the curve's maximum through one.

Post-metamorphic shape coefficient: The post-metamorphic shape coefficient, δ_M, of *Pisaster* was first estimated from the empirical relationship: $W_W = (\delta_M \cdot L_W)^3$, described using data of arm length (cm) and wet weight (g) from 457 individuals collected at Bodega Bay (38°18'16" N, 123°03'15" W). The estimate obtained from this analysis was then treated as an initial value in the covariation method. The new optimized estimate provided a closer approximation of the contribution of structure to body weight.

Parameter sensitivity analysis: A parameter sensitivity analysis was carried out by varying each parameter by 10% and quantifying the percent effect on observed length

at age 2y. Sensitivity is the ratio of the percent change in length at age 2y to the percent change in the parameter. This is equivalent to the partial derivative of length with respect to variation in a single parameter.

MODEL VALIDATION

Having estimated model parameter values for *Pisaster*, we validated the model predictions against growth data from 24 adult and juvenile sea stars kept individually by Feder (1956). His data were chosen because they are the only long-term time series available (~1.6y), produced using individuals kept under controlled laboratory conditions; food was provided *ad libitum* and water temperature is reported. Additionally, since growth was measured as a change in length and weight, we could use these data to evaluate our model's capacity to predict variation in body mass due to spawning events.

Because the estimated parameters varied around a mean (Table 4.1), we simulated 1000 possible growth trajectories resulting from combinations of parameter values sampled from normal distributions defined by their average and standard deviation (Table 4.1).

Statistical comparisons between observed and predicted data were performed using standard model skill metrics Mean Absolute Error (MAE), Mean Absolute Percent Error (MAPE), and Root Mean Square Error (RMSE), a conservative measure of the absolute magnitude of error (Hyndman & Koehler 2006). Generally, we regarded a fit to be good when MAPE did not exceed 10%.

The statistical language R (R Core Team 2013) was used to carry out all calculations.

116

Model training results

DEB model parameter values for *Pisaster* were successfully estimated through the covariation method using data from both, experiments conducted specifically to determine DEB quantities and from the literature (Table 4.1). Note that while some parameters could be estimated with high accuracy, others suffer from important variance. Given the generality of a model designed to characterize a broad range of physiological processes regulating life-history traits throughout ontogeny, it is expected that some parameters are harder to determine. In particular, maturity at puberty, E_H^p, shape coefficient of larvae, $\delta_{M.lrv}$, and maturity-maintenance rate coefficient, $\dot{k}_J$, showed high variability (Table 4.1) because we lacked direct observations to estimate them. Future applications of this model should consider the uncertainties of these parameters, and possibly work towards reducing them.

The half-saturation coefficient, Arrhenius temperature, and post-metamorphic shape coefficient were estimated directly from our data (Kooijman et al. 2008). The non-linear least square regression from the feeding experiment yielded an estimate of 13.9±2.3 mussels m^{-2} for the half-saturation coefficient (Fig. 4.2). The grid-search for the thermal-sensitivity parameter yielded a RMSE between scaled data and model predictions of 0.22 (Fig. 4.3). The post-metamorphic shape coefficient, δ_M, first empirically estimated to be 0.59±0.05, was then optimized with the covariation method, yielding a final value of 0.52±0.03 (Fig. 4.4).

We combined these empirically determined parameters with data from the literature, in an effort to simultaneously determine the remaining DEB parameter values using the covariation method (except for $[\dot{p}_{VM}]$, which was determined last) (Table 4.1), along with calibrating the model so it could capture important landmarks of the life-history of *Pisaster*, including size and age at transitions between life stages and maximum reproductive output index (*RO*). Simulating ideal conditions (*f*=1), the model predicted "birth" (first feeding larval stage) at 4.2d after fertilization, when the larval size is 0.02cm wide (vs. training values 9d and 0.03cm, respectively); settlement around day 59.9, when larval width is ~0.38cm (vs. training values 50d and 0.37cm, respectively); and puberty around day 264, when wet weight is ~66.7g (vs. training values 5y and 70-90g, respectively). The same simulation projects an estimate for *RO* of 0.21 (vs. training value 0.23). These predictions, along with the maximum size reported for *Pisaster* (20-cm arm length; Feder 1956) allowed estimation of growth curves for both larval and post-metamorphic stages. The model's ability to precisely track changes in larval body size (MAPE=12.27%, RMSE=0.005cm) is illustrated in Figure 4.5. The comparison between observed and predicted growth data for the adult life stage further revealed the model's good performance (overall RMSE=1.01cm) (Fig. 4.6). The training data for this adult stage were collected at two temperatures: 9 and 12°C (Sanford 2002a). When running our model at each of these temperatures, agreement between observations and predictions was slightly better at 12°C (RMSE=0.82cm) than 9°C (RMSE=1.18cm). Although Sanford (2002a) did not find differences in growth between individuals kept at 9 and 12°C, our model's built-in thermal sensitivity (independently estimated) predicts the 3°C difference in temperature would cause a significant change in growth (from 27 to 42% of

maximal value). The lack of coherence between these model predictions, which suggest large changes on growth between temperatures on the steep part of the thermal performance curve, and Sanford's data, which showed no difference in growth between 9° and 12°C, remains unexplained.

Finally, our long-term starvation experiment together with the parameterized DEB model allowed estimation of the shrinkage volume-specific cost of maintenance parameter that applies during prolonged starvation, $\left[\dot{p}_{VM}\right]$ (Table 4.1). Individuals subjected to food deprivation lost weight at a steady rate of 0.12 ± 0.02g d^{-1} (mean±1SD, N=6). The values for $\left[\dot{p}_{VM}\right]$ that minimized the RMSE between observed and predicted wet weight varied between 8 and 15J d^{-1} cm^{-3} (Fig. 4.7). We used the mean, 11.5J d^{-1} cm^{-3}, as the value for this parameter.

Model validation results

We ran the parameterized DEB model simulating conditions of food and water temperature, and compared the outputs to Feder's (Feder 1956) observations (Fig. 4.8). Similar to the conclusion obtained from the training protocol, the validation confirmed the model's capacity to describe the increase in arm length of *Pisaster* through time, with an overall relative error MAPE=9.22% (RMSE=1.23cm, MAE=0.99cm) when comparing observed data with the simulated growth trajectory obtained using the average parameter values (Fig. 4.8A). Note that agreement between observed and simulated data decreased with the size of the organism. The observed data lie within the envelope of the family of curves from the Monte Carlo simulations accounting for variability in parameter values and the simulations clearly track the change in arm length of *Pisaster* (Fig. 4.8A).

The model's overall capacity to describe changes in wet weight appeared less satisfactory than for arm length (Fig. 4.8B). The indicator of relative error, MAPE, reaches 24.59% (RMSE=147.56g, MAE=93.81g) when comparing observed data with the simulated growth trajectory obtained using the average parameter values (Fig. 4.8B). The model's lack of skill in predicting wet weight in *Pisaster* is further evidenced by the large spread of the family of growth curves from the Monte Carlo simulations that accounted for the variability in parameter estimates (Fig. 4.8B).

We performed a sensitivity analysis to evaluate the relative influence of the DEB parameters on *Pisaster* size at age 2 years (Table 4.1). Generally, the effect of increasing parameter values on the model output was approximately mirrored by the effect of decreasing the parameter values, and vice versa, indicating that most parameters had linear effects on growth. Effects were only nonlinear for thermal sensitivity parameters T_L and T_H. An increase in the value of the former had a strong negative effect on the model output (sensitivity -0.99), while a reduction caused a weak positive effect (sensitivity 0.04). In contrast, while increasing the value of the latter did not affect the model output, reducing it produced a strong negative effect (sensitivity -0.99, not shown in Table 4.1). This analysis revealed that the model was most sensitive to both increases in T_L and reductions in T_H. The model also showed a high sensitivity to increases in the parameters maximum surface area-specific assimilation rate, $\{\dot{p}_{Am}\}$ (sensitivity 0.20), volume-specific somatic maintenance cost, $[\dot{p}_M]$ (sensitivity -0.14), and the proportion of energy allocated to somatic maintenance and growth, k (sensitivity 0.11, Table 4.1). Changing the parameters half-saturation coefficient, X_κ, post-metamorphic shape

coefficient, δ_M, energy conductance, $\dot{v}$, volume-specific cost of structure, $[E_G]$, energy investment to transition between life stages (birth E_H^b, metamorphosis E_H^j, and puberty E_H^p), maturity maintenance rate coefficient, $\dot{k}_J$, Arrhenius temperature, T_A, and Arrhenius temperature at upper and lower limits (T_{AL} and T_{AH}) had little effect on growth (sensitivity < 0.10). Finally, because the exercise was performed assuming *ad libitum* food supply of a post-metamorphic individual, varying parameters volume-specific cost of maintenance during starvation, $[\dot{p}_{VM}]$, and larval shape coefficient, $\delta_{M.lrv}$, had no effect on the model's output (Table 4.1).

DISCUSSION

We satisfactorily parameterized a Dynamic Energy Budget model for the quintessential keystone predator *Pisaster ochraceus*, although independent tests of the model reveal varying estimates of model skill. By combining the theoretical framework of DEB with empirical data collected for modeling purposes, we estimated a set of parameters (Table 4.1) that describe dynamics of underlying physiological processes related to development, maintenance, growth and reproduction, which in turn define the physiological and ecological performance of *Pisaster* (Figs. 4.5-4.8).

Model sensitivity

Future applications of this model should recognize that different parameters have a different relative influence on the model's output. Thus, depending on users' specific study objectives, one should consider the precision with which certain parameter values were determined, and whether further tuning is required. Our model sensitivity analysis

provided a useful means for assessing this. Those parameters with high sensitivity have a

big impact on the output of the model (e.g. thermal sensitivity parameters T_{AL} and T_{AH}),

and therefore future efforts should focus on methods for improving their estimation. In

contrast, because parameters with low sensitivity should have little influence on the

output of the model, their estimation could be treated with less care. Consequently,

despite the large variability observed in some of the parameters, their relative importance

could be minor if their sensitivity is low (e.g. maturity-maintenance rate coefficient, $\dot{k}_J$).

Reserves and starvation

The model allows discriminating between the contributions from reserves, structure, and

gonads to the total wet weight of an individual experiencing different levels of food

availability (Fig. 4.9). Notably, the contribution of the reserve to the animal's body mass

is very small, albeit enough to fuel its metabolic demands. Similarly, a study conducted

with the Atlantic Bluefin Tuna (*Thunnus thynnus*) found a low contribution from reserves

(7%) (Jusup et al. 2011) which, according to the authors' analysis, explains their limited

ability to survive starvation and the need to forage voraciously. Despite the even smaller

reserve compartment in *Pisaster* (3.8%), its ability to readily draw energy from structure

appears as a strategy to cope with naturally uncertain food conditions. The observation

that individuals facing food limitation not only show a steady body mass loss but also a

reduction in arm length (i.e. structural length) suggests that individuals readily draw

energy from the structure compartment to supplement energy allocation from reserves.

Now consider a well fed individual (~250g wet mass) suddenly deprived of food; the

model predicts an exponential decrease in body mass, in accordance with our empirical

observations (Fig. 4.7). Figure 4.9B illustrates the very short period needed to empty the

reserve compartment (~67d to reach 1% of the maximum reserve density). Then, as

mobilized energy cannot satisfy the maintenance requirements, structure is used as an

energy source contributing to the subsequent mass loss. Figure 9 also shows the

contribution of gonads to total body mass, which fluctuates annually between 0 and

20.7% in a well-fed individual. Structure, in turn, comprises most of *Pisaster* weight: up

to 96.1% (Fig. 4.9A). Food deprivation further impacts the amount of gonads produced

during this initial period, which falls to zero after the annual spawning event (Fig. 4.9B).

It should also be mentioned that the contribution to total wet weight from the model's

reserve compartment does not reflect the relative contribution from pyloric caecum,

which is traditionally regarded as the sea star energy reserve organ (Harrold & Pearse

1980, Nimitz 1971, 1976, Pearse & Eernisse 1982). Although DEB reserves do not

account for a large portion of the weight of *Pisaster* (Fig. 4.9), pyloric caecum is known

to reach relative values comparable to reproductive output (~0.15-0.20 of total body

mass) when prey is available *ad libitum* (Sanford & Menge 2007). This seeming

contradiction may be explained by the location of the DEB reserve compartment in the

energy flow pathway (Fig. 4.1), which differs from the role of the pyloric caecum in sea

stars. Although the pyloric caecum can be considered as an energy storage organ, our

assumption is that it is located down-stream from the reserve compartment, in closer

proximity to the reproductive buffer. We make this argument based on two lines of

evidence. First, DEB theory assumes that when food supply is constant, the DEB reserve

density should not vary (Kooijman 2010, Sousa et al. 2010). The cyclic nature of the

pyloric caecum in *Pisaster*, even when prey is available *ad libitum* and individuals'

feeding does not fluctuate (Mauzey 1966, Pearse & Eernisse 1982, Pearse et al. 1986),

123

conflicts with the idea of equating the DEB reserve compartment with pyloric caecum. Second, studies have shown strong relationships between the volumes of pyloric caecum accumulated during the feeding period of *Pisaster*, and the gonadal tissue produced subsequently during the spawning period (Pearse & Eernisse 1982, Pearse et al. 1986, Sanford & Menge 2007). Thus, while it is possible that maintenance is paid in part by pyloric reserves, especially during starvation (Nimitz 1976), most of that energy is allocated to gonadal growth. For simplicity, we did not include a pyloric caecum compartment in the model. Future versions of DEB models for *Pisaster* or any other sea star could consider its dynamics explicitly although notably, model results did not appear to be sensitive to its absence. Because the dynamics in pyloric and gonadal indexes are driven by photoperiod regimes, these models would benefit by incorporating photoperiod in their structure.

To better predict changes in size following starvation, specifically when energy diverted to somatic maintenance and growth is not enough to cover the former, we subjected individuals to complete food deprivation and monitored weight-loss over time (Fig. 4.7). These data allowed us to define and estimate a new parameter, $\left[\dot{p}_{VM}\right]$, which not only describes energy flows from structure to pay for somatic maintenance, but also provides a good match between observed and simulated reductions in size due to starvation. Although the literature suggests that mobilizing energy from structure to pay for somatic maintenance should be less efficient than from reserves (Kooijman 2010, Sousa et al. 2010), our data revealed a lower value of $\left[\dot{p}_{VM}\right]$ than $\left[\dot{p}_{M}\right]$ (Table 4.1). This might be a consequence from the drop in activity and metabolism shown by individuals during prolonged starvation.

Interestingly, animals lost weight smoothly throughout the duration of the starvation experiment (Fig. 4.7). Previous studies both with vertebrates (Cherel et al. 1988) and invertebrates (Ren & Schiel 2008) have shown that the rate of weight loss changes from steep to shallow once reserves are depleted and structure is used as substrate. The observation that reserves make up a small portion of *Pisaster* biomass (Fig. 4.9) is likely masking the change in rate of weight loss expected based on the literature. Finally, it must be recognized that shrinkage of structure directly translates into a decrease in maintenance costs, consequently allowing the organism to stay alive. This is a key adaptive trait in challenging environments such as the rocky intertidal (Sebens 1987). Efforts to account for the effect of starvation on organisms that routinely undergo periods of reduced feeding thus represents a crucial step if we are to predict real world dynamics.

Model performance

Because of varying levels of skill amongst different growth metrics, it is important to highlight the instances when the model predictions can be expected to be reliable, and when they should be viewed with caution. The model accurately predicted larval width (Fig. 4.7) and arm length (Fig. 4.8A) trajectories. An important strength of DEB is indeed its ability to incorporate the entire life-history of an organism using the same parameter values. Like other species modeled through DEB – including bivalves (Rico-Villa et al. 2010) and fish (Jusup et al. 2011), *Pisaster* undergoes morphological changes between larval and post-metamorphic stages. Accounting for this in the model required application of stage-specific shape coefficients ($\delta_{M.lrv}$, δ_M) to transform structural lengths to physical lengths and a shape correction function (Eq. 1) to capture growth

acceleration. These adjustments provided a good correspondence between real and simulated larval growth. Note that, although the time period covered by the real data is only half of that required for larval competency, the model projection (59.9d) is close to observations from the literature (~50d for well-fed larvae) (Vickery & McClintock 2000). While our validation exercise was limited to laboratory conditions with abundant food supply, the feeding functional response embedded in the model structure allows assessments under scenarios of reduced energy availability. If food is limited, the model predicts longer times to larval competency, although maturity level at metamorphosis remains constant. These predictions are consistent with Hart's (1995) study of the urchin *Strongylocentrotus droabachiensis*, and suggest a mechanism for understanding the wide distribution in settlement times previously reported for *Pisaster* (76-228d) (Strathmann 1978). The model, however, ignores potentially important features of *Pisaster* embryonic and larval developmental stages. For instance, it does not account for the capacity of their larvae to clone when food is abundant and of high quality (Vickery & McClintock 2000). Additionally, the model assumes that energy density, $[E]$, is equal between mothers and offspring, contradicting previous experimental observations revealing that bigger females produced small, low-quality eggs, and small females produced larger, high-quality eggs (George 1999). Although we disregarded these aspects for simplicity, including them in future versions of the model would certainly increase its potential for bridging the gap between individual and population level processes for *Pisaster*.

Our simulated growth for juveniles and adults also showed good correspondence with empirical data, although precision varied with the size metric considered (predictions for arm length were more precise than for wet weight) (Fig. 4.8). Several

mechanisms may partially explain the reduced precision in predicting wet weight

trajectories. First, it is quite common that the weight-at-age data are more scattered than

the corresponding length-at-age data, meaning that the former is impossible to capture

with the same level of precision as the latter (Karasov & Martínez del Rio 2007). From a

DEB perspective this is not surprising given that weight contains contributions from three

state variables (including the structural length) each being a source of the prediction error

that adds to the overall amount of the scatter. The physical length, on the other hand, is

predicted solely from the structural length, meaning that the corresponding prediction

error is the only source of the scatter. Second, precision may be reduced by assuming *ad*

libitum food, reserve density remains constant and structural mass increases smoothly

with time. Gonadal tissue, however, fluctuates yearly due to spawning events triggered

by photoperiodic cycles (Pearse & Eernisse 1982, Pearse et al. 1986). By assuming that

all mature individuals release their gonads accumulated during the previous year, based

entirely on energetic criteria, the model does not capture individual and population level

variability in the timing of spawning given by unaccounted potential cues (e.g. body

temperature, presence of conspecifics (Himmelman et al. 2008), or by photoperiod

(Pearse & Eernisse 1982, Pearse et al. 1986)). Due to the large portion of body mass that

can be attributed to gonads during spring-summer period (Fraser et al. 1981, Sanford &

Menge 2007), discrepancies in the exact timing of spawning between the model and

empirical data can translate into large differences in wet weight at specific times. Note

that, when accurate estimates of spawning time are a key modeling goal, reducing the

time resolution of the model from days (default) to weeks would improve the value of

model's skill metric; in addition, using a day-length cue for spawning would also

improve skill metric. The model's precision may be even less in case individuals fail to spawn on spring-summer (after accumulating gonads), and/or if the handling time of prey items varies, affecting their capacity to process energy efficiently. Both scenarios are possible under lab and certainly field conditions (Feder 1956).

An additional source of error when modeling wet weight trajectories may come from the observation that relative investment in gonads negatively correlates with food availability across sites in *Pisaster* (Sanford & Menge 2007), which deviates from DEB theory's assumption that the relative investment (k) is constant. Sanford and Menge (2007) hypothesized that such an adaptation may increase the likelihood for larvae produced at poor sites to reach worthier locations. For simplicity, and because the mechanism is not completely understood, our model ignores this hypothesis.

Because of the ecological importance of the age at puberty, it is worth touching on the large discrepancy between the modeled and observed values (264d and 5y, respectively). Two aspects may be determining the mismatch. First, the observed value is an estimate calculated using field observations (Menge 1975), where environmental conditions (notably food and temperature) are uncertain and individuals probably do not forage constantly. In contrast, our estimate is based on growth measurements collected in controlled, constant lab settings, where *Pisaster* could feed *ad libitum*. Second, the difference between observed and modeled age at puberty may be due to the uncertainty in the estimates of some of the DEB parameter values. For example, our estimate for maturity maintenance rate coefficient was 0.0000029±0.018 (mean±SD) (Table 4.1).

Environmental dependency

Throughout its wide geographic range, *Pisaster* often copes with extremely challenging

conditions inherent to the rocky intertidal. Stress may arise from both physical and

biological forces whose impacts vary spatially and temporally. Here we focused on body

temperature and food availability because of their overarching influence on physiological

and ecological performance (Karasov & Martínez del Rio 2007). First, our thermal

sensitivity experiment yielded a complete thermal performance curve for respiration rate

(hereafter, TPC) for *Pisaster* (Fig. 4.3). A number of different approaches have been

proposed to analytically characterize TPCs (e.g. Angilletta 2006, Shi & Ge 2010), most

of which typically arrive at the same general shape; namely, an increase in performance

with temperature, followed by a leveling off at an intermediate temperature (optimal

performance), and a subsequent drop leading to minimum performance and death at

extreme temperatures (Angilletta 2009). The five parameters we estimated here

determine this general shape. TPCs are becoming an increasingly popular tool to readily

assess the effect of temperature on relevant ecological and physiological performance

traits, as well as for predicting impacts of climate change (Angilletta 2009, Monaco &

Helmuth 2011). When used in a DEB framework, one can further discriminate among

the effects of temperature on the various physiological processes being modeled

(maturity, maintenance, growth, reproduction). Since the relative importance of these

processes may vary depending on the organism's maturity (e.g. reproduction is only a

defining trait after maturity has been reached), being able to quantify their responses to

temperature separately should prove useful when working across life-stages. Note,

however, that our thermal sensitivity parameters were estimated based on oxygen

consumption measurements, and we rely on the assumption that all physiological rates

respond to temperature following the same formulation. While empirical evidence

sustains this assumption (Kooijman 2010), we recommend testing it against independent

measurements of feeding or growth rates at a range of temperatures, particularly at

extreme ends of the curve, where different processes are expectedly less coupled

(Levinton 1983, Sanford 2002b). In addition, our model assumes that temperature exerts

the same effect on metabolism, regardless of whether individuals are aerially exposed at

low tide or submerged at high tide. We based this on a recent study conducted on

Pisaster, which showed that thermal sensitivity is virtually equal between submerged and

exposed animals subjected to a range of temperatures; Q_{10} values being 2.18 and 2.12,

respectively (Fly et al. 2012). However, despite finding similar sensitivities, the study

also revealed a significant reduction in oxygen consumption rates (metabolic depression)

for sea stars exposed to air compared to those kept submerged in water at the same

temperatures (Fly et al. 2012). The mechanism by which some intertidal organisms

reduce metabolism during aerial exposure is unclear, and therefore we did not consider it

in the model. Note, however, that if animals are exposed daily, cumulative metabolic

depressions may potentially have important consequences for long-term energy budgets.

It should also be pointed that, since our TPC was described based on aquatic conditions,

our model may not work when body temperature during aerial exposure exceeds the peak

of our curve (~295K, or 22°C). Since aerial body temperatures above that threshold are

known to occur for *Pisaster* (Fly et al. 2012, Pincebourde et al. 2008), models employed

to describe its condition during periods of aerial exposure should add an additional set of

thermal sensitivity parameters. While the value for Arrhenius temperature (T_A) would

130

not change, the parameters that define the curve's shape at extreme temperatures (T_{AL},

T_{AH}, T_L and T_H) should be re-estimated based, for example, on information of critical

temperatures (Pincebourde et al. 2008). Finally, temperature sensitivity parameters are

likely to vary as a function of both prevalent body temperatures at the collecting

sites/intertidal height (i.e. acclimatization) and details related to experimental design (e.g.

acclimation time; chronic vs. acute) (Pincebourde et al. 2008). Future studies must

therefore carefully consider these and other caveats reported elsewhere (Schulte et al.

2011), in order to avoid misinterpreting modeling results.

Moreover, our feeding experiment yielded a scaled Type II functional response

curve (Fig. 4.2) which, based on a half-saturation coefficient, X_κ, provides means for

assessing the effect of changing food density on the rate of energy intake (Kooijman

2010). To our knowledge, this curve had not been described for *Pisaster* before.

Conclusions

In a period of increasing anthropogenic pressure, anticipating changes in the dynamics of

ecological systems represents a complex, yet necessary challenge that ecologists must

face in order to prevent further collapses of natural resources (Mumby et al. 2011).

Difficulties arise, in part, as a result of the multiple processes taking place across levels

of biological organization, which appear linked to nonlinearities emerging at broad scales

(Peters et al. 2007). Predicting dynamics of complex systems requires first uncovering

the mechanisms behind such nonlinearities (Denny & Helmuth 2009), and then their

incorporation in a coherent modeling framework (Sousa et al. 2010). By blending the

virtues of experimental and theoretical biology (Nisbet et al. 2012), recent advances are

providing increasingly accurate predictions of interdependent physiological and

ecological processes occurring simultaneously, thus advancing our understanding of emergent properties that would otherwise remain obscure.

The DEB model presented here represents a step forward in our efforts to bring data and theory together, to help illuminate key physiological properties and their dependence on biotic and abiotic environmental drivers. Given the keystone role of *Pisaster* (Estes et al. 1998, Paine 1974), insights obtained from this individual-based mechanistic model can potentially shed light on dynamics at population and community levels (Pincebourde et al. 2008, Sanford 2002b), especially when comparable models are developed for other ecologically key players in the intertidal ecosystem.

Table 4.1 *Pisaster ochraceus* DEB parameter values, and results of sensitivity analysis. Sensitivity is the percent change in arm length at age 2y divided by the percent change in a single parameter value (10%). Analyses were carried out using *ad libitum* food, at a temperature of 13°C. Parameters with a negative relation to growth are printed in bold type. Sensitivity of parameters not estimated is NaN.

Parameter	Symbol	Value±SD	Units	Sensitivity
Primary parameters				
Half-saturation coefficient[1]	X_κ	13.9±2.3	mussel m^{-2}	-0.01
Maximum surface area-specific assimilation rate[2]	$\{\dot{p}_{Am}\}$	43.2±4.1	J d^{-1} cm^{-2}	0.20
Energy conductance[2]	$\dot{v}$	0.04±0.01	cm d^{-1}	0.07
Fraction of energy used for somatic maintenance and growth[2]	k	0.58±0.07	-	0.11
Volume-specific cost of maintenance[2]	$[\dot{p}_M]$	40.43±1.41	J d^{-1} cm^{-3}	-0.14
Volume-specific cost of maintenance during starvation[1]	$[\dot{p}_{VM}]$	11.5±2.74	J d^{-1} cm^{-3}	0.00
Volume-specific cost of structure[2]	$[E_G]$	2743±97.22	J cm^{-3}	0.00
Maturity at birth[2]	E_H^b	0.012±4.8×10^{-4}	J	-0.03
Maturity at larval settlement[2]	E_H^j	100±4.21	J	0.00
Maturity at puberty[2]	E_H^p	13.9×10^6±99×10^6	J	0.00
Shape coefficient of larvae[2]	$\delta_{M.lrv}$	0.959±144.56	-	0.00
Post-metamorphic shape coefficient[1]	δ_M	0.52±0.03	-	-0.09

Maturity-maintenance rate coefficient[2]	$\dot{k}_J$	$2.9 \times 10^{-6} \pm 0.018$	d^{-1}	0.00

Temperature dependence

Arrhenius temperature[1]	T_A	6000 ± 335	K	-0.02
Lower limit of tolerance range[3]	T_L	280	K	-0.99
Upper limit of tolerance range[3]	T_H	297	K	0.00
Arrhenius temperature at lower limit[3]	T_{AL}	31000	K	0.01
Arrhenius temperature at upper limit[3]	T_{AH}	190000	K	0.00
Reference temperature[4]	T_{ref}	293	K	NaN

Conversion parameters

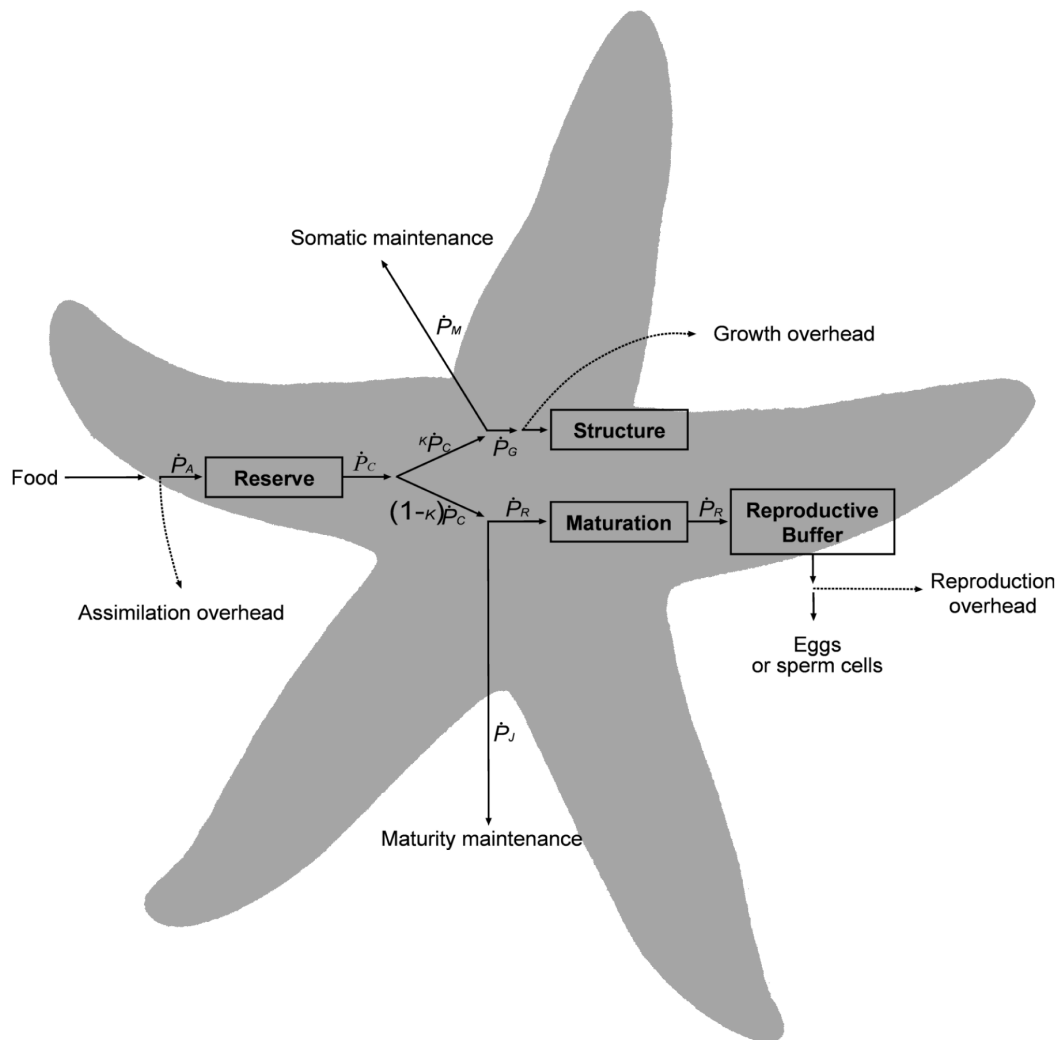|				
Density of structure[4]	d_V	1	$g\ cm^{-3}$	NaN
Weight-energy coupler for reserves[4]	ρ_E	4.35×10^{-5}	$g\ J^{-1}$	NaN
Molecular weight of reserves[4]	w_E	23.9	$g\ mol^{-1}$	NaN
Chemical potential of reserves[4]	$\bar{\mu}_E$	550	$kJ\ mol^{-1}$	NaN

[1] Estimated directly from data.

[2] Estimated using covariation method (DEBtool).

[3] Estimated using grid-search.

[4] Kept fixed.

Figure 4.1. Schematic representation of standard Dynamic Energy Budget model. Arrows represent energy fluxes (J d^{-1}) that drive the dynamics of the four state variables, depicted in boxes (Reserve, Structure, Maturation, and Reproductive Buffer). Energy enters the animal as food, and then assimilated at a rate $\dot{P}_A$ into Reserves. Mobilization rate, $\dot{P}_C$, regulates energy fluxes to cover the demands from somatic maintenance, $\dot{P}_M$, structural growth, $\dot{P}_G$, maturity maintenance, $\dot{P}_J$, maturation, $\dot{P}_R$ (immature individuals), and reproduction, $\dot{P}_R$ (mature individuals). The parameter kappa (k) is the proportion of mobilized energy diverted to $\dot{P}_M$ and $\dot{P}_G$, while the rest (1 - k) is used for $\dot{P}_J$ and $\dot{P}_R$. Formulations explaining these fluxes are given in the Appendix B. Overheads associated to assimilation, growth and reproduction arise due to thermodynamic inefficiencies when transforming between substrates.
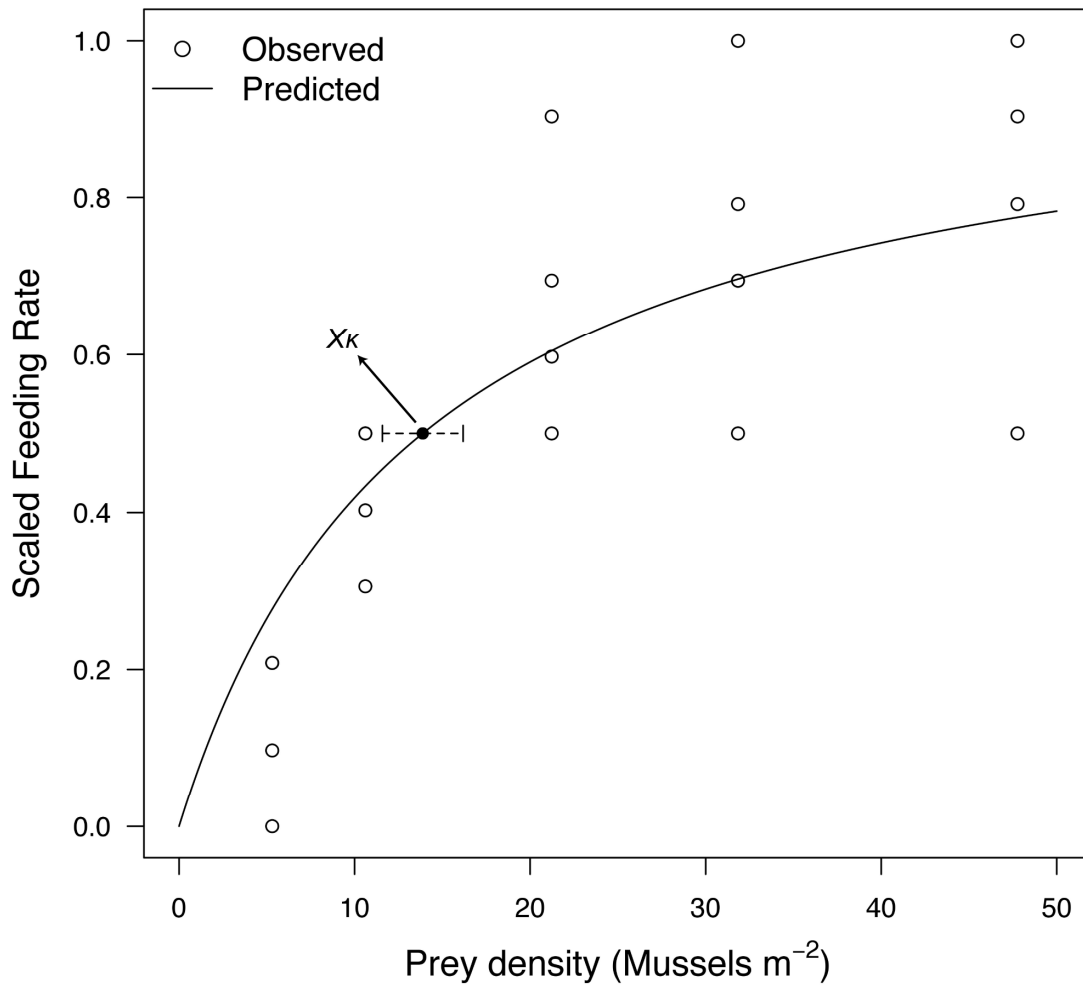
Figure 4.2 Scaled feeding rate as a function of prey density. Observed values (circles) and projection (line), based on a type II feeding functional response (Appendix B, Eq. 1), are shown for mussels with 2-cm shell length. The estimated value for the half-saturation parameter X_κ was 13.9±2.3 (Mean±1SD) mussels m^{-2}.
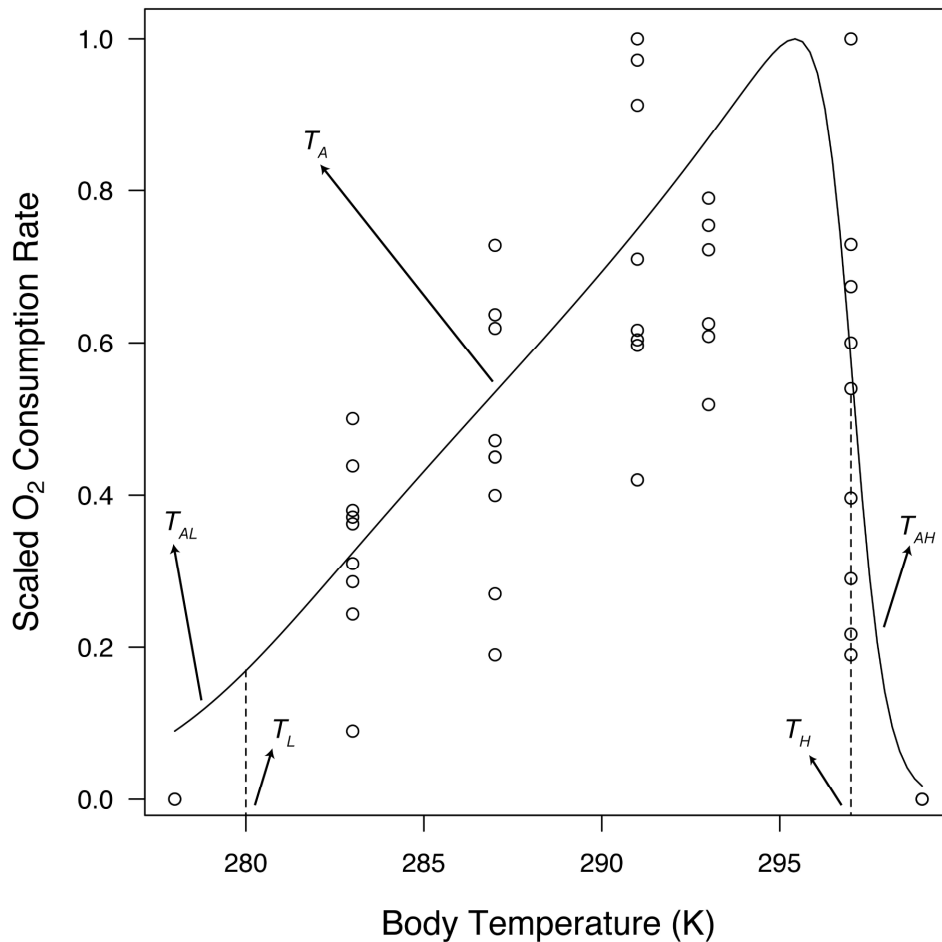
Figure 4.3 Temperature sensitivity. Observed values (circles) represent relative values of oxygen consumption and feeding rate (coldest temperature treatment) determined at a range of water temperatures from 278 to 299K. The line of best fit was obtained by first estimating Arrhenius temperature, T_A, and then running a grid-search to find the combination of parameter values for T_L (lower limit of tolerance range), T_H (higher limit of tolerance range), T_{AL} (Arrhenius temperature at lower limit), and T_{AH} (Arrhenius temperature at higher limit) that minimized the RMSE between observed and simulated data.
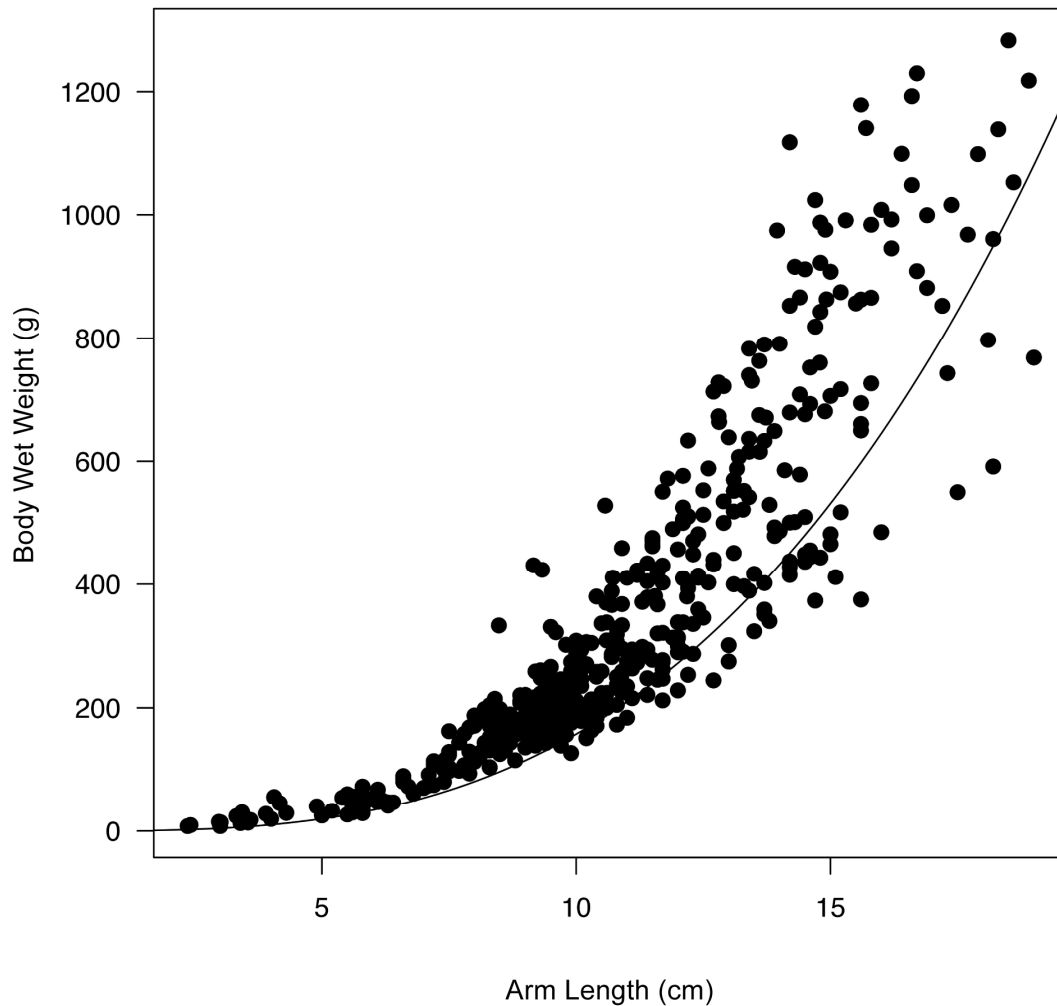
Figure 4.4 Body wet weight in (W_W) relation to arm length (L_W). Observed values are shown as dots (N=457 individuals). By fitting the equation $W_W = (\delta_M \cdot L_W)^3$, we estimated the post-metamorphic shape coefficient (δ_M). The estimate was then optimized through the covariation method (DEBtool), yielding 0.52±0.03 (Mean±1SD). The trajectory described by this model is shown as a line crossing the cloud of points below their center, thus better representing the contribution of structure to body weight.
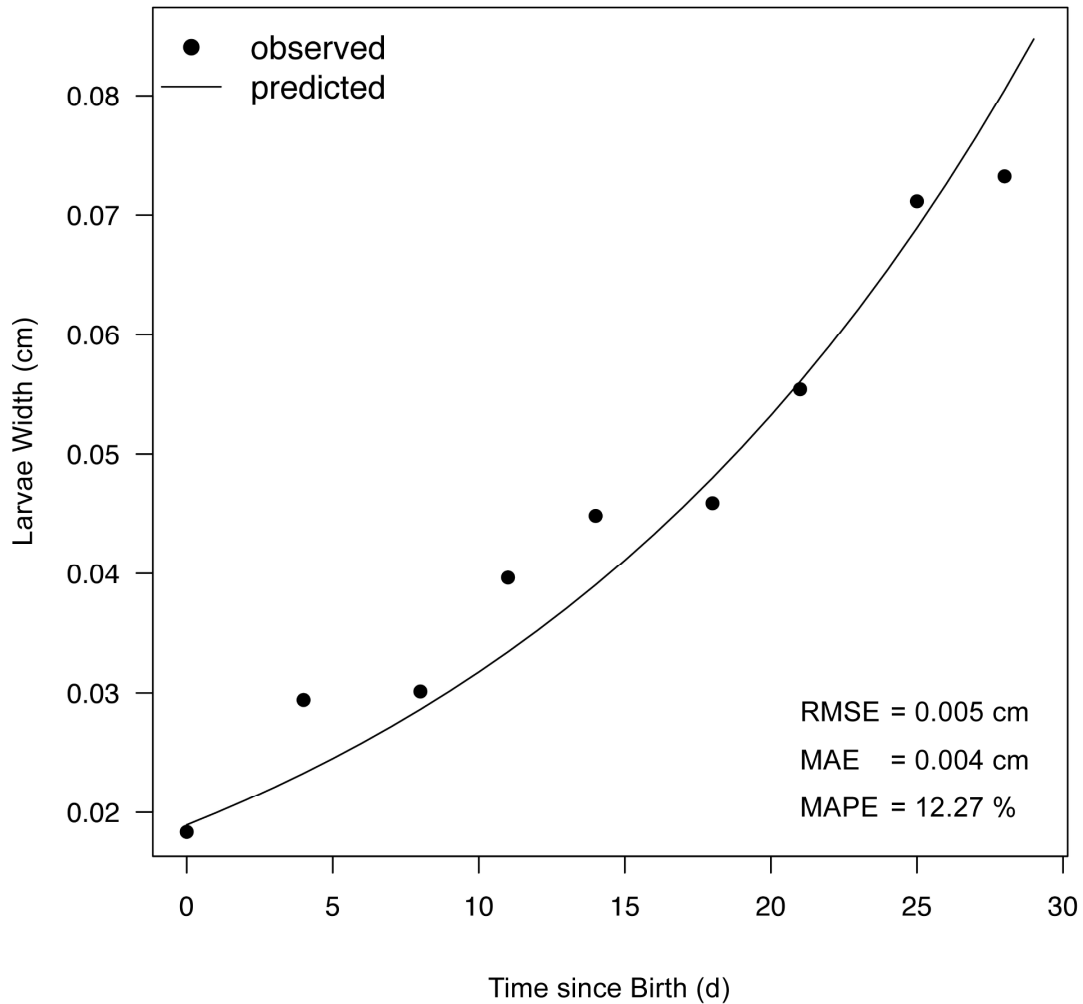
Figure 4.5 Larval growth from 0 to 27d after birth. Birth is considered as the day when larvae begin feeding. Laboratory data (from (George 1999)) are shown as dots. The line comes from a Dynamic Energy Budget model simulation, assuming *ad libitum* food and 12˚C water temperature. Root Mean Square (RMS) error, Mean Absolute Error (MAE), and Mean Absolute Percent Error (MAPE) are shown.
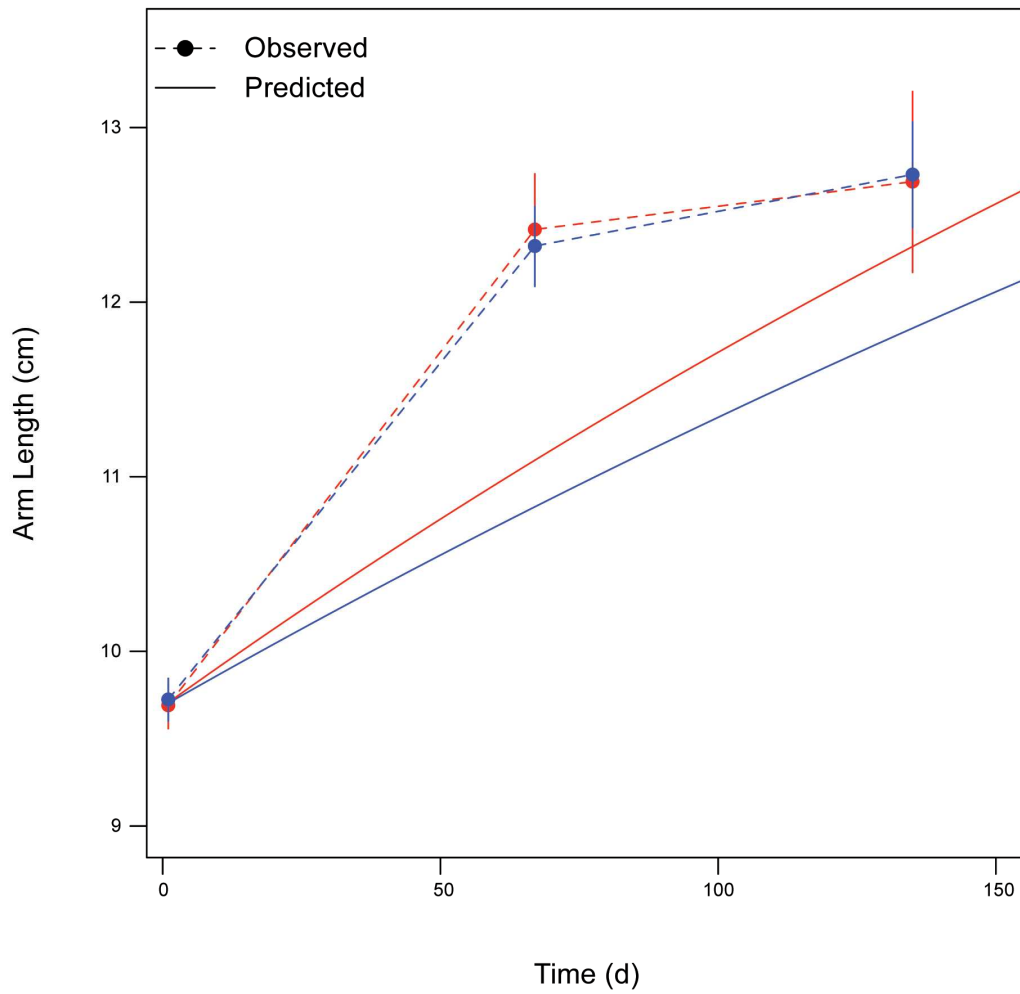
Figure 4.6 Post-metamorphic change in arm length over time at two water temperature treatments. Laboratory data from *ad libitum* feeding experiment (from (Sanford 2002a)) are shown as dots. Solid symbols and black line are from 9˚C treatment, open symbols and grey line are from 12˚C treatment. Dotted lines are DEB predictions, grey levels as above.
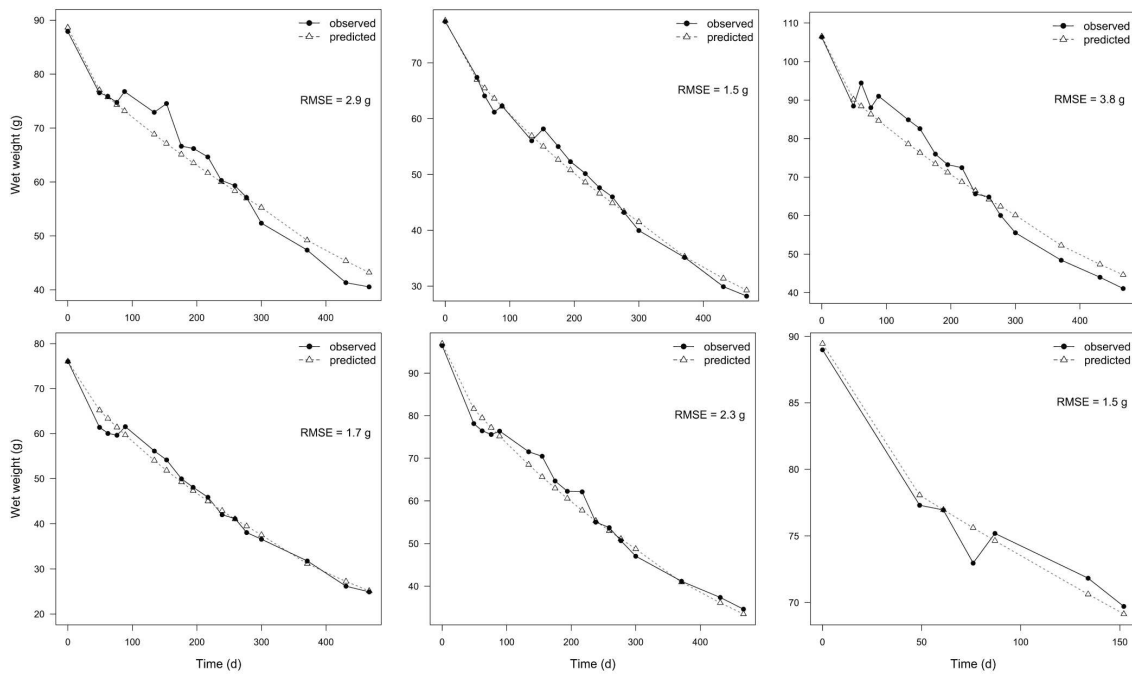
Figure 4.7 Post-metamorphic change in wet weight over time as a result of complete starvation. Each panel shows data for a different individual. Laboratory observations from long-term starvation trials are shown by dots and solid lines. Triangles and dotted lines are DEB predictions using the value for parameter $\left[\dot{p}_{VM}\right]$ that minimized the RMSE between observed and predicted data. The mean of the six estimates of $\left[\dot{p}_{VM}\right]$, 11.5 J d^{-1} cm^{-3}, was used in the DEB model.
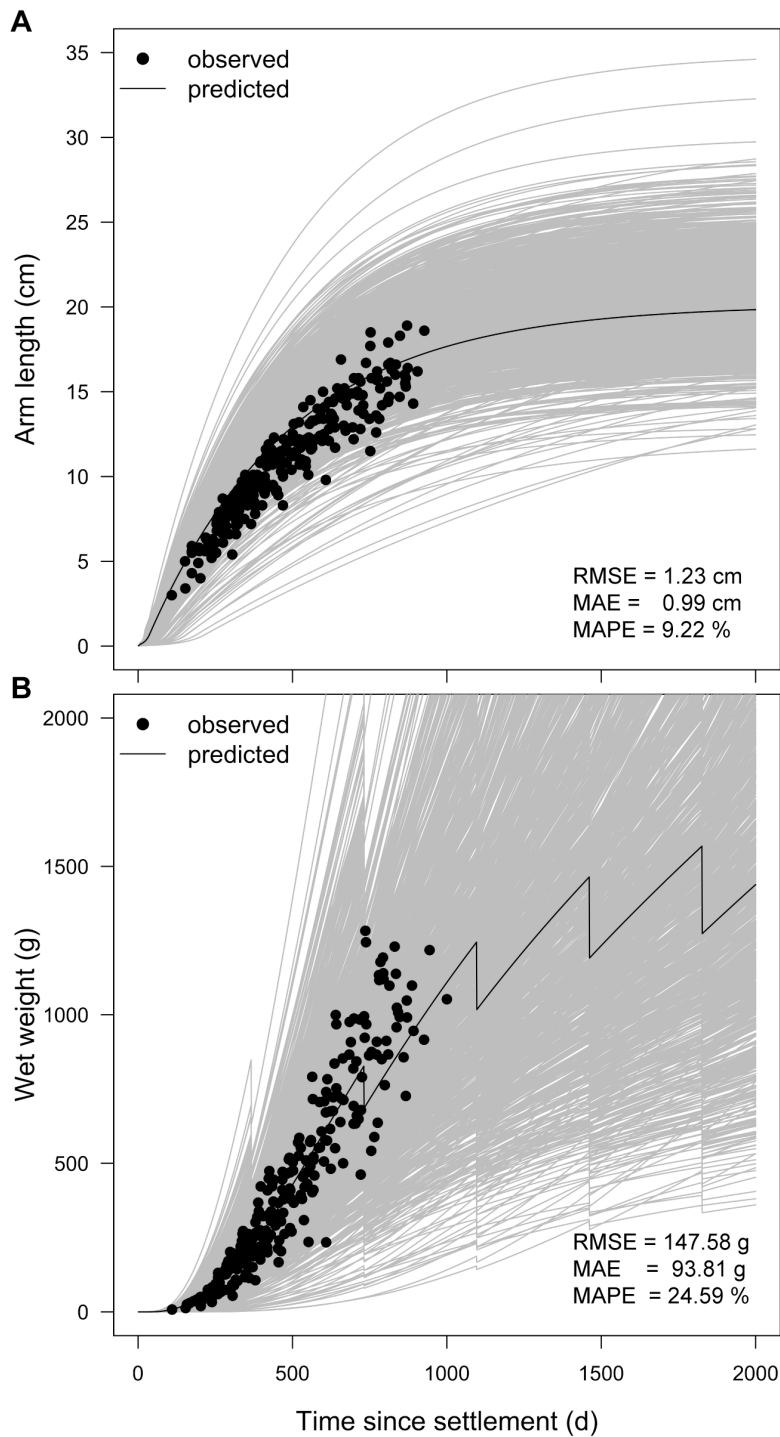
Figure 4.8 Post-metamorphic change in arm length and wet weight over time since larval settlement. Panel A illustrates arm length, and B wet weight. Laboratory observations (from citation [31]) are shown as dots. Food was provided *ad libitum*, and water temperature kept at 14.5˚C, in accordance to the average reported by Feder (1956). Grey

lines are results of 1000 Monte Carlo DEB simulations, which simultaneously sampled parameter values from normal distributions with parameter means and standard deviations (Table 4.1). Black line is DEB simulation using mean values for all parameters (Table 4.1). Root Mean Square Error (RMSE), Mean Absolute Error (MAE), and Mean Absolute Percent Error (MAPE) are relative to the DEB simulation that used mean parameter values.
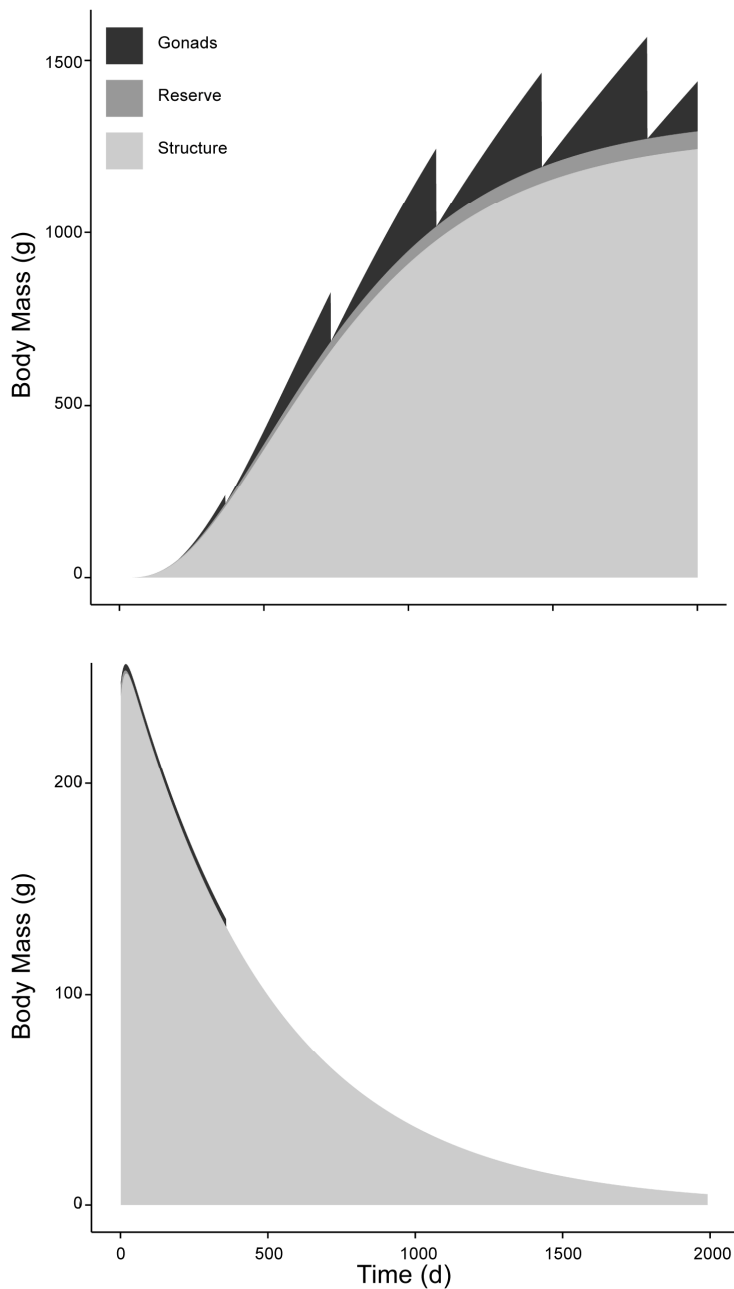
Figure 4.9 Change in wet weight under abundant food versus starvation. Values are results of DEB simulation using mean parameter values at a temperature of 13°C. Wet weights of gonad (black), reserve (dark grey), and structure (light grey). Panel A is trajectory with food *ad libitum*, and B is trajectory during complete starvation.

144

CHAPTER 5

CONCLUSION

Predator-prey interaction systems are key components of natural communities, which can determine their dynamics and the state of ecosystems (Estes & Palmisano 1974, Paine 1974). The ecological processes occurring at higher levels of organization can be traced down to the organism. Therefore, understanding how the environment impacts predators and prey can help predict ecological processes at higher levels. Such a mechanistic understanding is especially relevant in an era of ongoing and increasing climate change (Helmuth et al. 2006b, Parmesan & Yohe 2003), when accurate predictions are required by stakeholders and decision makers whom directly benefit from the various ecosystem services (CCSP 2009, Hoegh-Guldberg & Bruno 2010, IPCC 2007).

Much of the ecological theory available today has been developed within the rocky intertidal. Given the steep gradients in biotic and abiotic factors one can find there, investigators can readily test complex ecological phenomena that take place within a few meters (Benson 2002). Among the best-studied predator-prey systems is the interaction between the predatory sea star *Pisaster ochraceus* and its main prey the mussel *Mytilus californianus*. Because of the keystone role of *Pisaster* and the fact that *Mytilus* acts as a dominant competitor, numerous investigations have focused on the ecological consequences of this interaction (Paine 1966, Paine 1974, 1976). Recent work has begun exploring how environmental drivers may influence ecological dynamics by indirectly

regulating the interaction strength between these species (Pincebourde et al. 2012, Pincebourde et al. 2008, Pincebourde et al. 2009, Sanford 1999). Stemming from this work, the general goal of my dissertation was to explore aspects of behavior and physiology that may play important roles in controlling this interaction.

Chapter 2 ("Size-dependent intertidal height and refuge use in the keystone predator *Pisaster ochraceus*") aimed to examine detailed aspects of microhabitat use in *Pisaster*. While *Mytilus* is normally found on the mid to high intertidal, often exposed to the elements (solar radiation, wind speed, wave impact), *Pisaster* moves between exposed and protected (e.g. tide pools, crevices, under alga canopy) microhabitats. Because the intertidal may offer dramatically different conditions depending on where an ectotherm might be located (Denny et al. 2011, Seabra et al. 2011), knowing where sea stars are found would give a more detailed picture of the body temperatures experienced *in situ*, and the resulting physiological, and potentially population level, consequences. Furthermore, in this chapter I placed particular attention on the size-dependent distribution patterns displayed by *Pisaster*, and how they varied in time and space.

I found that at both sites analyzed, Bodega and Strawberry Hill, most *Pisaster* individuals were found protected in refugia during low tides, as had been previously reported (Burnaford & Vasquez 2008, Fly et al. 2012). I additionally learned that this risk-avoiding strategy does not vary much with time, and it takes place despite the seemingly benign thermal conditions animals would have been experiencing if located in exposed microhabitats or higher on the shore. The proportion of sea stars found protected was higher at Bodega than Strawberry Hill. I also found that, for sea stars found in refugia such as tide-pools or crevices, small individuals were located higher on

146

the shore than large ones. This size-dependent intertidal height (SDIH) pattern was not detected for individuals found exposed outside of refugia. While variables such as solar radiation, air temperature, and body temperature were positively related with the proportion of *Pisaster* found protected, no environmental variable seemed to explain SDIH. Concomitantly, lab experiments revealed that size-dependent sensitivity to temperature and desiccation did not help explain the distribution patterns either. These data suggested that *Pisaster* distribution patterns are not immediately driven by the environmental variables examined. However, given sea stars' persistent risk-avoiding behavior, the data seems to support the idea that "sub-optimal is optimal" (Martin & Huey 2008). This idea posits that ecotherms' mean performance is higher when maintaining body temperatures lower than what might be considered optimal. The tenets for this are: (1) thermal performance curves are asymmetrical with a strong tipping-point close to the optimal temperature, and (2) as imperfect thermoregulators, ectotherms might not respond fast enough to changes in body temperature, which may lead to critical temperatures. Given the highly thermally heterogeneous intertidal environment, it is conceivable that *Pisaster* favors refuges to prevent potential exposures to extreme events.

In Chapter 3 ("Thermal sensitivity and behavior's role in driving an intertidal predator-prey interaction") I proposed a novel approach for exploring the direct effects of temperature on both the predator *Pisaster* and its prey *Mytilus*, as well as the indirect effects on their interaction, based on the established frameworks of environmental stress models (ESM) (Menge & Olson 1990, Menge et al. 2002, Menge & Sutherland 1987) and thermal performance curves (TPC). In particular, this chapter asked: which species would be more greatly affected by environmental stress?

147

Although Petes et al. (2008b) had previously asked this question using the same model species, their methods lacked ecological realism. Their approach involved field caging experiments that deliberately allowed testing for the effect of an environmental thermal gradient on individuals' performance, but unintentionally constrained *Pisaster* ability to naturally move about the intertidal. Thus, while very informative, results obtained from these efforts might have yielded incorrect conclusions. As an alternative, by using thermal performance curves, body temperature records collected via biomimetic temperature loggers, and observations of *Pisaster* microhabitat use, I was able to assess thermal performance indirectly, thereby circumventing the caging problem.

First, describing thermal performance curves allowed comparing temperature sensitivities between species, aquatic/aerial condition, and sites. Thermal sensitivities appeared related to the body temperatures organisms experience in their habitats. For example, the parameter T_A (Arrhenius temperature) was lower for the site where body temperatures fluctuated the most. We argue that lower thermal sensitivity would provide organisms with a physiological buffer against increased temperature variability, and reduce the risk of reaching critical temperatures, which has indeed been observed in many species inhabiting thermally variable environments (Kooijman 2010).

Second, using this curves in combination with field body temperature records, we calculated mean relative thermal performance for both species. This analysis revealed that, contrary to previous accounts, *Mytilus* exhibited a lower thermal performance than *Pisaster*. Within the ESM framework, this means that the system behaves as a prey stress model. From here, we could speculate about the fate of rocky intertidal communities given, for example, increased pressure by climate change. One could hypothesize that

148

further temperature increases will raise thermal performance of both species; however, because T_A is greater for *Pisaster* than *Mytilus*, predation pressure should increase relative to levels observe today. When evaluating the role of behavior, I found no effects of including movement between microhabitats in *Pisaster* mean thermal performance. This was partially because there were little differences in potential body temperatures that *Pisaster* would have experienced in those microhabitats available. The latter in turn, is likely due to another behavior exploited by *Pisaster* to maintain body temperatures; namely, its ability to incorporate seawater into its coelomic cavity during high tides, which buffers temperature fluctuations during subsequent low tides (Pincebourde et al. 2009).

And third, I paired these indirect calculations of thermal performance with direct measurements of overall physiological condition (body mass index) and a marker for extreme thermal stress (heat-shock proteins 70kDa). These data suggested that both species *Pisaster* and *Mytilus* are more responsive to extreme thermal conditions than to the means. Notably, however, both species appear equipped either physiologically or behaviorally to cope with current levels of thermal stress.

Predicting ecological dynamics as a function of temperature requires more than simple analyses of organisms' overall thermal sensitivities. Their fitness depends on underlying physiological processes that can be captured by energy budget models. In Chapter 4 ("A Dynamic Energy Budget (DEB) model for the keystone predator *Pisaster ochraceus*"), I described a DEB model for *Pisaster*, the first one published for an echinoderm (Monaco et al. 2014). The model parameters estimated allowed characterizing individual sea stars' growth throughout ontogeny, including larvae,

149

juvenile, and adult. The model also captured shrinkage that takes place when food supply

is limited to a point where somatic maintenance requirements cannot be fulfilled.

Including this feature in the model was especially important because it underpins the

ability of *Pisaster* to cope with conditions of food scarcity (Sebens 1987), which are

common in many sites where this species is found (George 1999). Additionally, because

the parameterization included functions for a feeding functional response and a

temperature response, the model was suited with the ability to deal with combined effects

of changes in temperature and food availability.

This DEB model provides a baseline for future efforts to better understand the

physiological underpinnings of the *Pisaster-Mytilus* predator-prey interaction. Since we

already have a model for the prey (Matzelle et al. 2014), a natural next step could be to

first pair them and test their ability to capture dynamics observed in the field, and then

make projections of population level processes across geographical scales in a climate

change context.

REFERENCES

Addison JA, Ort BS, Mesa KA, Pogson GH (2008) Range-wide genetic homogeneity in the California sea mussel (Mytilus californianus): a comparison of allozymes, nuclear DNA markers, and mitochondrial DNA sequences. Mol Ecol 17:4222-4232

Allen BJ, Rodgers B, Tuan Y, Levinton JS (2012) Size-dependent temperature and desiccation constraints on performance capacity: Implications for sexual selection in a fiddler crab. Journal of Experimental Marine Biology and Ecology 438:93-99

André J, Haddon M, Pecl GT (2010) Modelling climate-change-induced nonlinear thresholds in cephalopod population dynamics. Global Change Biology 16:2866-2875

Angilletta MJJ (2006) Estimating and comparing thermal performance curves. Journal of Thermal Biology 31:541-545

Angilletta MJJ (2009) Thermal adaptation: a theoretical and empirical synthesis. Oxford University Press, Oxford

Augustine S, Litvak MK, Kooijman SALM (2011) Stochastic feeding of fish larvae and their metabolic handling of starvation. Journal of Sea Research 66:411-418

Bates AE, Hilton BJ, Harley CDG (2009) Effects of temperature, season and locality on wasting disease in the keystone predatory sea star *Pisaster ochraceus*. Dis Aquat Org 86:245-251

Bayne BL, Bayne CJ, Carefoot TC, Thompson RJ (1976) The physiological ecology of
    Mytilus californianus Conrad. 1. Metabolism and energy balance. Oecologia
    22:211-228

Benson KR (2002) The study of vertical zonation on rocky intertidal shores - A historical
    perspective. Integrative and Comparative Biology 42:776-779

Berlow EL, Navarrete SA (1997) Spatial and temporal variation in rocky intertidal
    community organization: Lessons from repeating field experiments. Journal of
    Experimental Marine Biology and Ecology 214:195-229

Bertness MD (1977) Behavioral and ecological aspects of shore-level size gradients in
    Thais lamellosa and *Thais emarginata*. Ecology 58:86-97

Bertness MD, Leonard GH (1997) The role of positive interactions in communities:
    Lessons from intertidal habitats. Ecology 78:1976-1989

Bertness MD, Leonard GH, Levine JM, Schmidt PR, Ingraham AO (1999) Testing the
    relative contribution of positive and negative interactions in rocky intertidal
    communities. Ecology 80:2711-2726

Bertness ME, Schneider DE (1976) Temperature relations of Puget Sound Thaids in
    reference to their intertidal distribution. The Veliger 19

Broitman BR, Szathmary PL, Mislan KAS, Blanchette CA, Helmuth B (2009) Predator-
    prey interactions under climate change: the importance of habitat vs body
    temperature. Oikos 118:219-224

Bruno JF, Stachowicz JJ, Bertness MD (2003) Inclusion of facilitation into ecological
    theory. Trends in ecology & evolution 18:119-125

Buckley LB (2013) Get real: putting models of climate change and species interactions in
practice. Annals of the New York Academy of Sciences 1297:126-138

Burnaford JL, Vasquez M (2008) Solar radiation plays a role in habitat selection by the
sea star *Pisaster ochraceus*. Marine Ecology Progress Series 368:177-187

Burrows MT, N. HR (1989) Natural foraging of dogwhelk, *Nucella lapillus* (Linnaeus);
the weather and whether to feed. Journal of Molluscan Studies 55:285-295

Burrows MT, Schoeman DS, Buckley LB, Moore P, Poloczanska ES, Brander KM,
Brown C, Bruno JF, Duarte CM, Halpern BS, Holding J, Kappel CV, Kiessling
W, O'Connor MI, Pandolfi JM, Parmesan C, Schwing FB, Sydeman WJ,
Richardson AJ (2011) The pace of shifting climate in marine and terrestrial
ecosystems. Science 334:652-655

Cartwright SR, Williams GA (2012) Seasonal variation in utilization of biogenic
microhabitats by littorinid snails on tropical rocky shores. Marine Biology
159:2323-2332

CCSP (2009) Thresholds of Climate Change in Ecosystems. A report by the U.S. Climate
Change Science Program and the Subcommittee on Global Change Research
[Fagre, D.B., C.W. Charles, C.D. Allen, C. Birkeland, F.S. Chapin III, P.M.
Groffman, G.R. Guntenspergen, A.K. Knapp, A.D. McGuire, P.J. Mulholland,
D.P.C. Peters, D.D. Roby, and George Sugihara]. In: Survey USG (ed), Reston,
VA

Chase JM, Leibold MA (2003) Ecological Niches: Linking Classical and Contemporary
Approaches. The University of Chicago Press, Chicago, IL

Cherel Y, Robin J-P, Maho YL (1988) Physiology and biochemistry of long-term fasting in birds. Canadian Journal of Zoology 66:159-166

Connell JH (1961) The influence of interspecific competition and other factors on the distribution of the barnacle *Chthamalus stellatus*. Ecology 42:710-723

Connell JH (1972) Community Interactions on Marine Rocky Intertidal Shores. Annual Review of Ecology and Systematics 3:169-192

Connell SD, Russell BD, Irving AD (2011) Can strong consumer and producer effects be reconciled to better forecast `catastrophic' phase-shifts in marine ecosystems? Journal of Experimental Marine Biology and Ecology 400:296-301

Connor KM, Gracey AY (2012) High-resolution analysis of metabolic cycles in the intertidal mussel *Mytilus californianus*. American Journal of Physiology - Regulatory, Integrative and Comparative Physiology 302:R103-R111

Dahlhoff EP, Buckley BA, Menge BA (2001) Physiology of the rocky intertidal predator *Nucella ostrina* along an environmental stress gradient. Ecology 82:2816-2829

Dahlhoff EP, Menge BA (1996) Influence of phytoplankton concentration and wave exposure on the ecophysiology of Mytilus californianus. Marine Ecology-Progress Series 144:97-107

Dell AI, Pawar S, Savage VM (2011) Systematic variation in the temperature dependence of physiological and ecological traits. Proceedings of the National Academy of Sciences 108:10591–10596

Dell AI, Pawar S, Savage VM (2013) Temperature dependence of trophic interactions are driven by asymmetry of species responses and foraging strategy. J Anim Ecol 83:70-84

Denny M, Helmuth B (2009) Confronting the physiological bottleneck: A challenge from ecomechanics. Integrative and Comparative Biology 49:197-201

Denny MW, Daniel TL, Koehl MAR (1985) Mechanical Limits to Size in Wave-Swept Organisms. Ecological Monographs 55:69-102

Denny MW, Dowd WW, Bilir L, Mach KJ (2011) Spreading the risk: Small-scale body temperature variation among intertidal organisms and its implications for species persistence. Journal of Experimental Marine Biology and Ecology 400:175-190

Duggins DO (1980) Kelp Beds and Sea Otters: An Experimental Approach. Ecology 61:447-453

Elvin DW, Gonor JJ (1979) The thermal regime of an intertidal *Mytilus californianus* Conrad population on the central Oregon coast. Journal of Experimental Marine Biology and Ecology 39:265-279

Emlet RB, Sadro SS (2006) Linking stages of life history: How larval quality translates into juvenile performance for an intertidal barnacle (*Balanus glandula*). Integrative and Comparative Biology 46:334-346

Estes JA, Palmisano JF (1974) Sea otters - Their role in structuring nearshore communities. Science 185:1058-1060

Estes JA, Tinker MT, Williams TM, Doak DF (1998) Killer Whale Predation on Sea Otters Linking Oceanic and Nearshore Ecosystems. Science 282:473-476

Fauth JE, Resetarits WJ, Jr. (1991) Interactions between the salamander *Siren intermedia* and the keystone predator *Notophthalmus viridescens*. Ecology 72:827-838

Feder HM (1956) Natural history studies on the starfish *Pisaster ochraceus* (Brandt, 1835) in Monterey bay area. PhD, Stanford University,

Feder ME, Hofmann GE (1999) Heat-shock proteins, molecular chaperones, and the stress response: Evolutionary and ecological physiology. Annual Review of Physiology 61:243-282

Fields PA, Graham JB, Rosenblatt RH, Somero GN (1993) Effects of expected global climate change on marine faunas. Trends in Ecology & Evolution 8:361-367

Filgueira R, Rosland R, Grant J (2011) A comparison of scope for growth (SFG) and dynamic energy budget (DEB) models applied to the blue mussel (*Mytilus edulis*). Journal of Sea Research 66:403-410

Fitzgerald-Dehoog L, Browning J, Allen BJ (2012) Food and heat stress in the California mussel: Evidence for an energetic trade-off between survival and growth. The Biological Bulletin 223:205-216

Fitzhenry T, Halpin PM, Helmuth B (2004) Testing the effects of wave exposure, site, and behavior on intertidal mussel body temperatures: applications and limits of temperature logger design. Marine Biology 145:339-349

Fly EK, Monaco CJ, Pincebourde S, Tullis A (2012) The influence of intertidal location and temperature on the metabolic cost of emersion in *Pisaster ochraceus*. Journal of Experimental Marine Biology and Ecology 422-423:20-28

Flye-Sainte-Marie J, Jean F, Paillard C, Kooijman SALM (2009) A quantitative estimation of the energetic cost of brown ring disease in the Manila clam using Dynamic Energy Budget theory. Journal of Sea Research 62:114-123

Fraser A, Gomez J, Hartwick EB, Smith MJ (1981) Observations on the reproduction and development of *Pisaster ochraceus* (Brandt). Canadian Journal of Zoology 59:1700-1707

Freitas V, Campos J, Fonds M, Van der Veer HW (2007) Potential impact of temperature change on epibenthic predator-bivalve prey interactions in temperate estuaries. Journal of Thermal Biology 32:328-340

Garrity SD (1984) Some adaptations of gastropods to physical stress on a tropical rocky shore. Ecology 65:559-574

Garza C, Robles C (2010) Effects of brackish water incursions and diel phasing of tides on vertical excursions of the keystone predator Pisaster ochraceus. Marine Biology 157:673-682

Gebauer P, Paschke K, Anger K (1999) Costs of delayed metamorphosis: reduced growth and survival in early juveniles of an estuarine grapsid crab, *Chasmagnathus granulata*. Journal of Experimental Marine Biology and Ecology 238:271-281

George SB (1999) Egg quality, larval growth and phenotypic plasticity in a forcipulate seastar. Journal of Experimental Marine Biology and Ecology 237:203-224

Gooding RA, Harley CDG, Tang E (2009) Elevated water temperature and carbon dioxide concentration increase the growth of a keystone echinoderm. Proceedings of the National Academy of Sciences of the United States of America 106:9316-9321

Hallett TB, Coulson T, Pilkington JG, Clutton-Brock TH, Pemberton JM, Grenfell BT (2004) Why large-scale climate indices seem to predict ecological processes better than local weather. Nature 430:71-75

Halpin PM, Menge BA, Hofmann GE (2004) Experimental demonstration of plasticity in the heat shock response of the intertidal mussel *Mytilus californianus*. Marine Ecology Progress Series 276:137-145

Harley CDG, Hughes AR, Hultgren KM, Miner BG, Sorte CJB, Thornber CS, Rodriguez
LF, Tomanek L, Williams SL (2006a) The impacts of climate change in coastal
marine systems. Ecology Letters 9:228-241

Harley CDG, Pankey MS, Wares JP, Grosberg RK, Wonham MJ (2006b) Color
polymorphism and genetic structure in the sea star *Pisaster ochraceus*. The
Biological Bulletin 211:248-262

Harrold C, Pearse JS (1980) Allocation of pyloric caecum reserves in fed and starved sea
stars, *Pisaster giganteus* (Stimpson): somatic mantenaince comes before
reproduction. Journal of Experimental Marine Biology and Ecology 48:169-183

Hart MW (1995) What are the costs of small egg size for a marine invertebrate with
feeding planktonic larvae? American Naturalist 146:415-426

Helmuth B (2002) How do we measure the environment? Linking intertidal thermal
physiology and ecology through biophysics. Integrative and Comparative Biology
42:837-845

Helmuth B, Broitman BR, Blanchette C, Gilman S, Halpin P, Harley CDG, O`Donnell
MJ, Hofmann GE, Menge B, Strickland D (2006a) Mosaic patterns of thermal
stress in the rocky intertidal zone: implications for climate change. Ecological
Monographs 76:461-479

Helmuth B, Harley CDG, Halpin PM, O'Donnell M, Hofmann GE, Blanchette CA (2002)
Climate change and latitudinal patterns of intertidal thermal stress. Science
298:1015-1017

Helmuth B, Kingsolver JG, Carrington E (2005) Biophysics, physiological ecology, and climate change: Does mechanism matter? Annual Review of Physiology 67:177-201

Helmuth B, Mieszkowska N, Moore P, Hawkins SJ (2006b) Living on the edge of two changing worlds: Forecasting the responses of rocky intertidal ecosystems to climate change. Annual Review of Ecology Evolution and Systematics 37:373-404

Helmuth BST (1998) Intertidal mussel microclimates: predicting the body temperature of a sessile invertebrate. Ecological Monographs 68:51-74

Helmuth BST, Hofmann GE (2001) Microhabitats, thermal heterogeneity, and patterns of physiological stress in the rocky intertidal zone. Biological Bulletin 201:374-384

Hettinger A, Sanford E, Hill TM, Lenz EA, Russell AD, Gaylord B (2013) Larval carry-over effects from ocean acidification persist in the natural environment. Global Change Biology 19:3317-3326

Himmelman JH, Dumont CP, Gaymer CF, Vallieres C, Drolet D (2008) Spawning synchrony and aggregative behaviour of cold-water echinoderms during multi-species mass spawnings. Marine Ecology-Progress Series 361:161-168

Hobday A (1995) Body-size variation exhibited by an intertidal limpet: Influence of wave exposure, tidal height and migratory behavior. Journal of Experimental Marine Biology and Ecology 189:29-45

Hochachka PW, Somero GN (2002) Biochemical Adaptation. Oxford University Press, New York

Hoegh-Guldberg O, Bruno JF (2010) The impact of climate change on the world's marine
ecosystems. Science 328:1523-1528

Hofmann GE, Somero GN (1995) Evidence for protein damage at environmental
temperatures - Seasonal-changes in levels of ubiquitin conjugates and Hsp70 in
the intertidal mussel *Mytilus trossulus*. Journal of Experimental Biology
198:1509-1518

Hollander J (2008) Testing the grain-size model for evolution of phenotypic plasticity.
Evolution 62:1381-1389

Holling CS (1959) Some characteristics of simple types of predation and parasitism.
Canadian entomologist 91:385-398

Honkoop PJC, Beukema JJ (1997) Loss of body mass in winter in three intertidal bivalve
species: an experimental and observational study of the interacting effects
between water temperature, feeding time and feeding behaviour. Journal of
Experimental Marine Biology and Ecology 212:277-297

Howard J, Babij E, Griffis R, Helmuth B, Himes-Cornell A, Niemier P, Orbach M, Petes
L, Allen S, Auad G, Auer C, Beard R, Boatman M, Bond N, Boyer T, Brown D,
Clay P, Crane K, Cross S, Dalton M, Diamond J, Diaz R, Dortch Q, Duffy E,
Fauquier D, Fisher W, Graham M, Halpern B, Hansen L, Hayum B, Herrick S,
Hollowed A, Hutchins D, Jewett E, Jin D, Knowlton N, Kotowicz D, Kristiansen
T, Little P, Lopez C, Loring P, Lumpkin R, Mace A, Mengerink K, Morrison JR,
Murray J, Norman K, O'Donnell J, Overland J, Parson R, Pettigrew N, Pfeirrer L,
Pidgeon E, Plummer M, Polovina J, Quintrell J, Rowles T, Runge J, Rust M,
Sanford E, Send U, Singer M, Speir C, Stanitski D, Thornber C, Wilson C, Xue Y

(2013) Oceans and Marine Resources in a Changing Climate. Oceanography and Marine Biology 51:71-192

Huang X-w, Wang T-f, Ye Z-w, Han G-d, Dong Y-w (2014) Temperature relations of aerial and aquatic physiological performance in a mid-intertidal limpet Cellana toreuma: adaptation to rapid changes in thermal stress during emersion. Integrative Zoology:n/a-n/a

Huey RB (1991) Physiological consequences of habitat selection. American Naturalist 137:S91-S115

Huey RB, Kingsolver JG (1989) Evolution of thermal sensitivity of ectotherm performance. Trends in Ecology & Evolution 4:131-135

Huey RB, Stevenson RD (1979) Integrating thermal physiology and ecology of ectotherms: A discussion of approaches. American Zoologist 19:357-366

Hyndman RJ, Koehler AB (2006) Another look at measures of forecast accuracy. International Journal of Forecasting 22:679-688

Iacarella JC, Helmuth B (2012) Body temperature and desiccation constrain the activity of Littoraria irrorata within the Spartina alterniflora canopy. Journal of Thermal Biology 37:15-22

IPCC (2007) Climate Change 2007: Impacts, Adaptation and Vulnerability. Contribution of Working Group II to the Fourth Assessment Report of the Intergovernmental Panel on Climate Change. Cambridge University Press, Cambridge, UK

Jackson AC (2010) Effects of topography on the environment. Journal of the Marine Biological Association of the United Kingdom 90:169-192

Jones KMM, Boulding EG (1999) State-dependent habitat selection by an intertidal snail: the costs of selecting a physically stressful microhabitat. Journal of Experimental Marine Biology and Ecology 242:149-177

Jones SJ, Mieszkowska N, Wethey DS (2009) Linking Thermal Tolerances and Biogeography: Mytilus edulis (L.) at its Southern Limit on the East Coast of the United States. Biol Bull 217:73-85

Judge ML, Botton ML, Hamilton MG (2011) Physiological consequences of the supralittoral fringe: microhabitat temperature profiles and stress protein levels in the tropical periwinkle Cenchritis muricatus (Linneaus, 1758). Hydrobiologia 675:143-156

Jusup M, Klanjscek T, Matsuda H, Kooijman SALM (2011) A Full Lifecycle Bioenergetic Model for Bluefin Tuna. PLoS ONE 6:e21903

Karasov WH, Martínez del Rio C (2007) Physiological Ecology: How Animals Process Energy, Nutrients, and Toxins. Princeton University Press, Princeton

Kearney M (2006) Habitat, environment and niche: what are we modelling? Oikos 115:186-191

Kearney M, Shine R, Porter WP (2009) The potential for behavioral thermoregulation to buffer "cold-blooded" animals against climate warming. Proceedings of the National Academy of Sciences

Kearney M, Simpson SJ, Raubenheimer D, Helmuth B (2010) Modelling the ecological niche from functional traits. Philos Trans R Soc B-Biol Sci 365:3469-3483

Klaassen M, Ens BJ (1993) Habitat selection and energetics of the fiddler crab (Uca tangeri). Netherlands Journal of Sea Research 31:495-502

Kooijman SALM (1986) Energy budgets can explain body size relations. Journal of
Theoretical Biology 121:269-282

Kooijman SALM (2010) Dynamic Energy Budget Theory For Metabolic Organization.
Cambridge University Press, Cambridge

Kooijman SALM, Pecquerie L, Augustine S, Jusup M (2011) Scenarios for acceleration
in fish development and the role of metamorphosis. Journal of Sea Research
66:419-423

Kooijman SALM, Sousa T, Pecquerie L, van der Meer J, Jager T (2008) From food-
dependent statistics to metabolic parameters, a practical guide to the use of
dynamic energy budget theory. Biological Reviews 83:533-552

Kordas RL, Harley CDG, O'Connor MI (2011) Community ecology in a warming world:
The influence of temperature on interspecific interactions in marine systems.
Journal of Experimental Marine Biology and Ecology 400:218-226

Landenberger DE (1969) Effects of exposure to air on Pacific starfish and its relationship
to distribution. Physiological Zoology 42:220-&

Lawrence JM, Cowell BC (1996) The righting response as an indication of stress in
stichaster striatus (Echinodermata, asteroidea). Marine and Freshwater Behaviour
and Physiology 27:239-248

Leonard GH (2000) Latitudinal variation in species interactions: A test in the New
England rocky intertidal zone. Ecology 81:1015-1030

Levinton JS (1983) The latitudinal compensation hypothesis: Growth data and a model of
latitudinal growth differentiation based upon energy budgets. I. Interspecific

comparison of *Ophryotrocha* (POLYCHATE: DORVILLEIDAE). Biological

Bulletin 165:686-698

Lika K, Kearney MR, Freitas V, van der Veer HW, van der Meer J, Wijsman JWM,

Pecquerie L, Kooijman SALM (2011a) The "covariation method" for estimating

the parameters of the standard Dynamic Energy Budget model I: Philosophy and

approach. Journal of Sea Research 66:270-277

Lika K, Kearney MR, Kooijman SALM (2011b) The "covariation method" for estimating

the parameters of the standard Dynamic Energy Budget model II: Properties and

preliminary patterns. Journal of Sea Research 66:278-288

Linton DL, Taghon GL (2000) Feeding, growth, and fecundity of *Abarenicola pacifica* in

relation to sediment organic concentration. Journal of Experimental Marine

Biology and Ecology 254:85-107

Manzur T, Barahona M, Navarrete SA (2010) Ontogenetic changes in habitat use and diet

of the sea-star Heliaster helianthus on the coast of central Chile. Journal of the

Marine Biological Association of the UK 90:537-546

Marshall D, Baharuddin N, McQuaid C (2013) Behaviour moderates climate warming

vulnerability in high-rocky-shore snails: interactions of habitat use, energy

consumption and environmental temperature. Marine Biology:1-6

Marshall DJ, McQuaid CD (2011) Warming reduces metabolic rate in marine snails:

adaptation to fluctuating high temperatures challenges the metabolic theory of

ecology. Proceedings of the Royal Society B-Biological Sciences 278:281-288

Martin TL, Huey RB (2008) Why "Suboptimal" is optimal: Jensen's inequality and

ectotherm thermal preferences. American Naturalist 171:E102-E118

Matzelle A, Montalto V, Sarà G, Zippay M, Helmuth B (2014) Dynamic Energy Budget

    model parameter estimation for the bivalve *Mytilus californianus*: Application of

    the covariation method. Journal of Sea Research

Mauzey KP (1966) Feeding behavior and reproductive cycles in *Pisaster ochraceus*. Biol

    Bull 131:127-144

McQuaid CD (1982) The influence of desiccation and predation on vertical size gradients

    in populations of the gastropod *Oxystele variegata* (Anton) on an exposed rocky

    shore. Oecologia 53:123-127

Menge BA (1975) Brood or broadcast? The adaptive significance of different

    reproductive strategies in the two intertidal sea stars *Leptasterias hexactis* and

    Pisaster ochraceus. Marine Biology 31:87-100

Menge BA, Berlow EL, Blanchette CA, Navarrete SA, Yamada SB (1994) The keystone

    species concept: Variation in interaction strength in a rocky intertidal habitat.

    Ecological Monographs 64:250-286

Menge BA, Olson AM (1990) Role of scale and environmental factors in regulation of

    community structure. Trends in Ecololy and Evolution 5:52–57

Menge BA, Olson AM, Dahlhoff EP (2002) Environmental stress, bottom-up effects, and

    community dynamics: Integrating molecular-physiological and ecological

    approaches. Integrative and Comparative Biology 42:892-908

Menge BA, Sutherland JP (1976) Species diversity gradients: Synthesis of the roles of

    predation, competition, and temporal heterogeneity. The American Naturalist

    110:351-369

Menge BA, Sutherland JP (1987) Community regulation: Variation in disturbance, competition, and predation in relation to environmental stress and recruitment. The American Naturalist 130:730-757

Mills LS, Soulé ME, Doak DF (1993) The keystone-species concept in ecology and conservation. Bioscience 43:219-224

Mislan KAS, Helmuth B, Wethey DS (2014) Geographical variation in climatic sensitivity of intertidal mussel zonation. Global Ecology and Biogeography:n/a-n/a

Mislan KAS, Wethey DS, Helmuth B (2009) When to worry about the weather: role of tidal cycle in determining patterns of risk in intertidal ecosystems. Global Change Biology 15:3056-3065

Monaco CJ, Brokordt KB, Gaymer CF (2010) Latitudinal thermal gradient effect on the cost of living of the intertidal porcelain crab *Petrolisthes granulosus*. Aquatic Biology 9:23-33

Monaco CJ, Helmuth B (2011) Tipping points, thresholds and the keystone role of physiology in marine climate change research. In: Lesser M (ed) Advances in Marine Biology, Book 60. Elsevier, Oxford, UK

Monaco CJ, Wethey DS, Helmuth B (2014) A dynamic energy budget (DEB) model for the keystone predator *Pisaster ochraceus*. PLoS ONE 9:e104658

Moore P, Thompson RC, Hawkins SJ (2007) Effects of grazer identity on the probability of escapes by a canopy-forming macroalga. Journal of Experimental Marine Biology and Ecology 344:170-180

Moré J (1978) The Levenberg-Marquardt algorithm: Implementation and theory. In:

    Watson GA (ed) Numerical Analysis, Book 630. Springer Berlin Heidelberg

Mumby PJ, Iglesias-Prieto R, Hooten AJ, Sale PF, Hoegh-Guldberg O, Edwards AJ,

    Harvell CD, Gomez ED, Knowlton N, Hatziolos ME, Kyewalyanga MS, Muthiga

    N (2011) Revisiting climate thresholds and ecosystem collapse. Frontiers in

    Ecology and the Environment 9:94-96

Muñoz JLP, Camus PA, Labra FA, Finke GR, Bozinovic F (2008) Thermal constraints

    on daily patterns of aggregation and density along an intertidal gradient in the

    periwinkle Echinolittorina peruviana. Journal of Thermal Biology 33:149-156

Muñoz JLP, Finke GR, Camus PA, Bozinovic F (2005) Thermoregulatory behavior, heat

    gain and thermal tolerance in the periwinkle *Echinolittorina peruviana* in central

    Chile. Comparative Biochemistry and Physiology a-Molecular & Integrative

    Physiology 142:92-98

Newell RC (1970) Biology of Intertidal Animals. Logos, Great Britain

Nimitz AMS (1971) Histochemical study of gut nutrient reserves in relation to

    reproduction and nutrition in the sea stars, *Pisaster ochraceus* and *Patiria

    miniata*. The Biological Bulletin 140:461-481

Nimitz AMS (1976) Histochemical Changes in Gonadal Nutrient Reserves Correlated

    with Nutrition in the Sea Stars, *Pisaster ochraceus* and *Patiria miniata*.

    Biological Bulletin 151:357-369

Nisbet RM, Jusup M, Klanjscek T, Pecquerie L (2012) Integrating dynamic energy

    budget (DEB) theory with traditional bioenergetic models. The Journal of

    Experimental Biology 215:892-902

Nisbet RM, Muller EB, Lika K, Kooijman SALM (2000) From molecules to ecosystems through dynamic energy budget models. J Anim Ecol 69:913-926

O'Connor MI, Piehler MF, Leech DM, Anton A, Bruno JF (2009) Warming and Resource Availability Shift Food Web Structure and Metabolism. PLoS Biol 7:e1000178

Ohlberger J, Thackeray SJ, Winfield IJ, Maberly SC, Vøllestad LA (2014) When phenology matters: age–size truncation alters population response to trophic mismatch. Proceedings of the Royal Society B: Biological Sciences 281

Paine RT (1966) Food web complexity and species diversity. The American Naturalist 100:65-75

Paine RT (1974) Intertidal community structure: experimental studies on the relationship between a dominant competitor and its principal predator. Oecologia 15:93-120

Paine RT (1976) Size-limited predation: an observational and experimental approach with the Mytilus-Pisaster interaction. Ecology 57:858-873

Parmesan C, Yohe G (2003) A globally coherent fingerprint of climate change impacts across natural systems. Nature 421:37-42

Pearse JS, Eernisse DJ (1982) Photoperiodic regulation of gametogenesis and gonadal growth in the sea star *Pisaster ochraceus*. Marine Biology 67:121-125

Pearse JS, Eernisse DJ, Pearse VB, Beauchamp KA (1986) Photoperiodic Regulation of Gametogenesis in Sea Stars, with Evidence for an Annual Calendar Independent of Fixed Daylength. American Zoologist 26:417-431

Pechenik JA (2006) Larval experience and latent effects—metamorphosis is not a new beginning. Integrative and Comparative Biology 46:323-333

Peck LS, Clark MS, Morley SA, Massey A, Rossetti H (2009) Animal temperature limits and ecological relevance: effects of size, activity and rates of change. Functional Ecology 23:248-256

Peck LS, Souster T, Clark MS (2013) Juveniles are more resistant to warming than adults in 4 species of Antarctic marine invertebrates. PLoS ONE 8:e66033

Pecquerie L, Johnson LR, Kooijman SALM, Nisbet RM (2011) Analyzing variations in life-history traits of Pacific salmon in the context of Dynamic Energy Budget (DEB) theory. Journal of Sea Research 66:424-433

Pecquerie L, Petitgas P, Kooijman SALM (2009) Modeling fish growth and reproduction in the context of the Dynamic Energy Budget theory to predict environmental impact on anchovy spawning duration. Journal of Sea Research 62:93-105

Percy JA (1973) Thermal adaptation in Boreo-Arctic Echinoid Strongylocentrotus droabachiensis (O.F. Müler: 1776). II. Seasonal Acclimatization and Urchin Activity. Physiological Zoology 46:129-138

Peters D, Bestelmeyer B, Turner M (2007) Cross–scale interactions and changing pattern–process relationships: Consequences for system dynamics. Ecosystems 10:790-796

Petes LE, Menge BA, Harris AL (2008a) Intertidal mussels exhibit energetic trade-offs between reproduction and stress resistance. Ecological Monographs 78:387-402

Petes LE, Menge BA, Murphy GD (2007) Environmental stress decreases survival, growth, and reproduction in New Zealand mussels. Journal of Experimental Marine Biology and Ecology 351:83-91

Petes LE, Mouchka ME, Milston-Clements RH, Momoda TS, Menge BA (2008b) Effects of environmental stress on intertidal mussels and their sea star predators. Oecologia 156:671-680

Pia TS, Johnson T, George SB (2012) Salinity-induced morphological changes in *Pisaster ochraceus* (Echinodermata: Asteroidea) larvae. Journal of Plankton Research 34:590-601

Pincebourde S, Sanford E, Casas J, Helmuth B (2012) Temporal coincidence of environmental stress events modulates predation rates. Ecology Letters

Pincebourde S, Sanford E, Helmuth B (2008) Body temperature during low tide alters the feeding performance of a top intertidal predator. Limnology and Oceanography 53:1562-1573

Pincebourde S, Sanford E, Helmuth B (2009) An intertidal sea star adjusts thermal inertia to avoid extreme body temperatures. American Naturalist 174:890-897

Place SP, O'Donnell MJ, Hofmann GE (2008) Gene expression in the intertidal mussel Mytilus californianus: physiological response to environmental factors on a biogeographic scale. Marine Ecology-Progress Series 356:1-14

Porter W, Mitchell J, Beckman W, Tracy C (1975) Environmental constraints on some predator-prey interactions. In: Gates D, Schmerl R (eds) Perspectives of Biophysical Ecology. Springer-Verlag, New York

Pörtner HO (2002) Climate variations and the physiological basis of temperature dependent biogeography: systemic to molecular hierarchy of thermal tolerance in animals. Comparative Biochemestry and Physiology Part A 132:739-761

Pörtner HO (2006) Climate-dependent evolution of Antarctic ectotherms: An integrative analysis. Deep Sea Research Part II: Topical Studies in Oceanography 53:1071-1104

Potter KA, Woods HA, Pincebourde S (2013) Microclimatic challenges in global change biology. Global Change Biology 19:2932–2939

Power ME, Tilman D, Estes JA, Menge BA, Bond WJ, Mills LS, Daily G, Castilla JC, Lubchenco J, Paine RT (1996) Challenges in the quest for keystones. Bioscience 46:609-620

Quinn GP, Keough MJ (2002) Experimental Design and Data Analysis for Biologists. Cambridge University Press

R Core Team (2013) R: A Language and Environment for Statistical Computing. R Foundation for Statistical Computing, Vienna, Austria

Raffaelli DG, Hughes RN (1978) The effects of crevice size and availability on populations of *Littorina rudis* and *Littorina neritoides*. J Anim Ecol 47:71-83

Ren JS, Schiel DR (2008) A dynamic energy budget model: parameterisation and application to the Pacific oyster *Crassostrea gigas* in New Zealand waters. Journal of Experimental Marine Biology and Ecology 361:28-42

Richmond CE, Wethey DS, Woodin SA (2007) Climate change and increased environmental variability: Demographic responses in an estuarine harpacticoid copepod. Ecol Model 209:189-202

Rico-Villa B, Bernard I, Robert R, Pouvreau S (2010) A Dynamic Energy Budget (DEB) growth model for Pacific oyster larvae, *Crassostrea gigas*. Aquaculture 305:84-94

Robles C, Sherwood-Stephens R, Alvarado M (1995) Responses of a key intertidal predator to varying recruitment of Its prey. Ecology 76:565-579

Robles CD, Desharnais RA, Garza C, Donahue MJ, Martinez CA (2009) Complex equilibria in the maintenance of boundaries: experiments with mussel beds. Ecology 90:985-995

Rogers T, Elliott J (2013) Differences in relative abundance and size structure of the sea stars Pisaster ochraceus and Evasterias troschelii among habitat types in Puget Sound, Washington, USA. Marine Biology 160:853-865

Rogers-Bennett L, Kudela R, Nielsen KJ, Paquin A, O'Kelly C, Langlois G, Crane D, Moore J (2012) Dinoflagellate bloom coincides with marine invertebrate mortalities in northern California. Harmful Algae News, Book 46

Rojas JM, Castillo SB, Escobar JB, Shinen JL, Bozinovic F (2013) Huddling up in a dry environment: the physiological benefits of aggregation in an intertidal gastropod. Marine Biology 160:1119-1126

Russell BD, Harley CDG, Wernberg T, Mieszkowska N, Widdicombe S, Hall-Spencer JM, Connell SD (2011) Predicting ecosystem shifts requires new approaches that integrate the effects of climate change across entire systems. Biology Letters

Russell R, Wood SA, Allison G, Menge BA (2006) Scale, environment, and trophic status: the context dependency of community saturation in rocky intertidal communities. The American Naturalist 167:E158-E170

Sanford E (1999) Regulation of keystone predation by small changes in ocean temperature. Science 283:2095-2097

Sanford E (2002a) The feeding, growth, and energetics of two rocky intertidal predators

    (*Pisaster ochraceus* and *Nucella canaliculata*) under water temperatures

    simulating episodic upwelling. Journal of Experimental Marine Biology and

    Ecology 273:199-218

Sanford E (2002b) Water Temperature, Predation, and the Neglected Role of

    Physiological Rate Effects in Rocky Intertidal Communities. Integrative and

    Comparative Biology 42:881-891

Sanford E, Kelly MW (2011) Local adaptation in marine invertebrates. Annual Review of

    Marine Science 3:509-535

Sanford E, Menge BA (2007) Reproductive output and consistency of source populations

    in the sea star *Pisaster ochraceus*. Marine Ecology-Progress Series 349:1-12

Sarà G, Palmeri V, Montalto V, Rinaldi A, Widdows J (2013) Parameterisation of

    bivalve functional traits for mechanistic eco-physiological dynamic energy budget

    (DEB) models. Marine Ecology Progress Series 480:99-117

Saraiva S, van der Meer J, Kooijman SALM, Sousa T (2011) Modelling feeding

    processes in bivalves: A mechanistic approach. Ecol Model 222:514-523

Schneider KR, Van Thiel LE, Helmuth B (2010) Interactive effects of food availability

    and aerial body temperature on the survival of two intertidal Mytilus species.

    Journal of Thermal Biology 35:161-166

Schulte PM, Healy TM, Fangue NA (2011) Thermal Performance Curves, Phenotypic

    Plasticity, and the Time Scales of Temperature Exposure. Integrative and

    Comparative Biology 51:691-702

Seabra R, Wethey DS, Santos AM, Lima FP (2011) Side matters: Microhabitat influence on intertidal heat stress over a large geographical scale. Journal of Experimental Marine Biology and Ecology 400:200-208

Sebens KP (1987) The ecology of indeterminate growth in animals. Annual Review of Ecology and Systematics 18:371-407

Sharpe PJH, DeMichele DW (1977) Reaction kinetics of poikilotherm development. Journal of Theoretical Biology 64:649-670

Shi P, Ge F (2010) A comparison of different thermal performance functions describing temperature-dependent development rates. Journal of Thermal Biology 35:225-231

Sokolova IM (2013) Energy-Limited Tolerance to Stress as a Conceptual Framework to Integrate the Effects of Multiple Stressors. Integrative and Comparative Biology 53:597-608

Sokolova IM, Lannig G (2008) Interactive effects of metal pollution and temperature on metabolism in aquatic ectotherms: implications of global climate change. Clim Res 37:181-201

Somero GN (2010) The physiology of climate change: how potentials for acclimatization and genetic adaptation will determine 'winners' and 'losers'. Journal of Experimental Biology 213:912-920

Soto RE, Bozinovic F (1998) Behavioral thermoregulation of the periwinkle *Nodilittorina peruviana* inhabiting the rocky intertidal of central Chile: a laboratory and field study. Revista Chilena de Historia Natural 71:375-382

Sousa T, Domingos T, Kooijman SALM (2008) From empirical patterns to theory: a formal metabolic theory of life. Philosophical Transactions of the Royal Society B: Biological Sciences 363:2453-2464

Sousa T, Domingos T, Poggiale J-C, Kooijman SALM (2010) Dynamic energy budget theory restores coherence in biology. Philosophical Transactions of the Royal Society B: Biological Sciences 365:3413-3428

Stevenson RD (1985) Body size and limits to the daily range of body temperature in terrestrial ectotherms. The American Naturalist 125:102-117

Stickle WB (1988) Patterns of nitrogen excretion in the phylum echinodermata. Comparative Biochemistry and Physiology Part A: Physiology 91:317-321

Stillman JH (2002) Causes and Consequences of Thermal Tolerance Limits in Rocky Intertidal Porcelain Crabs, Genus *Petrolisthes*. Integrative and Comparative Biology 42:790-796

Stillman JH, Somero GN (2000) A Comparative analysis of the upper thermal tolerance limits of eastern Pacific porcelain crabs, genus *Petrolisthes*: Influences of latitude, vertical zonation, acclimation, and phylogeny. Physiological and Biochemical Zoology 73:200-208

Stokstad E (2014) Death of the Stars. Science Magazine 344:464-467

Strathmann R (1978) Length of pelagic period in echinoderms with feeding larvae from the Northeast Pacific. Journal of Experimental Marine Biology and Ecology 34:23-27

Strathmann RR (1971) The feeding behavior of planktotrophic echinoderm larvae: Mechanisms, regulation, and rates of suspensionfeeding. Journal of Experimental Marine Biology and Ecology 6:109-160

Szathmary PL, Helmuth B, Wethey DS (2009) Climate change in the rocky intertidal zone: predicting and measuring the body temperature of a keystone predator. Marine Ecology-Progress Series 374:43-56

Tenore KR, Chesney EJJ (1985) The effects of interaction of rate of food supply and population density on the bioenergetics of the opportunistic polychaete, *Capitella capitata* (type 1). Limnology and Oceanography 30

Tepler S, Mach K, Denny M (2011) Preference versus performance: Body temperature of the intertidal snail *Chlorostoma funebralis*. The Biological Bulletin 220:107-117

Tomanek L, Helmuth B (2002) Physiological ecology of rocky intertidal organisms: A synergy of concepts. Integrative and Comparative Biology 42:771-775

Trowbridge CD (1998) Stenophagous, herbivorous sea slugs attack desiccation-prone, green algal hosts (Codium spp.): indirect evidence of prey-stress models (PSMs)? Journal of Experimental Marine Biology and Ecology 230:31-53

Tummers B (2006) *DataThief III*. http://datathief.org/

van der Meer J (2006) An introduction to Dynamic Energy Budget (DEB) models with special emphasis on parameter estimation. Journal of Sea Research 56:85-102

van der Veer HW, Cardoso JFMF, van der Meer J (2006) The estimation of DEB parameters for various Northeast Atlantic bivalve species. Journal of Sea Research 56:107-124

Vermeij GJ (1972) Intraspecific shore-level size gradients in intertidal molluscs. Ecology 53:693-700

Vickery M, McClintock J (2000) Effects of food concentration and availability on the incidence of cloning in planktotrophic larvae of the sea star *Pisaster ochraceus*. Biological Bulletin 199:298-304

Von Bertalanffy L (1957) Quantitative laws in metabolism and growth. The Quarterly Review of Biology 32:217-231

Wernberg T, Russell BD, Moore PJ, Ling SD, Smale DA, Campbell A, Coleman MA, Steinberg PD, Kendrick GA, Connell SD (2011) Impacts of climate change in a global hotspot for temperate marine biodiversity and ocean warming. Journal of Experimental Marine Biology and Ecology 400:7-16

Wethey DS (1983) Geographic limits and local zonation - the barnacles Semibalanus (Balanus) and Chtamalus in New England. Biological Bulletin 165:330-341

Wethey DS (1984) Sun and shade mediate competition in the barnacles *Chthamalus* and *Semibalanus*: a field experiment. The Biological Bulletin 167:176-185

Wethey DS (2002) Biogeography, competition, and microclimate: The barnacle *Chthamalus fragilis* in New England. Integrative and Comparative Biology 42:872-880

Williams GA, De Pirro M, Cartwright S, Khangura K, Ng W-C, Leung PTY, Morritt D (2011) Come rain or shine: the combined effects of physical stresses on physiological and protein-level responses of an intertidal limpet in the monsoonal tropics. Functional Ecology 25:101-110

Williams GA, Morritt D (1995) Habitat partitioning and thermal tolerance in a tropical

limpet, *Cellana grata*. Marine Ecology Progress Series 124:89-103

Woodin SA, Hilbish TJ, Helmuth B, Jones SJ, Wethey DS (2013) Climate change,

species distribution models, and physiological performance metrics: predicting

when biogeographic models are likely to fail. Ecology and Evolution 3:3334-3346

Zarnetske PL, Skelly DK, Urban MC (2012) Biotic Multipliers of Climate Change.

Science 336:1516-1518

Zippay M, Hofmann G (2010) Physiological tolerances across latitudes: thermal

sensitivity of larval marine snails (Nucella spp.). Marine Biology 157:707-714

Zwarts L, Blomert AM (1992) Why knot *Calibris canutus* take medium-sized *Macoma*

balthica when six prey species are available. Marine Ecology Progress Series

83:113-128

APPENDIX A

EFFECT OF ENVIRONMENTAL VARIABLES ON *PISASTER* SIZE-DEPENDENT INTERTIDAL HEIGHT

Results of multiple regression analyses (conducted through generalized linear models, GLM) to test the effect of environmental variables (air temperature, solar radiation, seawater temperature, wind speed, and wave height) on *Pisaster* size-dependent intertidal height (SDIH). The significance of parameter estimates was computed via Likelihood Ratio Tests (LRT) using Type II sums of squares. The analysis was run separately for individuals found exposed and protected.

Variable/ Refuge use	Estimate	Std. Error	χ^2	df	P-value
Protected individuals					
Solar radiation	$-2.7*10^{-5}$	$6.3*10^{-5}$	0.19	1	0.66
Air temperature	$6.9*10^{-3}$	$1.3*10^{-2}$	0.28	1	0.59
Wave height	$-3.7*10^{-3}$	$9.5*10^{-3}$	0.16	1	0.69
Seawater temperature	$-1.3*10^{-3}$	$1.4*10^{-2}$	0.01	1	0.93
Wind speed	$-1.6*10^{-3}$	$7.8*10^{-3}$	0.04	1	0.84
Exposed individuals					
Solar radiation	$-5.4*10^{-5}$	$6.2*10^{-5}$	0.76	1	0.38
Air temperature	$8.4*10^{-3}$	$1.4*10^{-2}$	0.33	1	0.56
Wave height	$-2.8*10^{-3}$	$1.0*10^{-2}$	0.07	1	0.78
Seawater temperature	$1.9*10^{-2}$	$2.1*10^{-2}$	0.89	1	0.35
Wind speed	$4.0*10^{-3}$	$8.7*10^{-3}$	0.21	1	0.65

APPENDIX B

GENERALIZED DEB MODEL STRUCTURE

This section will describe some basic features of a standard DEB model (for deeper

discussions of the fundamentals behind the theory see (Kooijman 2010, Kooijman et al.

2008)). Standard versions of DEB models conceptually discriminate between the state

variables energy reserve, E (J), structural volume, V (cm^3), and maturation, E_H (J).

Once the threshold of puberty has been reached, the state variable reproductive buffer,

E_R (J), can be included. Reproductive buffer accounts for variability in the reproductive

potential of mature individuals. The mass of an organism at any given point in time is

defined by the contributions from reserve, structure, and reproductive buffer. Maturation,

in turn, is understood as energy or mass that dissipates in the form of heat or metabolites

as the organism increases its maturity; therefore, this state variable does not contribute to

total mass. A chief assumption in standard DEB models is that the biochemical

composition of reserve and structure are constant (i.e. strong homeostasis assumption).

Although the state variables cannot be measured directly, their dynamics are fully

described by a set of equations that will ultimately characterize an organism's

physiological condition (Sousa et al. 2008).

Before defining the processes that govern an individual's physiological condition,

it is worth elaborating on how DEB theory deals with matters of size and shape.

Assuming that the organism's shape does not change with growth (i.e. isomorphy), the

model relies on structural length L (cm), rather than physical length L_W (cm), to provide a measure of size. Structural length is preferred because (1) it only relates to structural volume discriminating between contributions from other state variables, and (2) it is not affected by the organism's shape, thus favoring inter-species comparisons (Kooijman 2010). The DEB parameter shape coefficient δ_M (dimensionless) serves to translate physical measurements taken from some representative length (e.g. arm length) to structural length: $L = \delta_M \cdot L_W$. In the model, structural length defines all physiological processes proportional to area or volume. The equations describing surface-area related processes are expressed in terms of L^2 (cm^2), while those proportional to volume are expressed in terms of L^3 (cm^3). All rates (units t^{-1}) are written with a dot as in $\dot{p}_A$. All surface-area specific quantities (units L^{-2}) are written in curly braces as in $\{\dot{p}_{Am}\}$. All volume-specific quantities (units L^{-3}) are written in square brackets as in $[\dot{p}_M]$.

Energy reserve changes as the organism acquires food. DEB theory makes use of a scaled version of Holling's type II functional response model (Holling 1959), f (dimensionless), to account for the effects of food availability, X (resource density, 2-cm shell length mussels m^{-2}), on feeding and assimilation flux. The amount of energy entering the body is assumed to be proportional to the surface-area of the structural volume, i.e. L^2 (cm^2). Thus, as the organism forages the energy assimilated through the gut, $\dot{p}_A$ (J d^{-1}), can be described by:

$$\dot{p}_A = M \cdot \{\dot{p}_{Am}\} \cdot L^2 \cdot f \qquad \text{with} \qquad f = \frac{X}{X + X_\kappa} \qquad (6),$$

where $\{\dot{p}_{Am}\}$ is a DEB parameter known as maximum surface area-specific assimilation rate (J d^{-1} cm^{-2}) and M is a shape correction function (dimensionless) explained in the main text (Eq. 1). The parameter X_κ represents the half-saturation coefficient or Michaellis-Menten constant (resource density at which feeding rate is one half of its maximum value) (Saraiva et al. 2011). The process of assimilation is not perfect; inefficiencies in transforming energy from food into energy reserve determine that a fraction of the available energy is dissipated.

The energy stored as reserve is balanced by all the metabolic needs of the organism, including growth, development (i.e. maturity), reproduction and maintenance (structural and maturity) (Sousa et al. 2010), as well as by the energy dissipated through the processes of growth and reproduction. The total energy allocated for those needs is known as utilization flux, $\dot{p}_C$ (J d^{-1}). Both the assimilation $\dot{p}_A$ and the utilization $\dot{p}_C$ fluxes define the dynamics of the reserve E:

$$\frac{dE}{dt} = \dot{p}_A - \dot{p}_C$$

(7)

$$\dot{p}_C = E \cdot \frac{M \cdot \dot{v} \cdot [E_G] \cdot L^2 + \dot{p}_M}{\kappa \cdot E + [E_G] \cdot L^3}$$

(8),

where three DEB parameters are introduced; energy conductance, $\dot{v}$ (cm d^{-1}), volume-specific cost of structure, $[E_G]$ (J cm^{-3}), and κ (dimensionless, explained below). The equation for estimating $\dot{p}_C$ has been derived assuming that reserve density, $[E] = E/V$ (J cm^{-3}), follows first order dynamics – i.e. the rate of decrease of reserve density is proportional to the amount of reserve density (van der Meer 2006). Notably, this aspect

of DEB theory offers a mechanism for filtering the effects of highly variable environmental conditions, thus suiting the organism with a homeostatic capacity. In depth explanations of the formal derivation of $\dot{p}_C$ can be found in Kooijman (2010) and Jusup et al. (2011).

The utilized energy is then distributed among the metabolic processes – somatic maintenance, $\dot{p}_M$ (J d^{-1}), structural growth, $\dot{p}_G$ (J d^{-1}), maturity maintenance, $\dot{p}_J$ (J d^{-1}), and maturation or reproductive buffer, $\dot{p}_R$ (J d^{-1}) (Fig. 1). The long-standing problem of allocation has been solved by DEB theory via the so-called *kappa* (κ) rule (Kooijman 1986, 2010). The parameter κ amounts to a fixed fraction of energy utilized from the reserves that goes to somatic maintenance and growth, the former having absolute priority over the latter. For ectothermic organisms, somatic maintenance amounts to the energetic costs associated with the turnover of structural proteins and the maintenance of metabolite concentration gradients across cell membranes. Since all these costs are proportional to structural volume, somatic maintenance can be described by:

$$\dot{p}_M = \left[\dot{p}_M \right] \cdot L^3$$

(9),

where $\left[\dot{p}_M \right]$ is a parameter known as volume-specific somatic maintenance cost (J d^{-1} cm^{-3}). Due to the priority given to somatic maintenance, the energy derived to structural growth can be calculated from $\dot{p}_G = \kappa \cdot \dot{p}_C - \dot{p}_M$. Growth is understood as a change in structure (excluding dynamics in body size due to fluctuations in energy reserve and reproductive buffer), which can be described by (Jusup et al. 2011):

$$\frac{dL}{dt} = \frac{1}{3 \cdot L^2} \cdot \frac{\dot{p}_G}{\left[E_G \right]}$$

(10).

Note that equation 5 includes the parameter volume-specific cost of structure $[E_G]$ to account for the cost of converting energy from reserve to structure (including tissue production and anabolic overheads). This formulation is equivalent to the traditional von Bertalanffy growth equation (Von Bertalanffy 1957), whose parameter von Bertalanffy growth coefficient, $\dot{r}_B$ (d^{-1}) describes the decreasing rate at which individuals reach their ultimate size L_∞ resulting from the balance between food assimilation and somatic maintenance (Sousa et al. 2010, van der Meer 2006). Furthermore, this mechanism is incorporated in DEB theory's formulation for this parameter;

$$\dot{r}_B = \frac{1}{3} \cdot \left(\frac{[\dot{p}_M]}{\kappa \cdot f \cdot [E_m] + [E_G]} \right)$$

. The validity of this formulation has been confirmed by successfully modeling the growth trajectories of many taxa reported in the literature (see Kooijman 2010 for details).

The utilized energy not going to somatic maintenance and growth, $\dot{p}_C \cdot (1 - \kappa)$, is channeled to cover costs of maturity maintenance, $\dot{p}_J$, and either increase the level of maturity or fill up the reproductive buffer, $\dot{p}_R$; energy allocated to maturation is assumed to increase from the age at birth until puberty, after which the available energy is directly used for building-up the reproductive buffer (Fig. 1). Maturity maintenance, $\dot{p}_J$ (J d^{-1}), which accounts for the maintenance of increased complexity attained throughout development, is assumed proportional to the level of maturity and can be modeled by:

$$\dot{p}_J = \dot{k}_J \cdot E_H \tag{11},$$

where the parameter $\dot{k}_J$ represents the maturity maintenance rate coefficient (d^{-1}). Once puberty is reached ($E_H \geq E_H^p$), maturity maintenance becomes constant. Knowing the energy allocated to maturity maintenance, the dynamics of $\dot{p}_R$ can be tracked through:

$$\dot{p}_R = \dot{p}_C \cdot (1-\kappa) - \dot{p}_J \tag{12}.$$

While $\dot{p}_R$ is equivalent to the rate of change of the maturation state variable (i.e. dE_H/dt) before puberty, it describes dynamics of the reproductive buffer state variable (i.e. dE_R/dt) after puberty is reached. Gonadal tissue is then synthetized from the reproductive buffer. The efficiency of turning reserve energy into eggs or sperm is determined by a reproductive efficiency coefficient k_R. We refer to the maturation state variable to determine the level of maturity at any given point in time, as well as the timing of transitions between developmental stages. Explicitly relying on the state variable maturation liberates the model from having to use size as a metric for developmental stage. This feature is particularly relevant for species that can grow or shrink indeterminately, such as sea stars (Feder, 1956; Sebens, 1987).

Physiological rates are temperature-dependent, and need to be corrected accordingly. DEB models make use of the Arrhenius relationship to describe the influence of body temperature on physiological rates over the range of temperatures where enzymes can be assumed to be active, delimited by the parameters T_L (K) and T_H (K). The parameter T_A, known as Arrhenius Temperature, allows capturing the thermal-sensitivity of the organism within these margins. Above and below the thermo-tolerance window enzymes become inactive, leading to a decline in physiological rates, which can

be traced by the parameters T_{AL} and T_{AH}, respectively (Freitas et al. 2007, Sharpe & DeMichele 1977). These five parameters fully define an organism's thermal performance curve, in accordance to the formula:

$$\dot{k}(T) = \dot{k}_1 \cdot \exp\left\{\frac{T_A}{T_1} - \frac{T_A}{T}\right\} \cdot \left(1 + \exp\left\{\frac{T_{AL}}{T} - \frac{T_{AL}}{T_L}\right\} + \exp\left\{\frac{T_{AH}}{T_H} - \frac{T_{AH}}{T}\right\}\right)^{-1}$$

(13),

where $\dot{k}(T)$ is the value of the physiological rate at a given body temperature T (K), and

$\dot{k}_1$ is the known value at a reference temperature T_1 (K).

Finally, DEB models explicitly acknowledge the existence of overhead costs associated with processes where energy-conversion inefficiencies between different compartments are observed. Such overhead costs, linked to assimilation, growth, and reproduction (Fig. 1), translate to energy losses in the form of heat and metabolites (Kooijman 2010).

APPENDIX C

PLoS ONE COPYRIGHT PERMISSION LETTER

Cristián Monaco <cristianmonaco@gmail.com>

Case 03510878: Question ref:_00DU0Ifis._500U0DEMrl:ref

one_production <one_production@plos.org>   Mon, Nov 3, 2014 at 12:35 PM
To: "cristianmonaco@gmail.com" <cristianmonaco@gmail.com>

Dear Dr. Monaco,

All PLOS publications are published under the Creative Commons Attribution License (CC BY 4.0,
http://creativecommons.org/licenses/by/4.0/). This means that you are free to use the material however you see
fit, as long as the original source is cited.

Best Regards,

Joseph S. Senate

PLOS I OPEN FOR DISCOVERY
Joseph Senate I Sr. Production Coordinator
1160 Battery Street, Suite 225, San Francisco, CA 94111
plos.org I Facebook I Twitter I Blog
[Quoted text hidden]